EIDGENÖSSISCHE TECHNISCHE HOCHSCHULE LAUSANNE
POLITECNICO FEDERALE DI LOSANNA
SWISS FEDERAL INSTITUTE OF TECHNOLOGY LAUSANNE

ÉCOLE POLYTECHNIQUE
FÉDÉRALE DE LAUSANNE

STRUCTURAL METALLIC MATERIALS BY INFILTRATION

Jean-François Despois, Randoald Müller, Ali Miserez,
Ludger Weber, Andreas Rossoll, Andreas Mortensen

Swiss Federal Institute of Technology in Lausanne
Institute of Materials
Laboratory for Mechanical Metallurgy

Report Documentation Page

Form Approved
OMB No. 0704-0188

1. REPORT DATE **18 MAR 2004**	2. REPORT TYPE **N/A**	3. DATES COVERED **-**
4. TITLE AND SUBTITLE **Structural Metallic Materials By Infiltration**		5a. CONTRACT NUMBER 5b. GRANT NUMBER 5c. PROGRAM ELEMENT NUMBER
6. AUTHOR(S)		5d. PROJECT NUMBER 5e. TASK NUMBER 5f. WORK UNIT NUMBER
7. PERFORMING ORGANIZATION NAME(S) AND ADDRESS(ES) **Swiss Federal Institute of Technology in Lausanne Institute of Materials Laboratory for Mechanical Metallurgy**		8. PERFORMING ORGANIZATION REPORT NUMBER
9. SPONSORING/MONITORING AGENCY NAME(S) AND ADDRESS(ES)		10. SPONSOR/MONITOR'S ACRONYM(S) 11. SPONSOR/MONITOR'S REPORT NUMBER(S)
12. DISTRIBUTION/AVAILABILITY STATEMENT **Approved for public release, distribution unlimited**		
13. SUPPLEMENTARY NOTES **See also ADM001672., The original document contains color images.**		
14. ABSTRACT		
15. SUBJECT TERMS		

16. SECURITY CLASSIFICATION OF:			17. LIMITATION OF ABSTRACT	18. NUMBER OF PAGES	19a. NAME OF RESPONSIBLE PERSON
a. REPORT	b. ABSTRACT	c. THIS PAGE			
NATO/unclassified	**unclassified**	**unclassified**	**UU**	**102**	

Standard Form 298 (Rev. 8-98)
Prescribed by ANSI Std Z39-18

Infiltration

The Infiltration Process

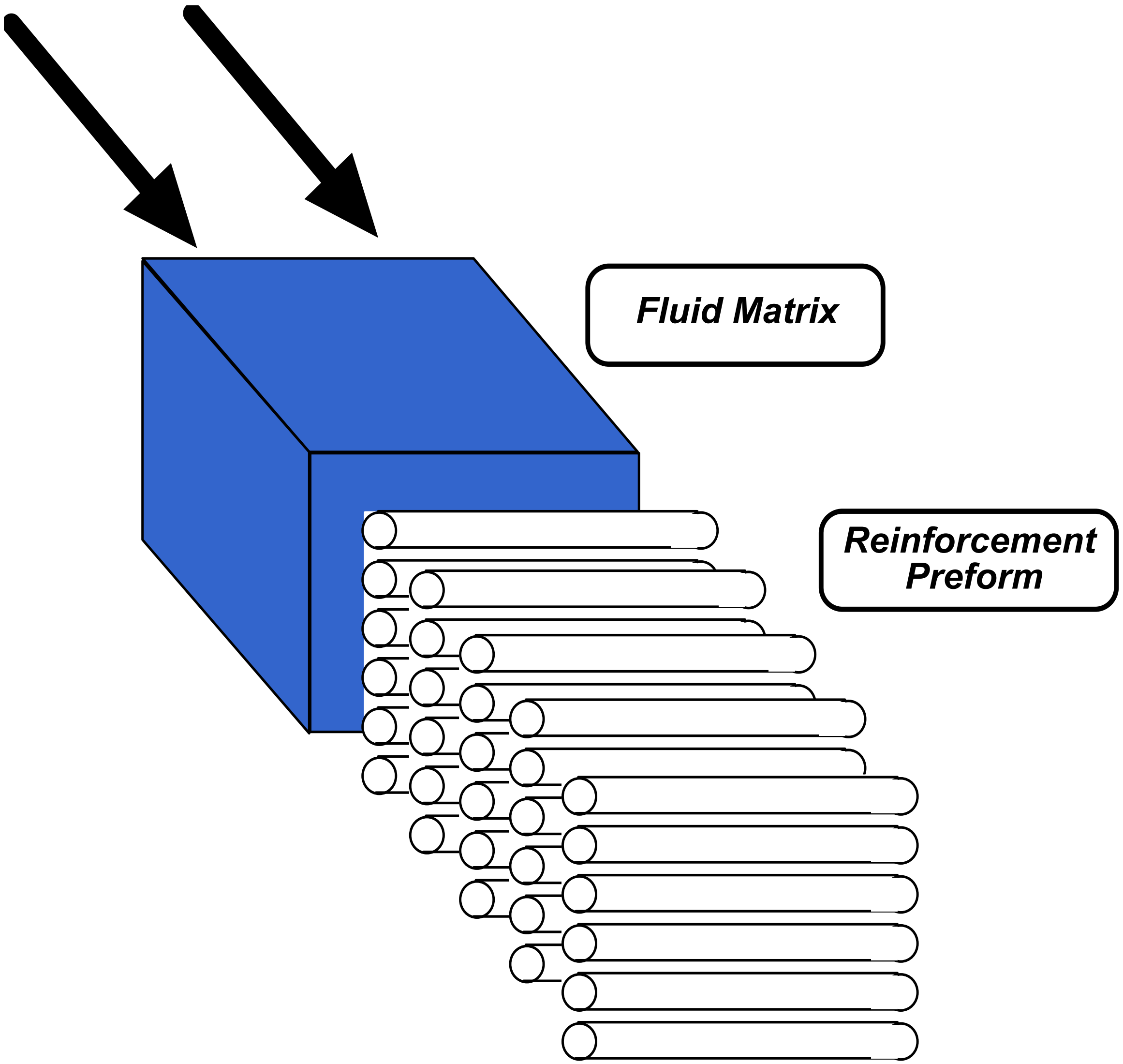

The Infiltration Process

General Characteristics for metals:

- high capillary forces

Material	Temperature (°C)	Surface Tension (N/m)
Polypropylene (PP)	180	0.0208
Polyethylene (PE)	180	0.0265
Polyethylene oxide (PEO)	180	0.0307
Nylon 6.6	270	0.0303
PE I	220	0.0357
PA 12	-	0.039
Epoxy, unreacted	-	0.03 to 0.04
Ethanol	20	0.022
Water	20	0.073
SiO_2	1800	0.31
Na_2SiO_3	1088	0.30
Al_2O_3	2050	0.63
$CaSiO_3$	1540	0.35
Al	700	0.87
Cu	1120	1.2
Ti	1670	1.53
Ag	970	0.92
Au	1070	1.13

The Infiltration Process

General Characteristics for metals:
- high capillary forces
- low viscosity

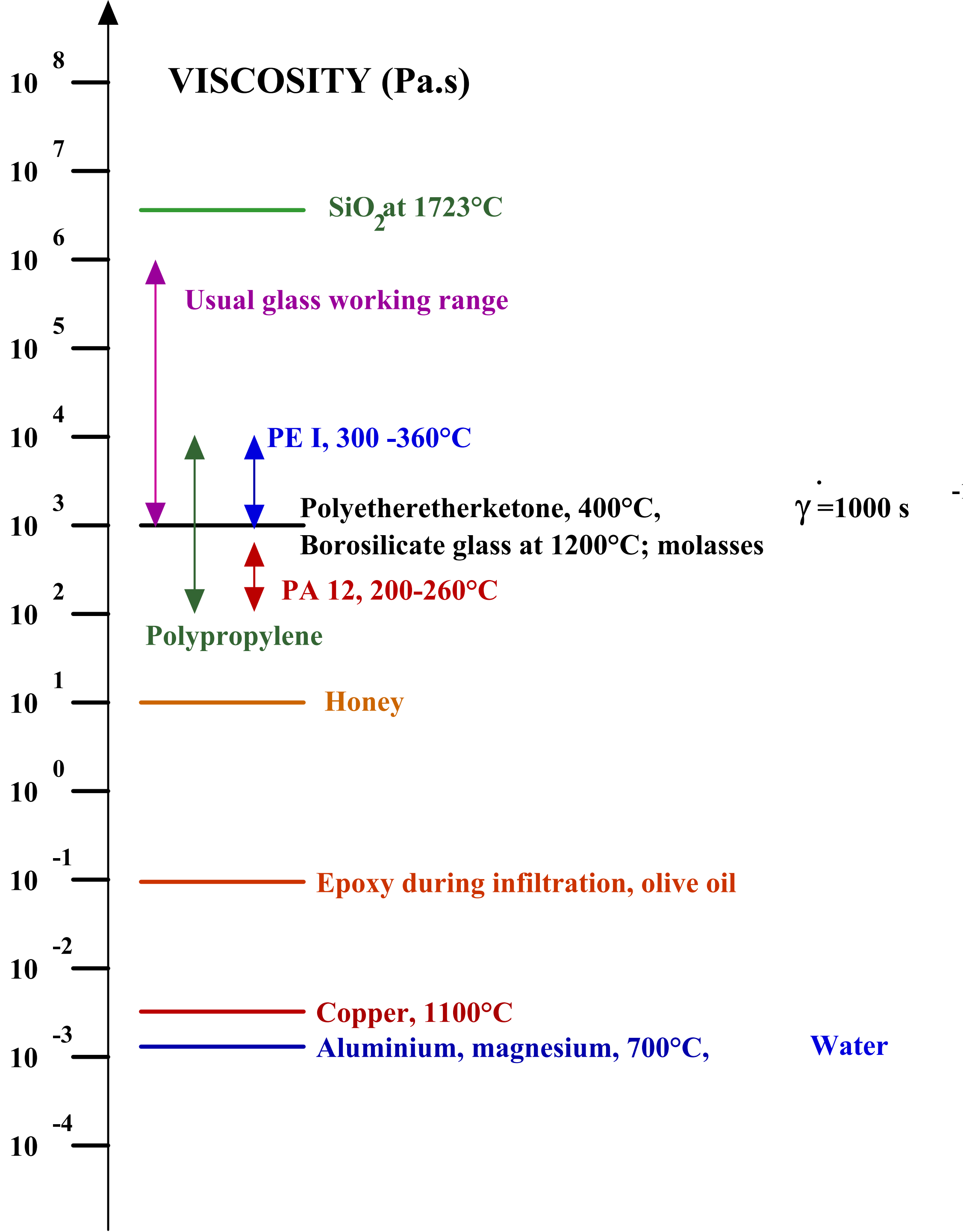

The Infiltration Process: Spontaneous Infiltration

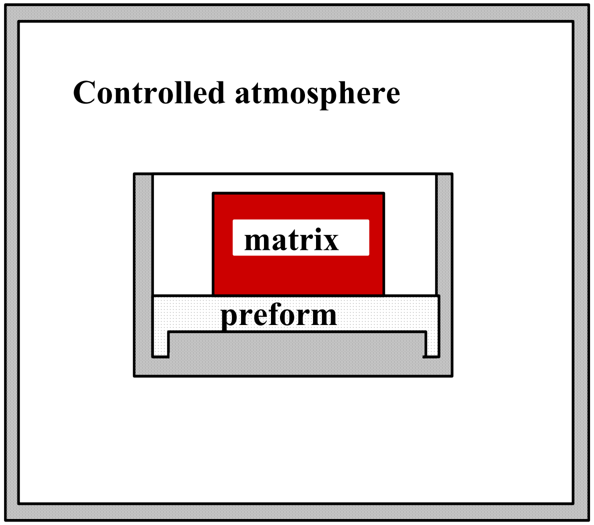

Place preform and metal in a furnace

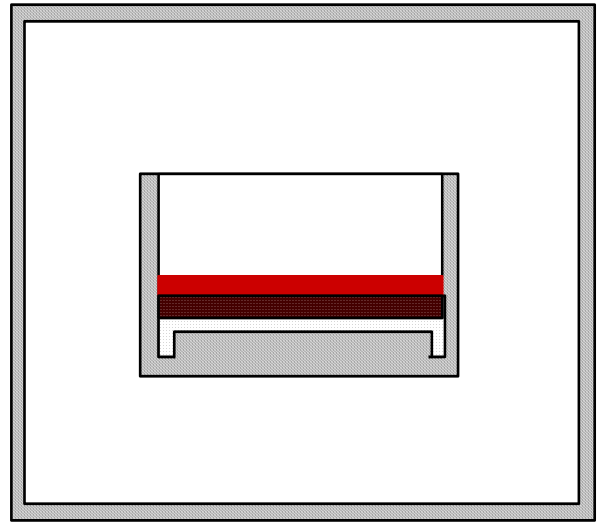

Infiltration proceeds

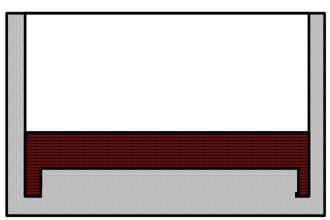

Composite is solidified

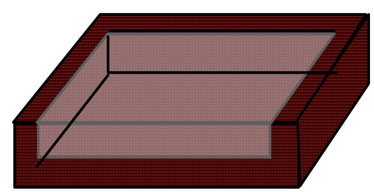

The infiltrated composite

The Infiltration Process: Squeeze Casting

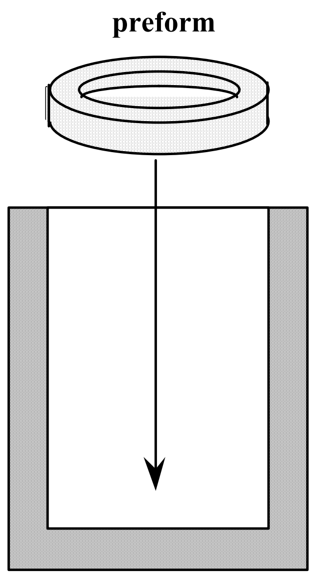

Preform preheating and placement

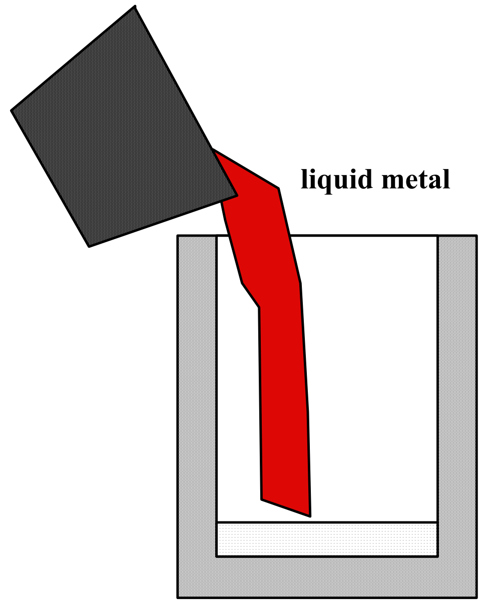

Metal pouring

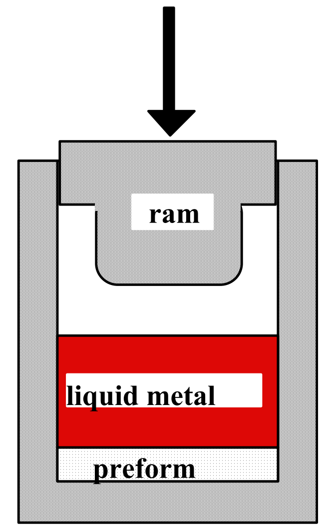

Ram movement initiation

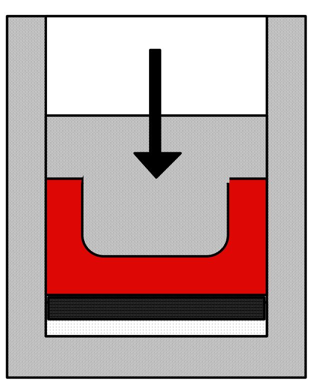

Infiltration

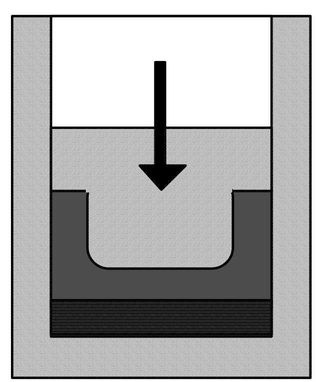

Solidification

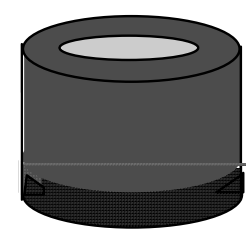

The infiltrated selectively reinforced cast composite component

The Infiltration Process: Pressure Infiltration

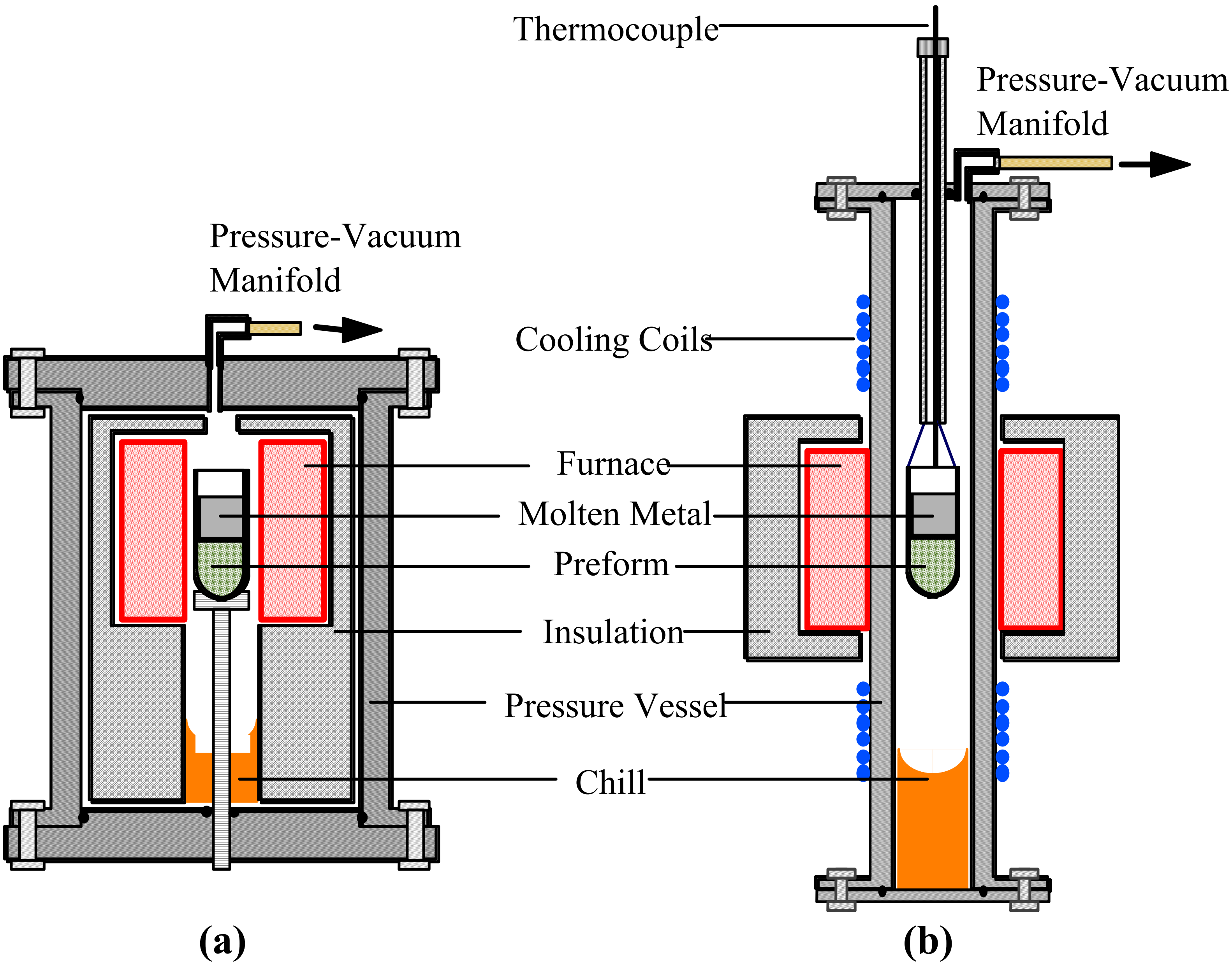

The infiltration Process

IN GENERAL

- Net-shape, rapid.

- Produces defect-free material if well engineered...

- ...with considerable flexibility in the material choice if pressure is used to drive the metal.

- Hence, well suited for the production of model multiphase materials.

50% ceramic

in

50% metal

A few good reasons to add ceramic to a metal or an alloy

A few good reasons to add ceramic to a metal or an alloy

- Increase wear and abrasion resistance;

- Increase the specific elastic modulus (E/ρ) above 26 $MJ \cdot kg^{-1}$;

- Tailor certain physical properties: thermal conductivity, coefficient of thermal expansion, …

- Increase the tensile strength (with ceramic fibers)

A few good reasons NOT to add ceramic to a metal or an alloy

- Lower ductility;
- Lower toughness;

(...frequently with consequences on strength.)

→ The volume fraction ceramic V_f is therefore generally kept below 25-30% in structural particle reinforced metals.

Why a high volume fraction ceramic might be desirable

Why a high volume fraction ceramic might be desirable

- The incremental benefit increases with the fraction ceramic;

Young's modulus of Al/Al_2O_{3p}

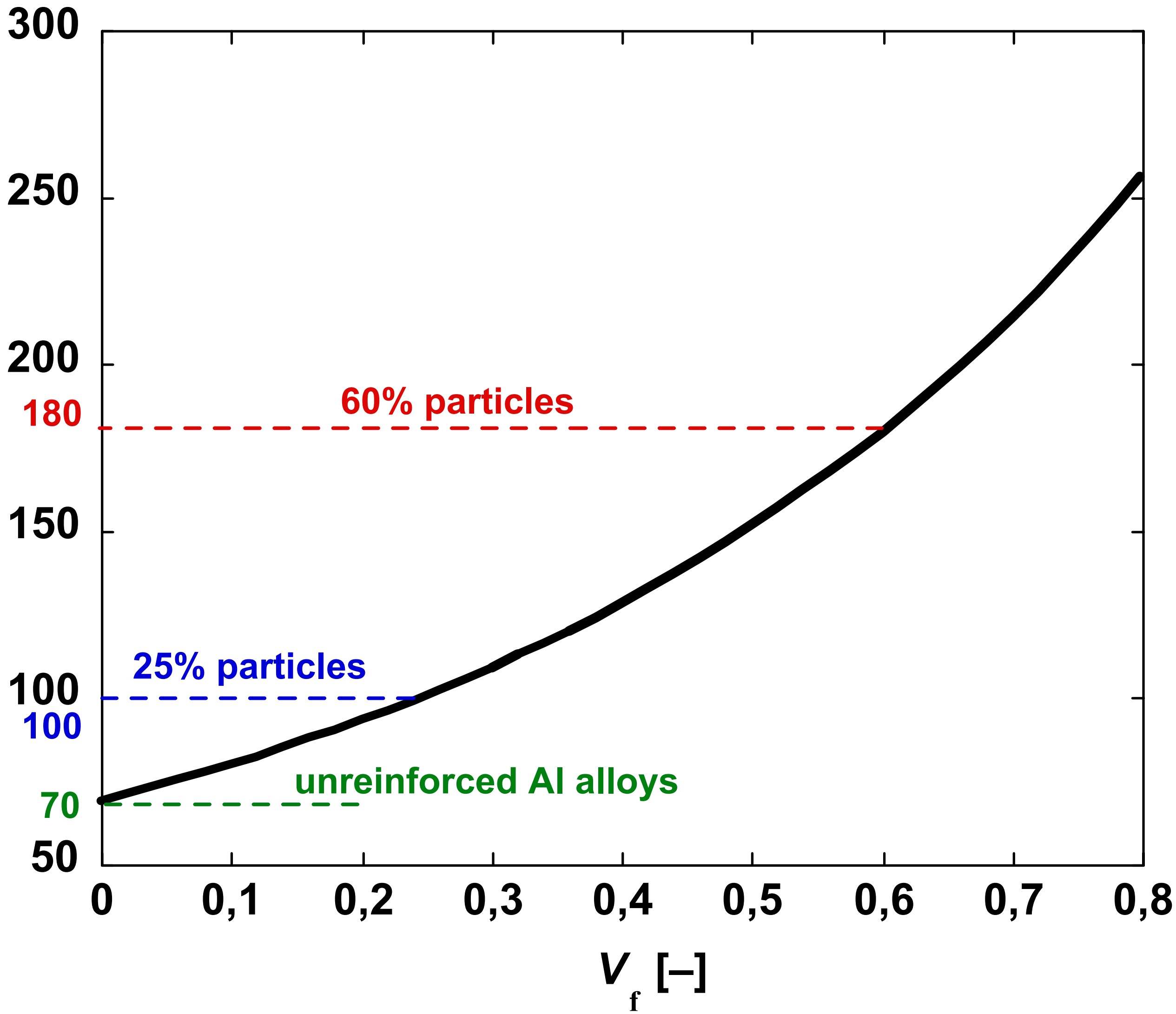

According to Christensen's 3-phase self-consistent model (E = 70 GPa and ν = 0.345 for Al, and E = 390 GPa and ν = 0.22 for Al_2O_3)

Why a high volume fraction ceramic might be desirable

- The incremental benefit increases with the fraction ceramic;

- Particle clustering.

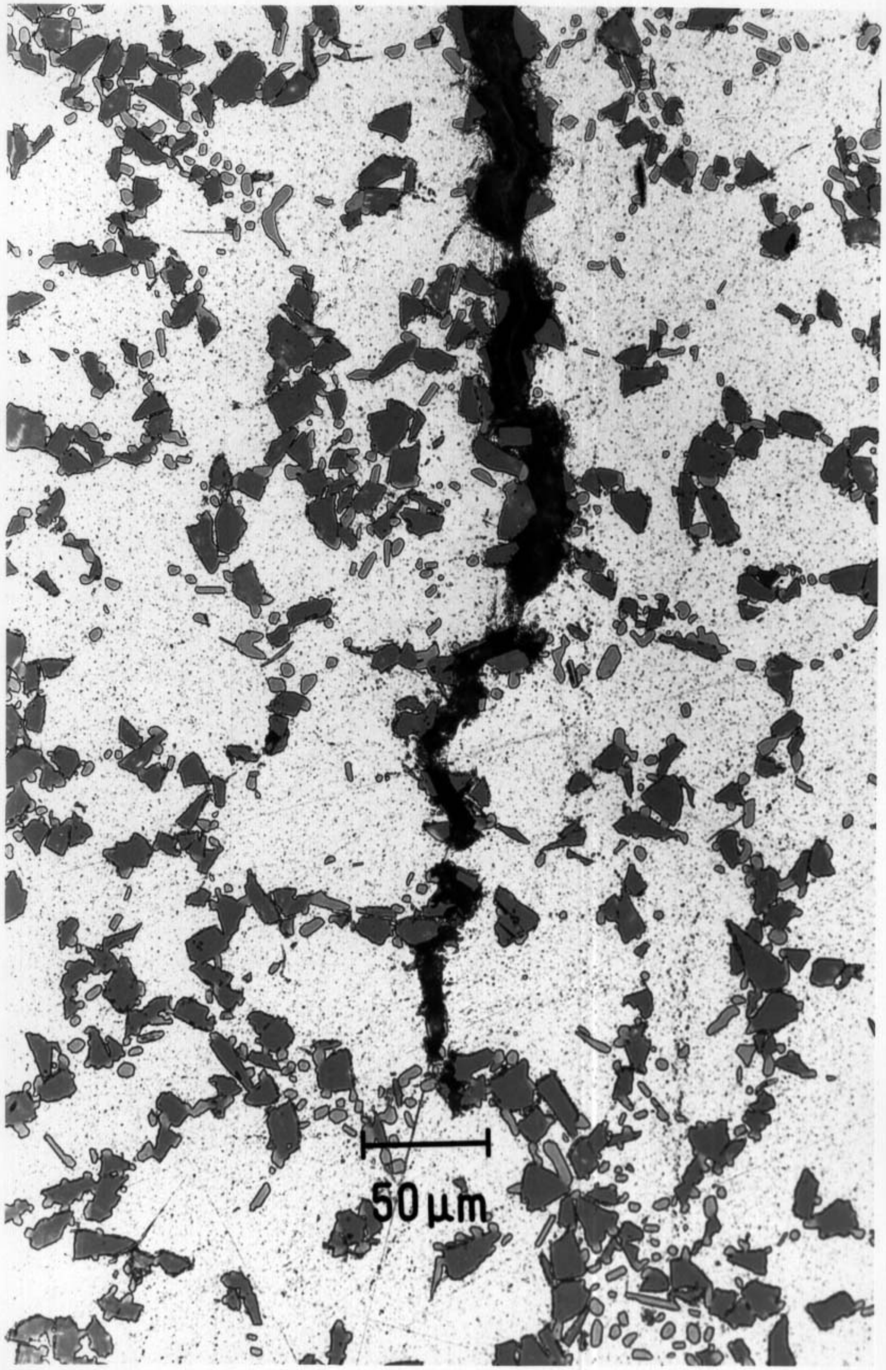

Influence of Particle Clustering:

...a somewhat extreme example, but a real one.

Gravity cast Al-356 / SiCp

Particle Reinforced Aluminium by Infiltration

Particle Reinforced Aluminium by Infiltration

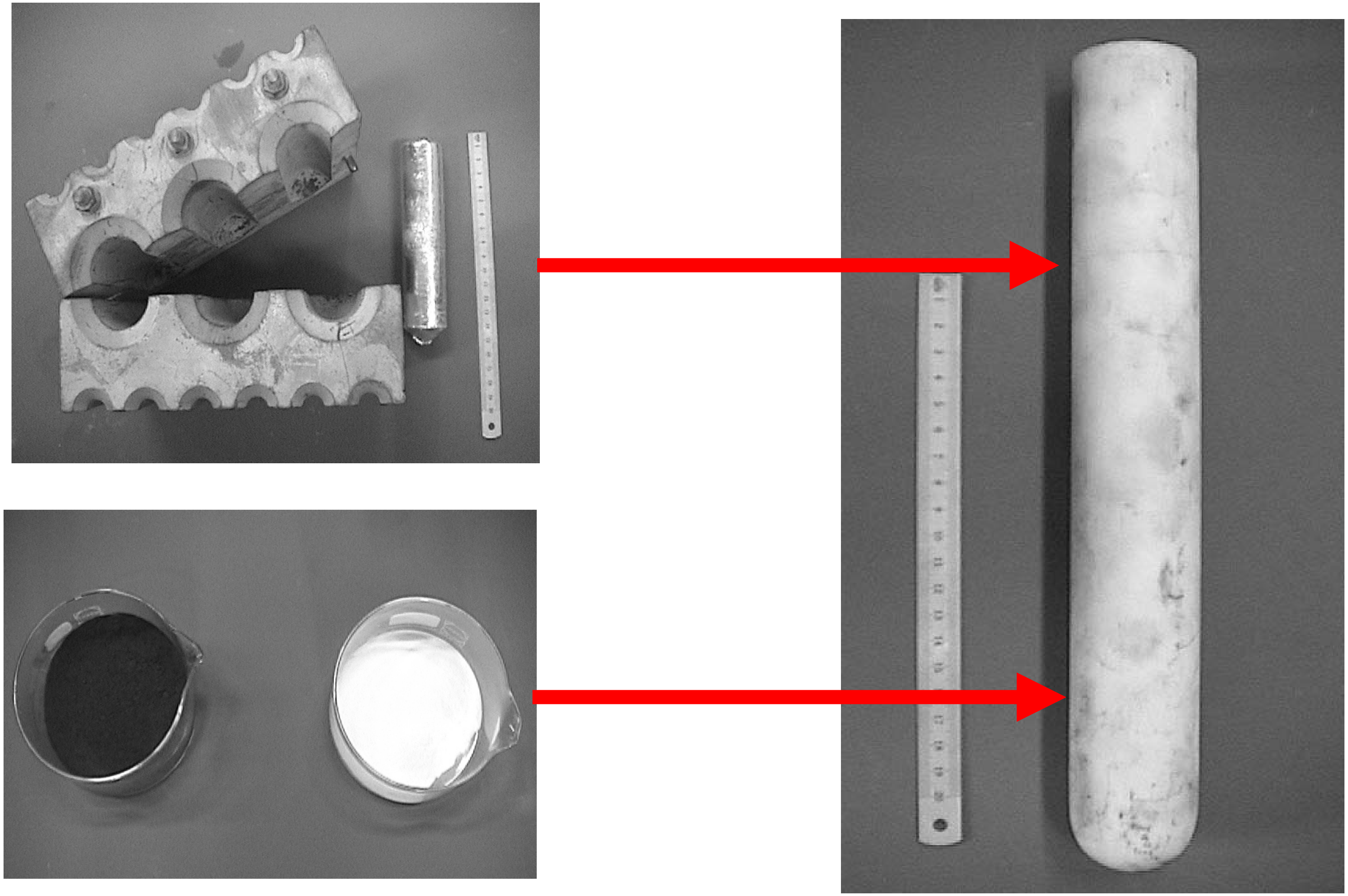

Ceramic particles and a cast metal ingot are packed, in that order, into an alumina crucible

Particle Reinforced Aluminium by Infiltration

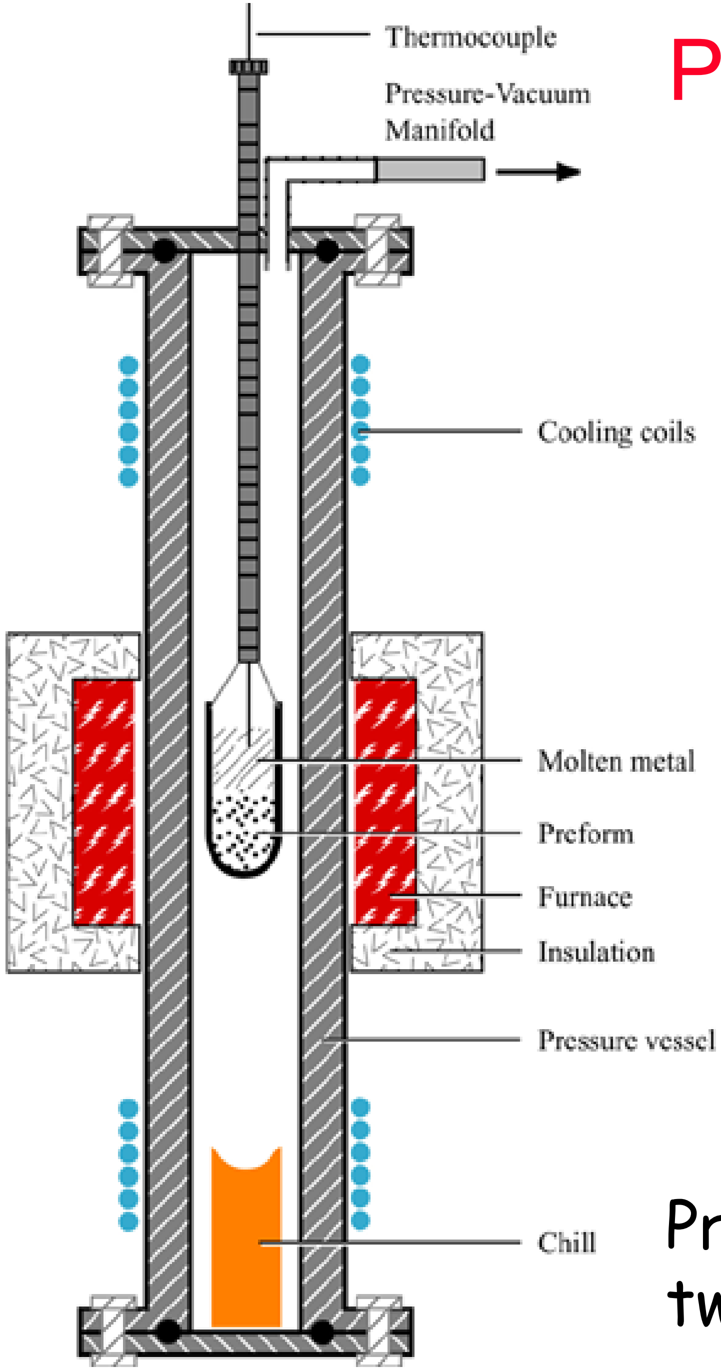

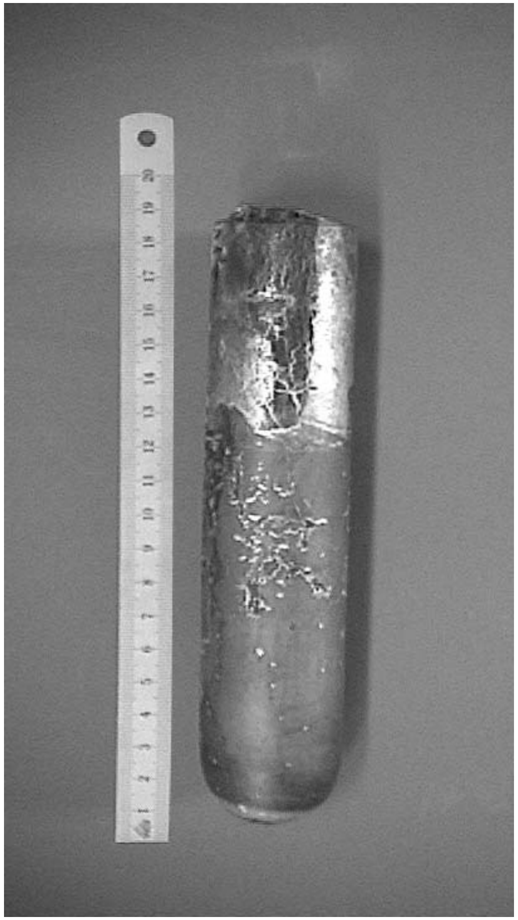

Pressure infiltration then combines the two into an ingot of composite

Three Matrices

- *99.99% pure Al*

- *Al-2wt.% Cu*
  (as-cast, T4 and T6)

- *Al-4.5wt.% Cu*
  (as-cast, T4 and T6)

Three Reinforcement Types

Angular Al_2O_3

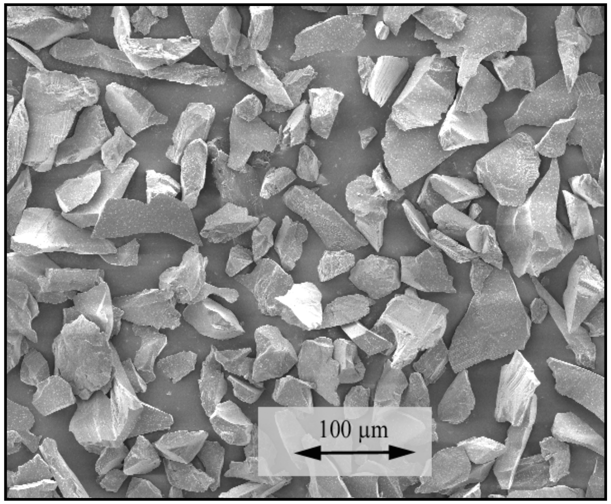

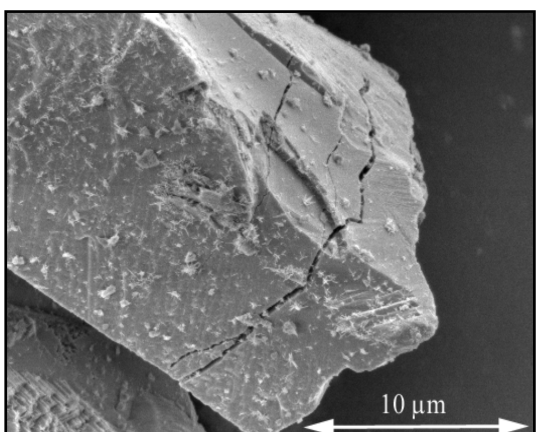

Polygonal Al_2O_3

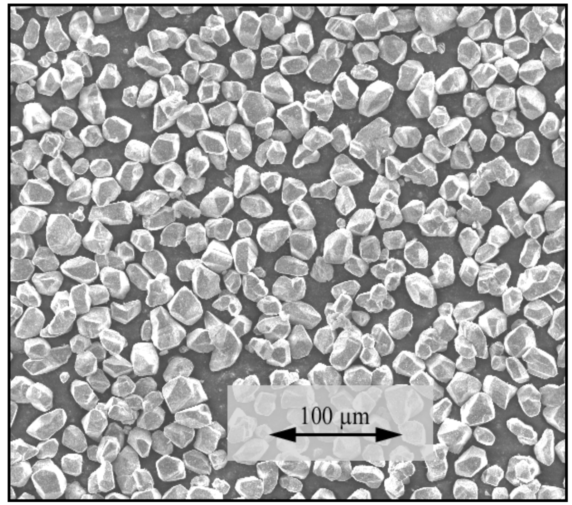

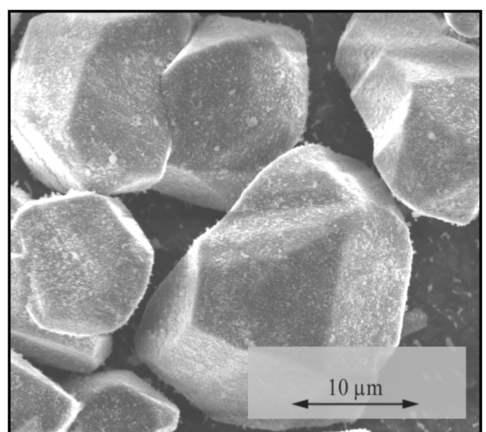

Angular B_4C

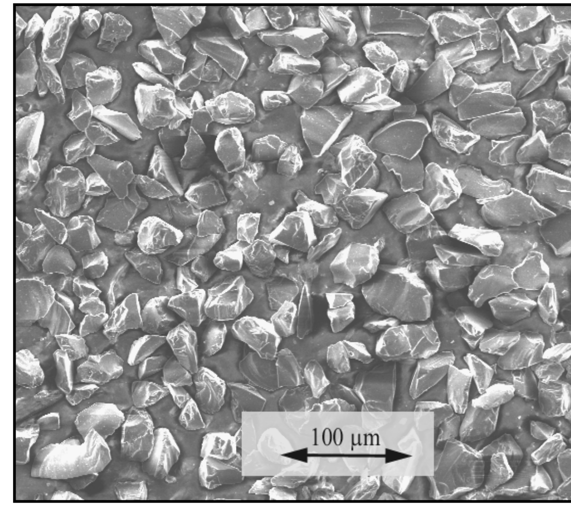

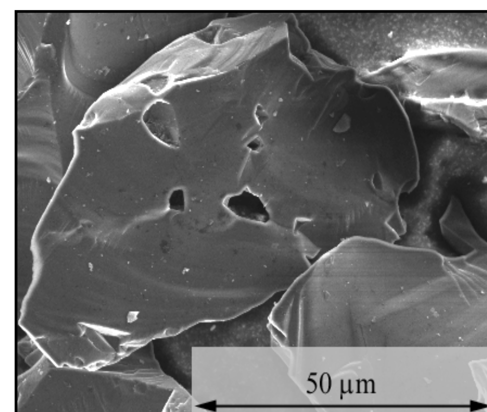

Infiltrated Particle Reinforced Aluminium

Angular Al_2O_3 | Polygonal Al_2O_3 | B_4C

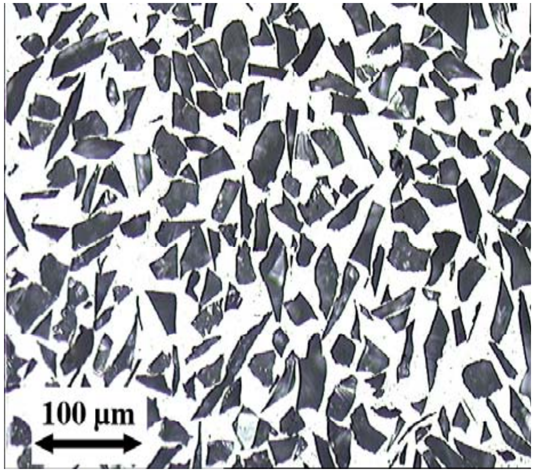

35 µm

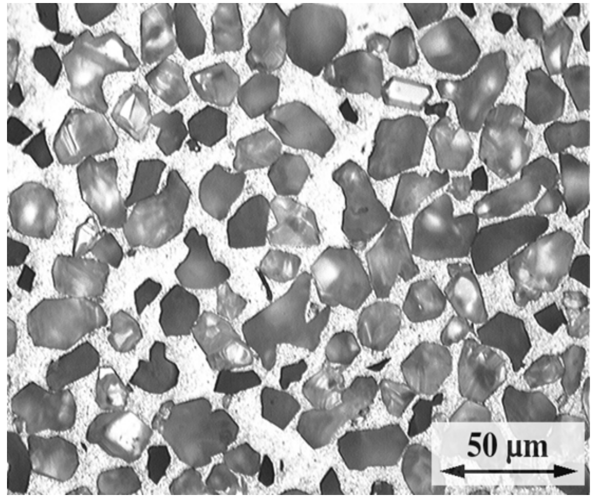

25 µm

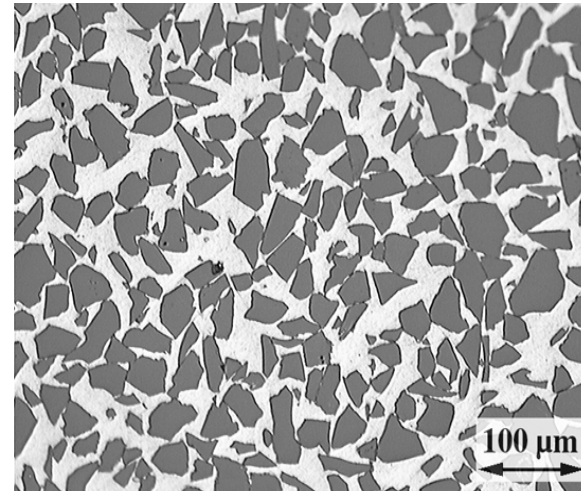

35 µm

5 µm

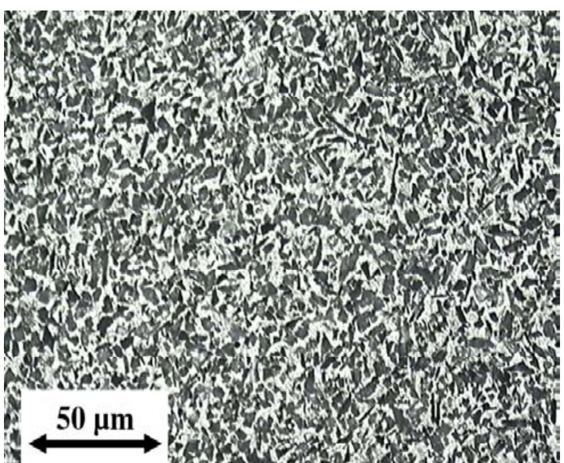

5 µm

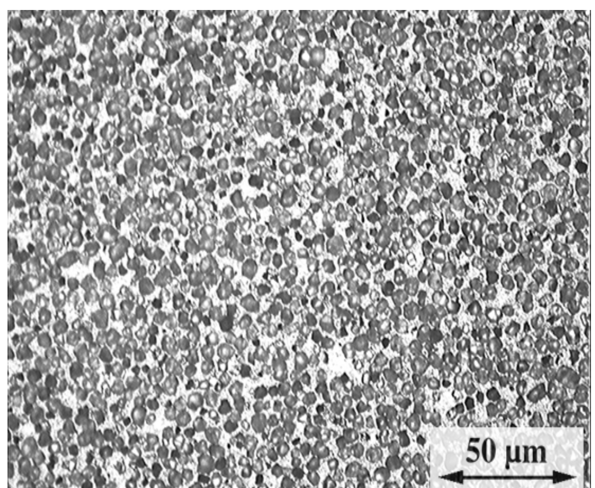

10 µm

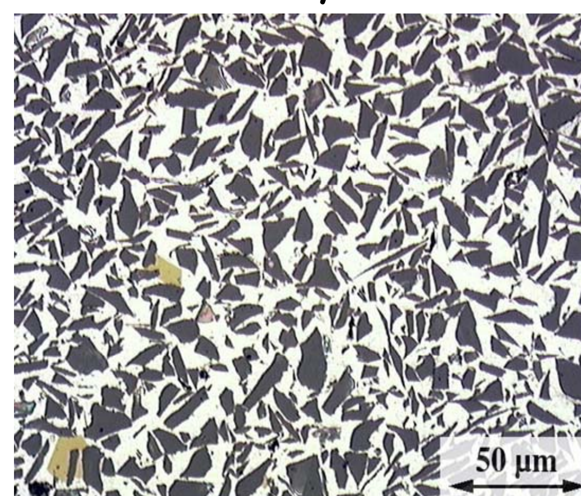

Tensile Behaviour

Tensile Behaviour

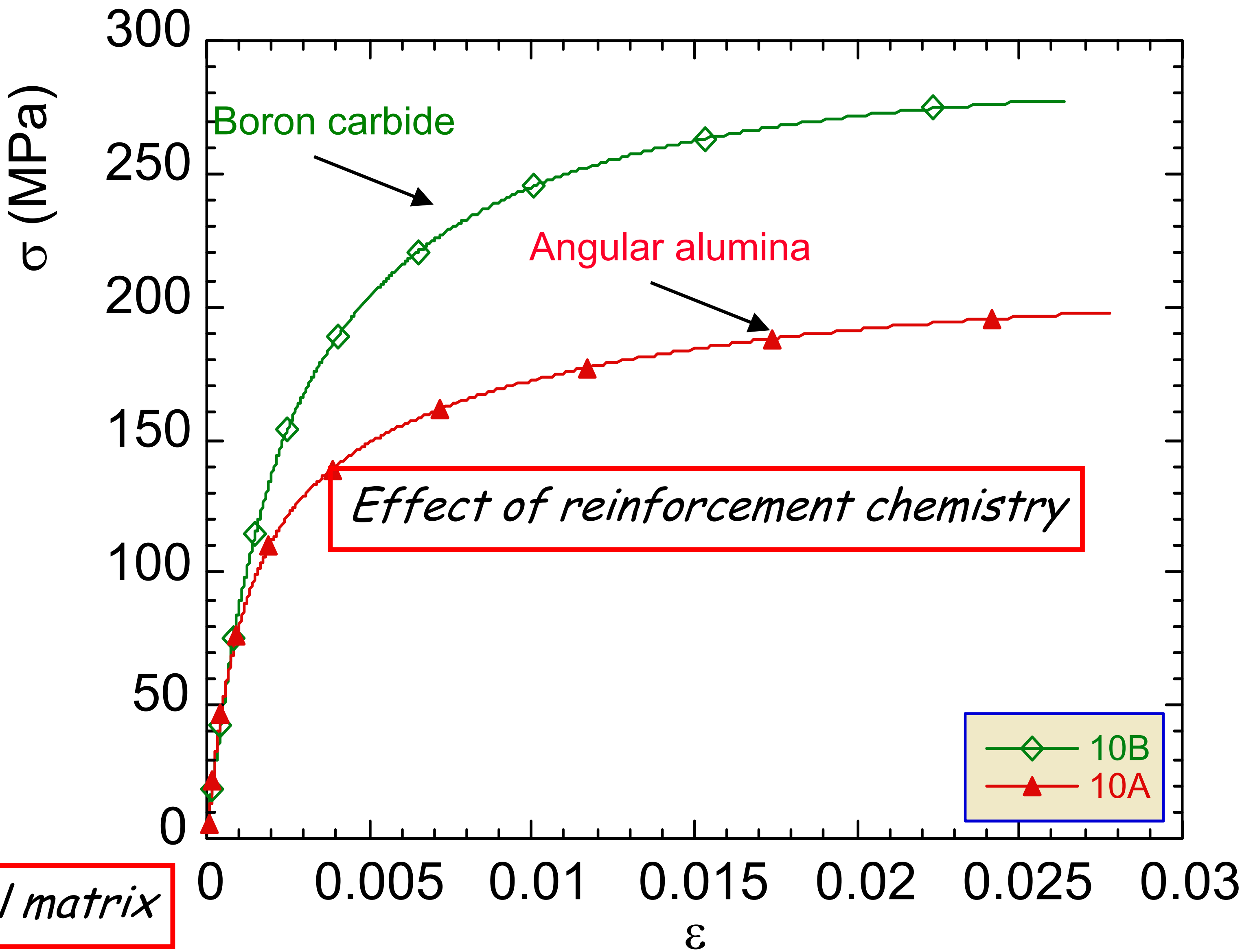

Pure Al matrix

Tensile Behaviour

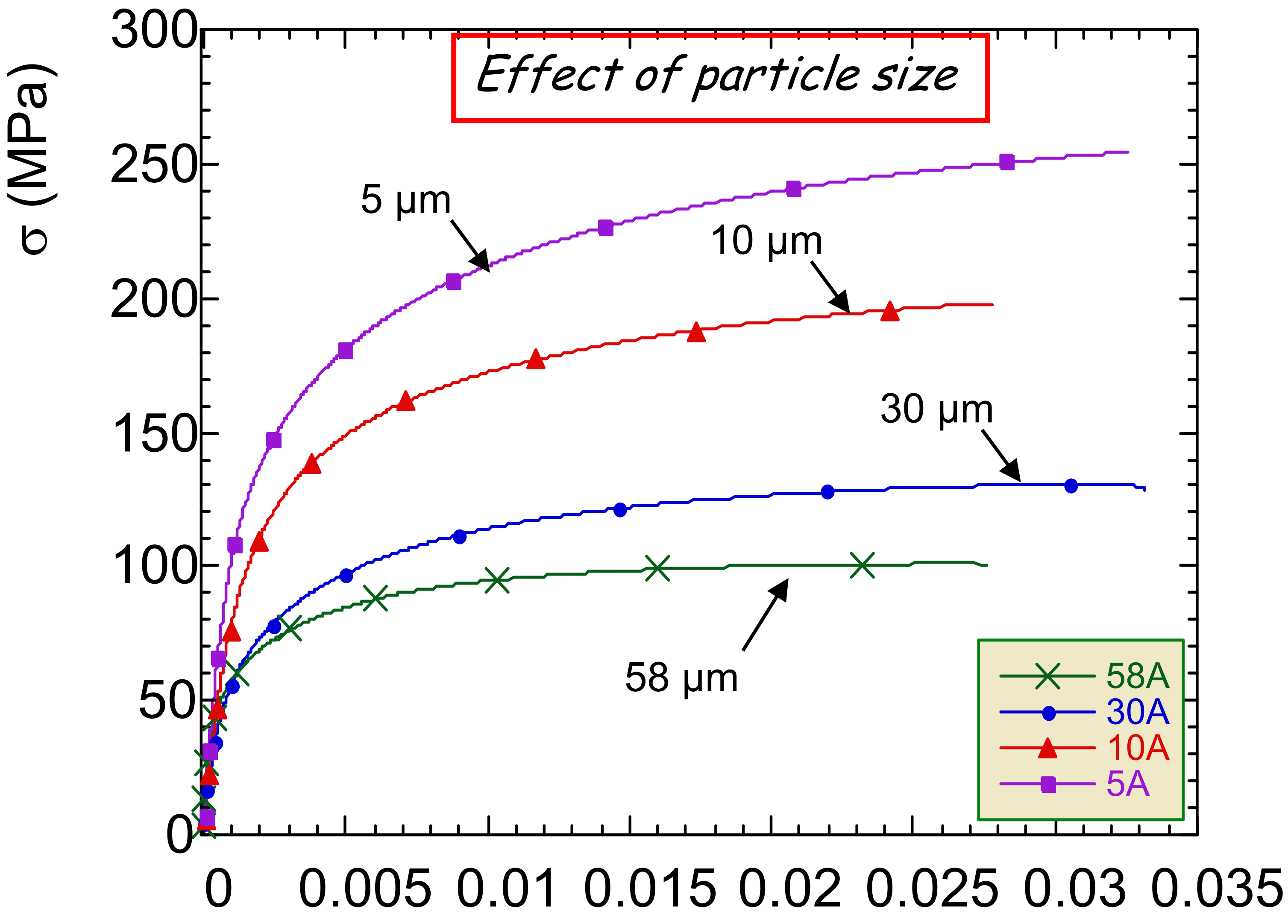

Pure Al/angular alumina)

The Size Effect

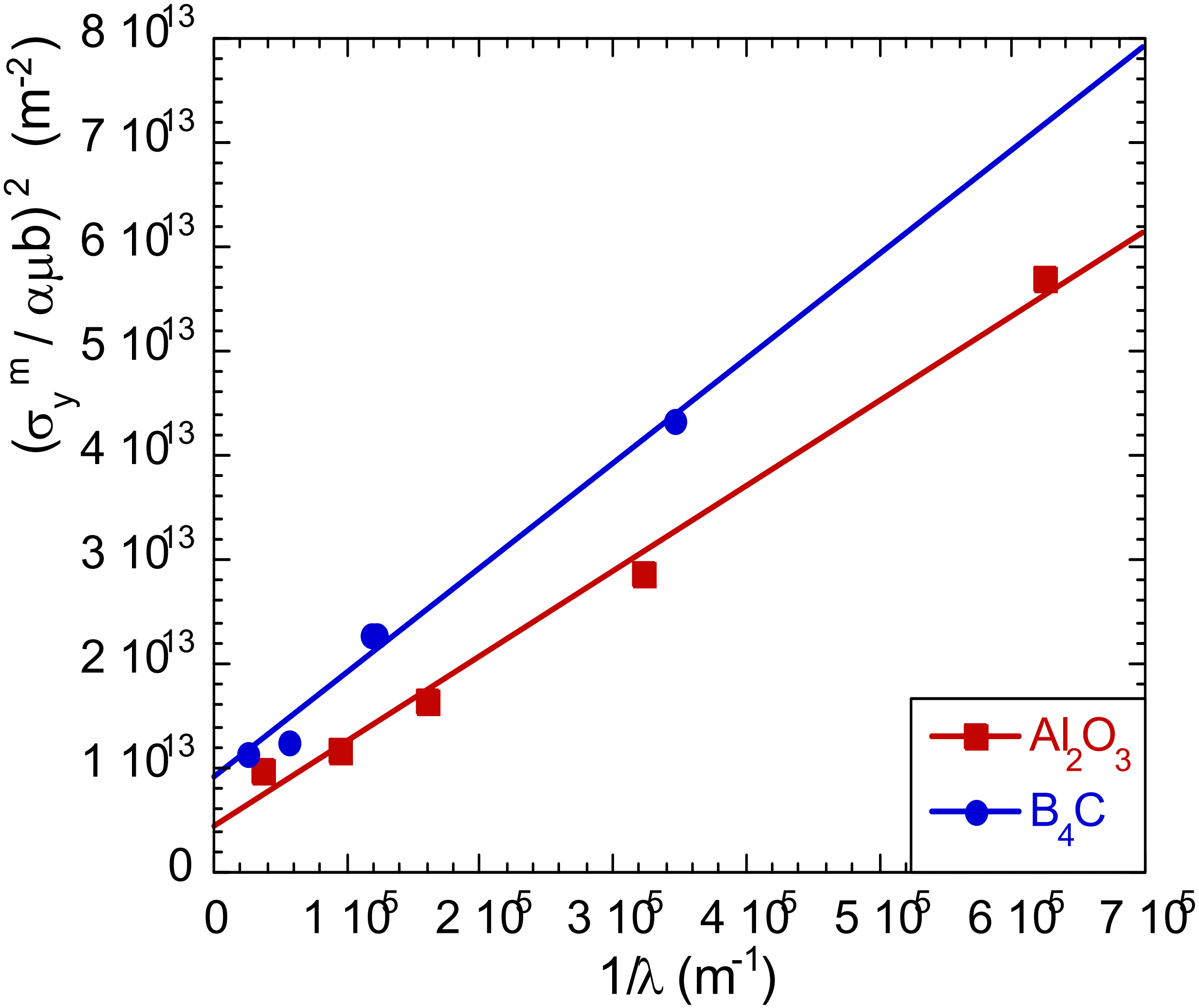

Comparing Al_2O_3 with B_4C:
- *ΔCTE* is 1.3 times higher for B_4C;
- the experimental slope is 1.25 times higher.

Tensile Behaviour

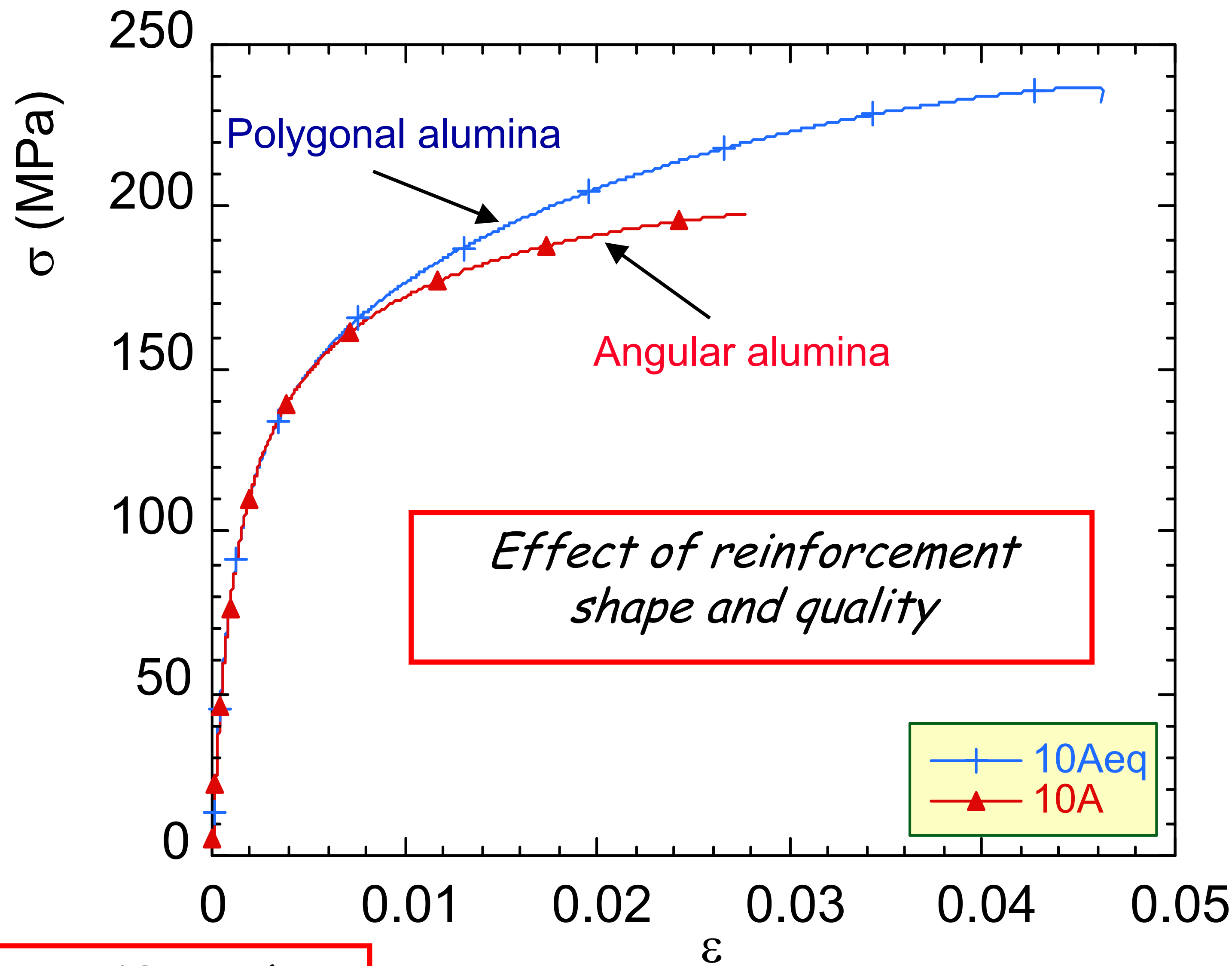

Pure Al matrix; 10µm Al_2O_3

Tensile behaviour

Illustrating the influence of particle type

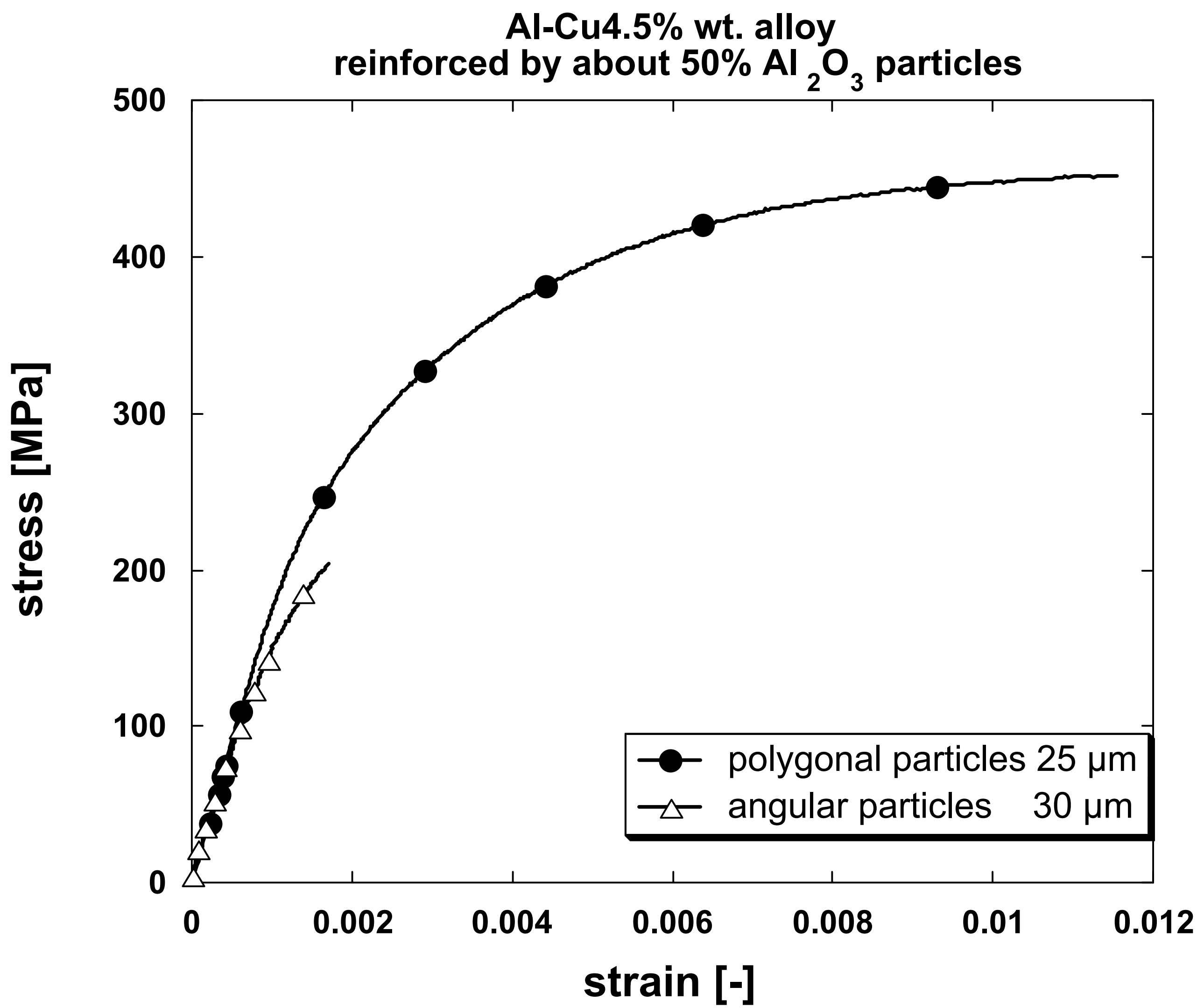

Damage

Damage

1 - Particle fracture followed by void nucleation in the matrix at particle cracks

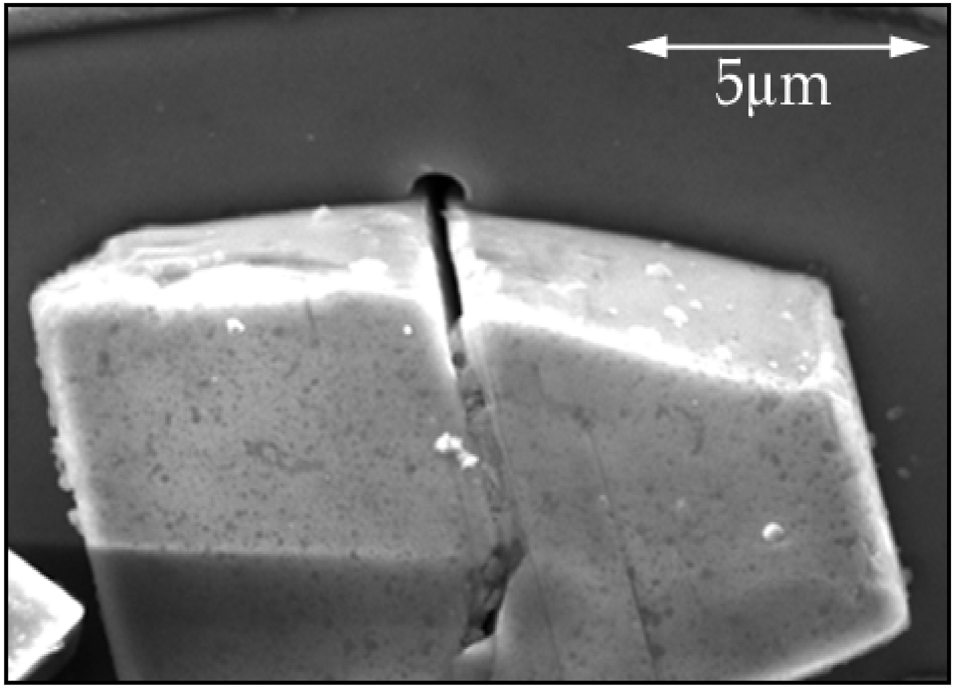

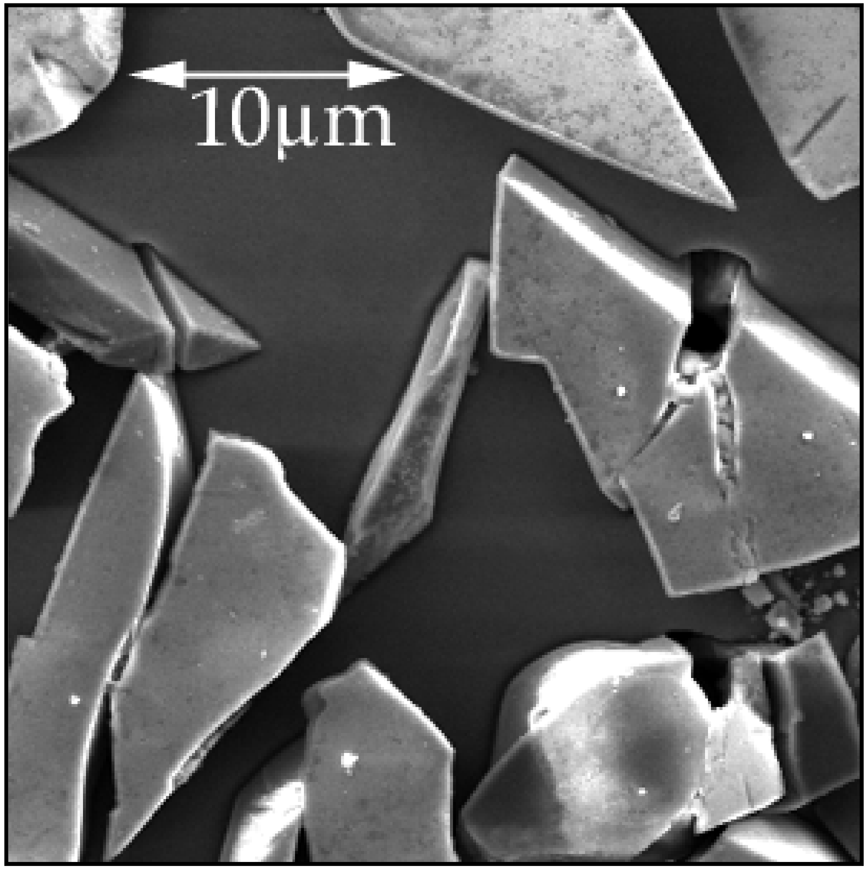

Al_2O_3 (angular) - Al

↔ σ

Damage

2 - Matrix voiding at sites of high stress triaxiality

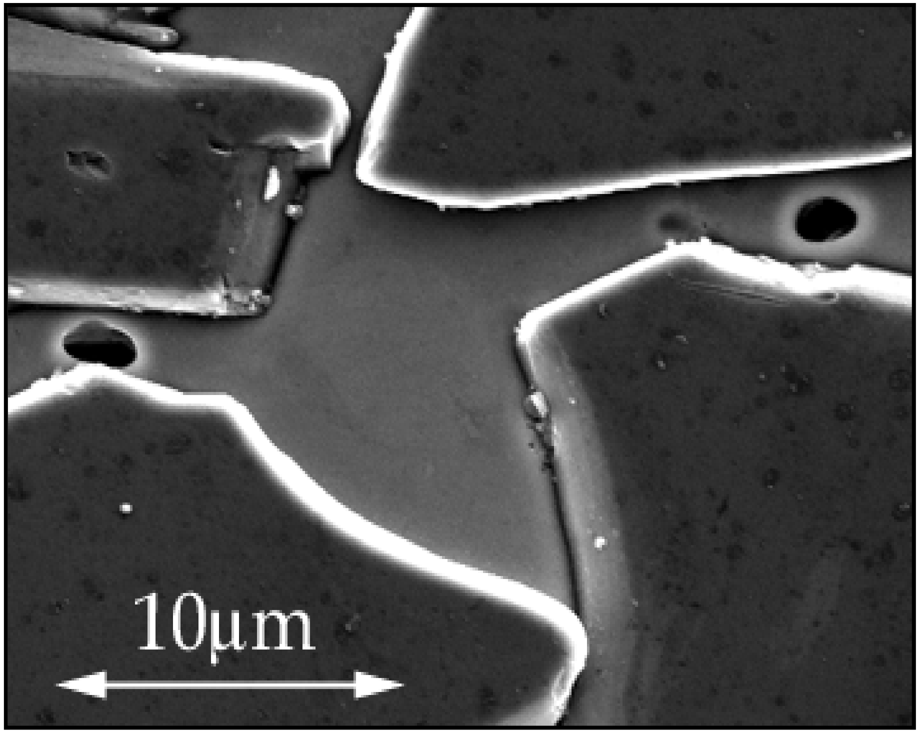

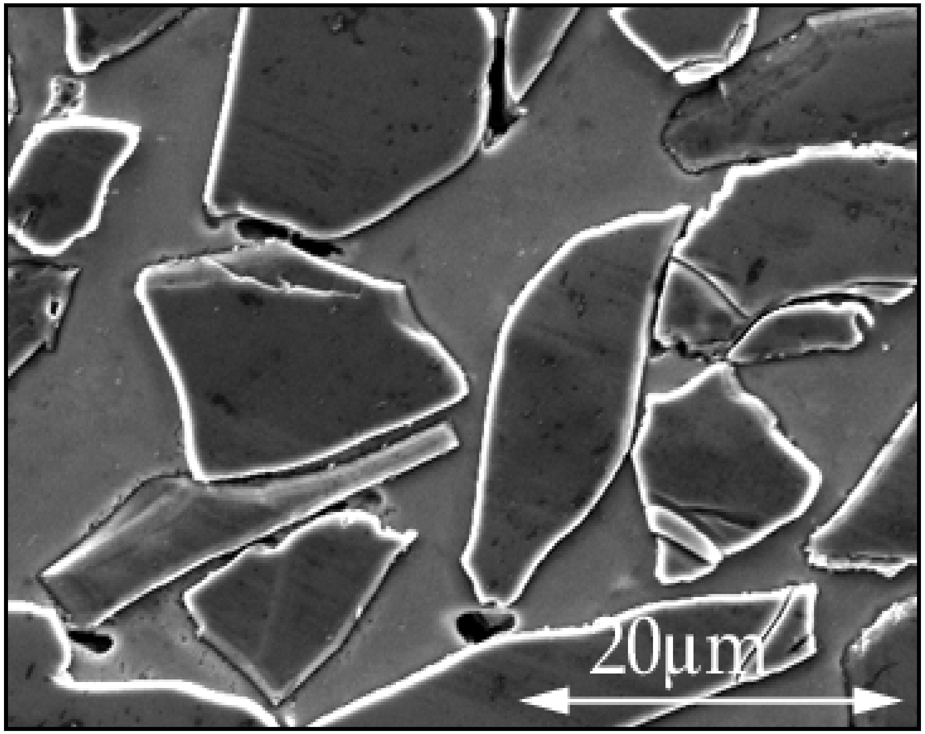

B_4C-Al

σ

Damage

Measurement:

- Young 's modulus evolution with strain
- Derived damage parameter: $D_E = 1 - E/E_0$

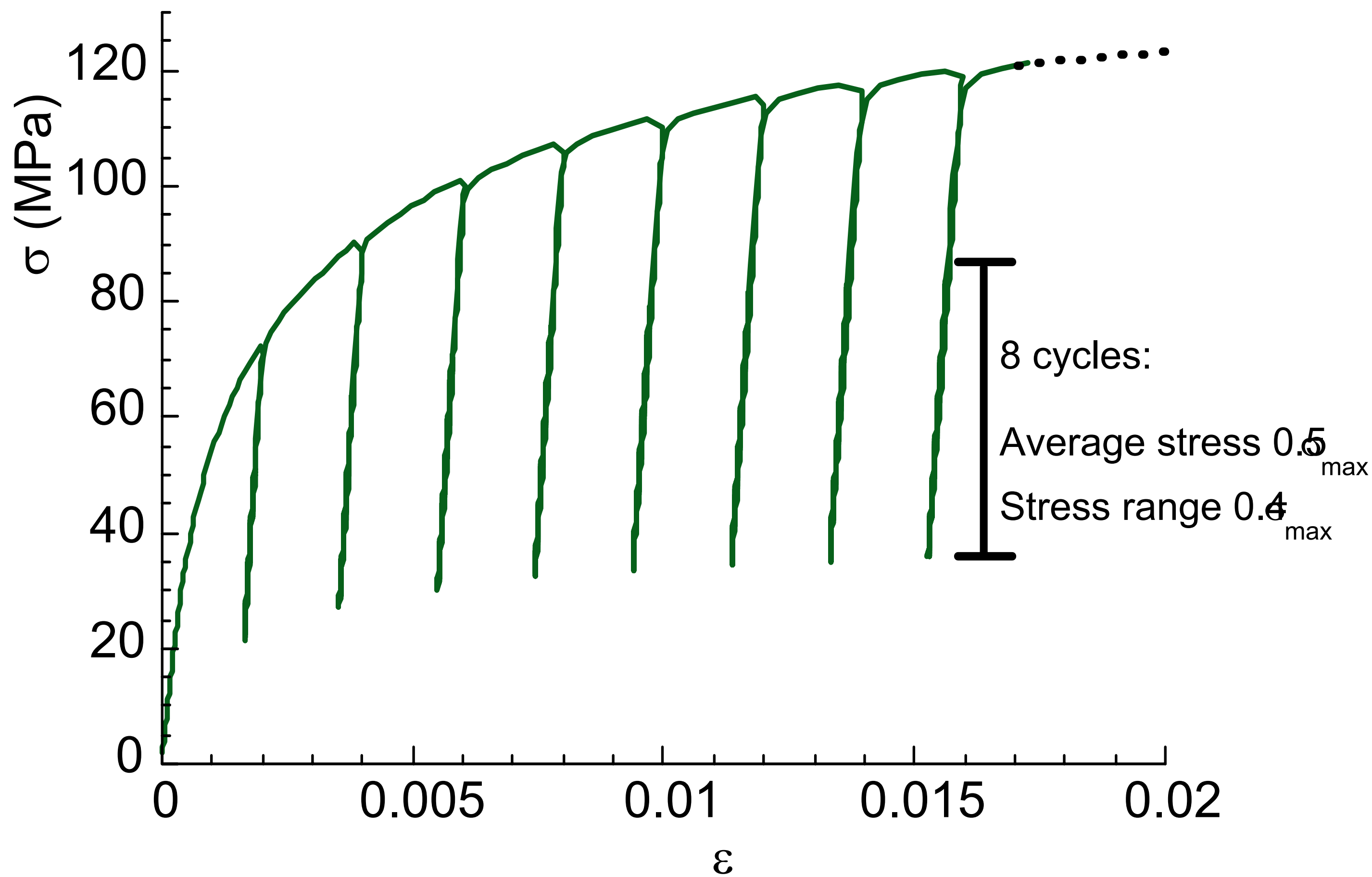

Damage

Measuring the rate of damage accumulation

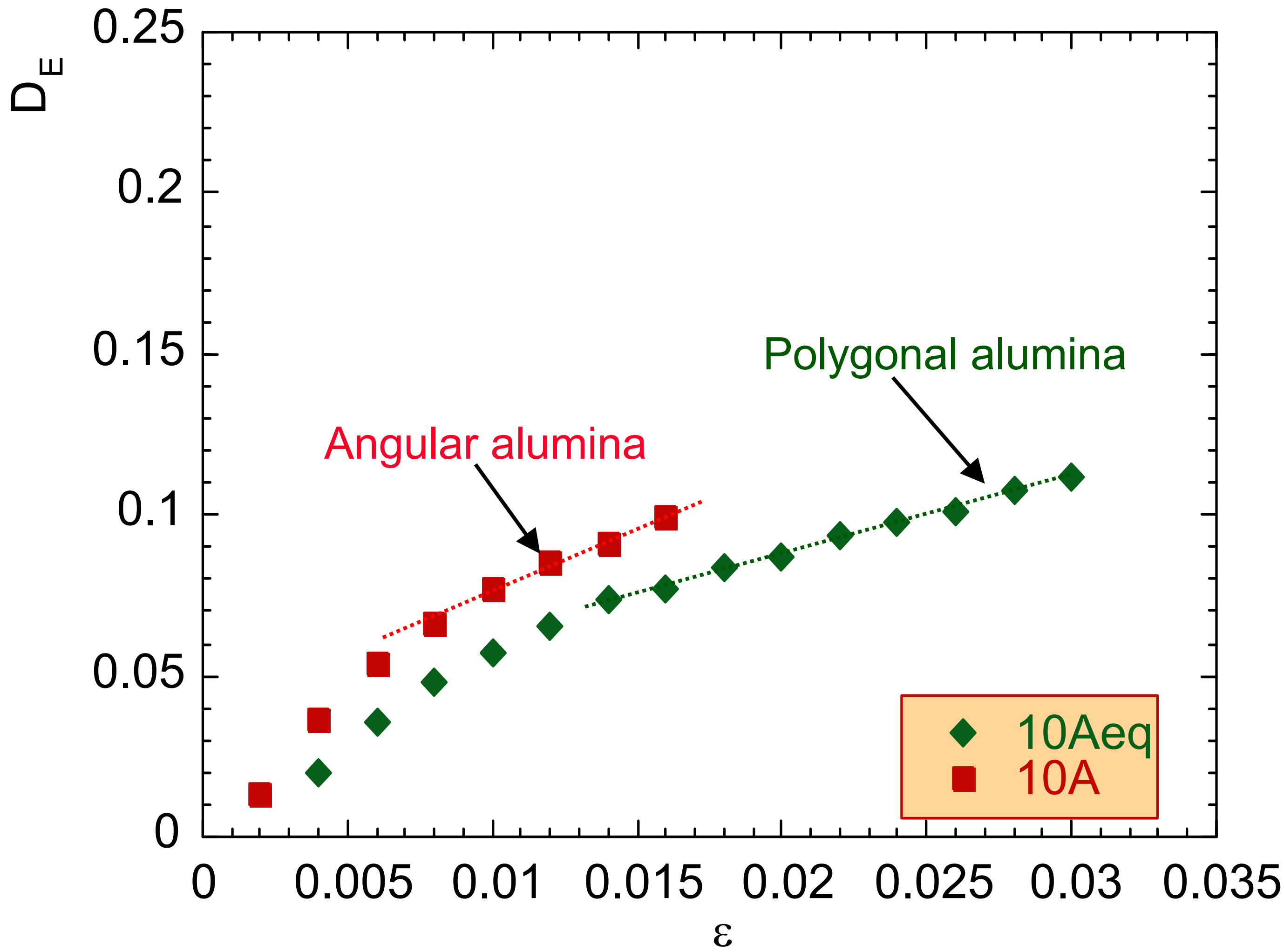

Link between Damage and Tensile Ductility

$$\varepsilon_f = \frac{n}{1 - \dfrac{d\ln\left(D_E\right)}{d\varepsilon}}$$

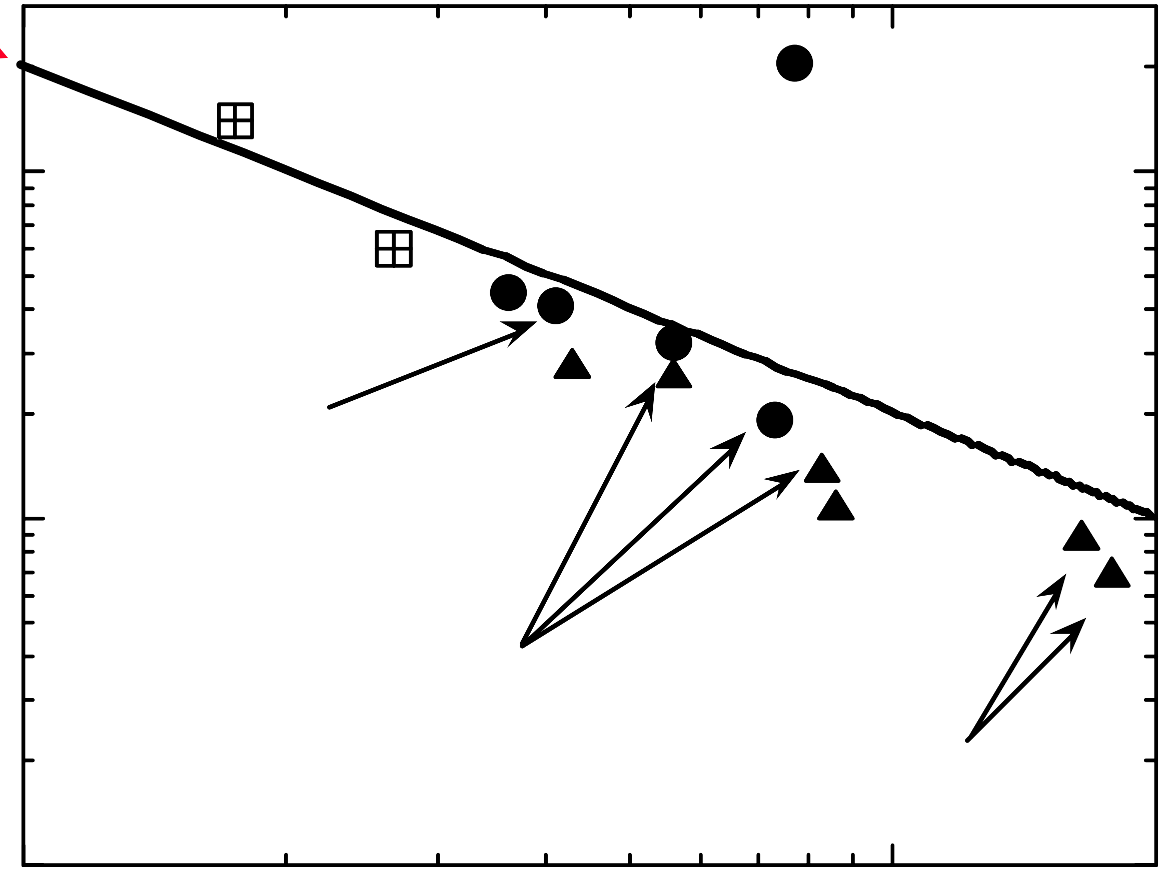

Fracture Toughness

Toughness

- J_R method for pure Al composites using precracked CT specimens (ASTM E-1737);
- Unloading compliance method used to monitor crack growth

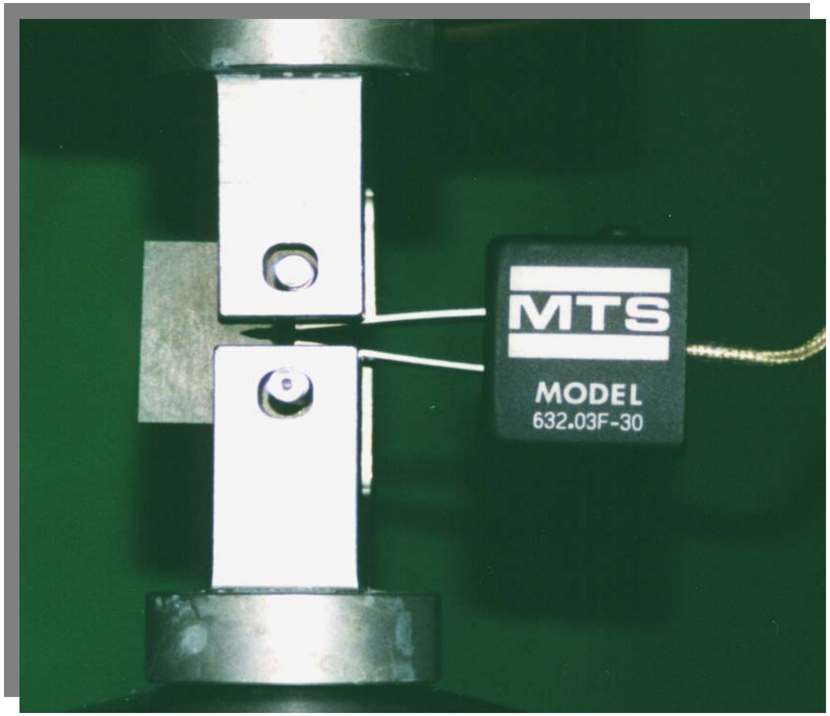

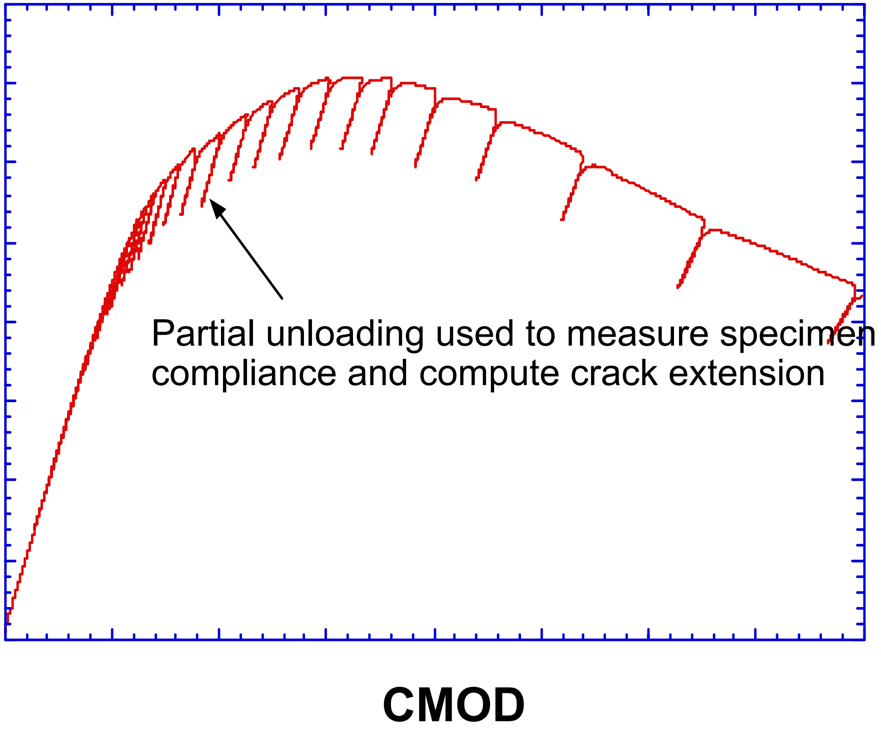

Toughness

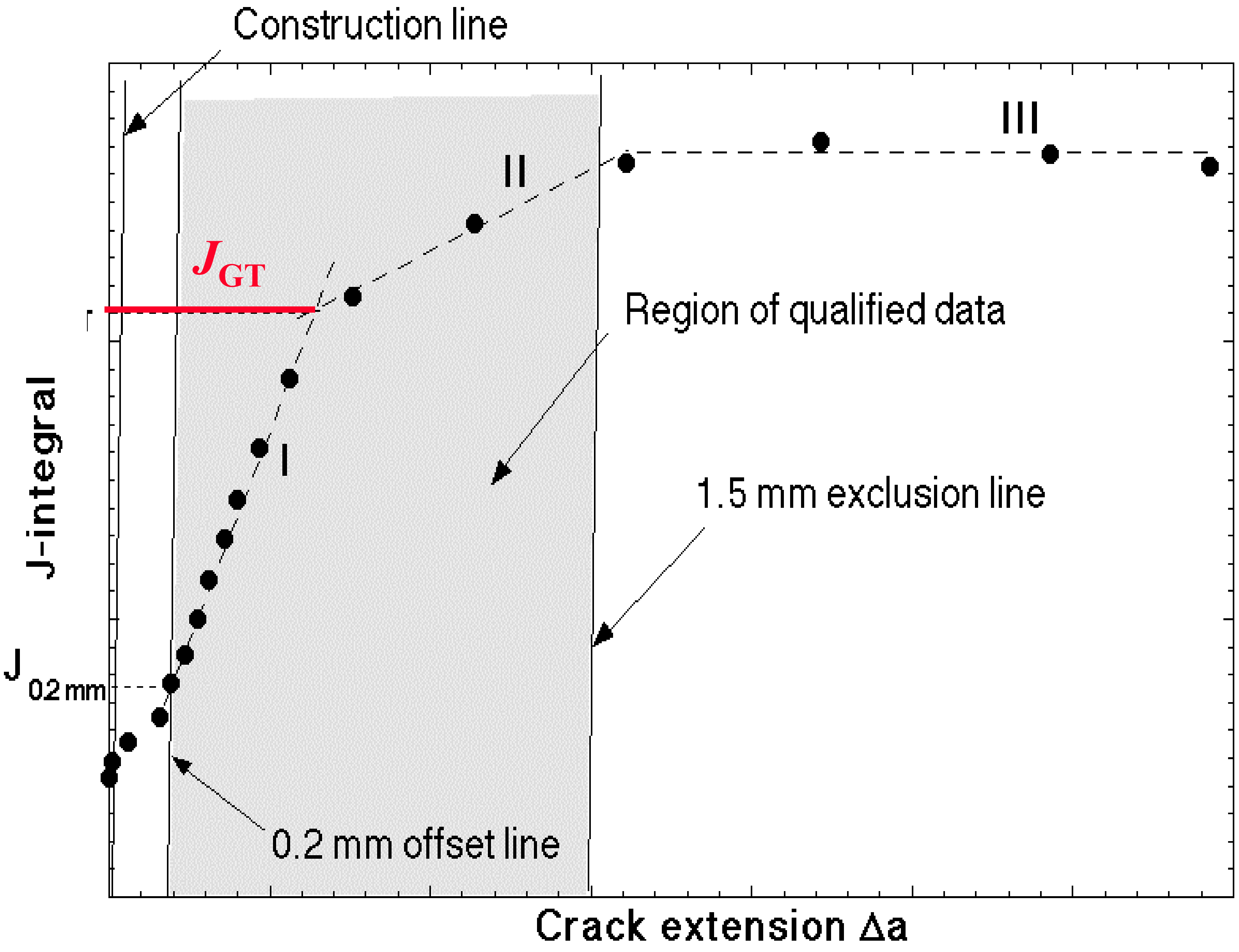
Construction line
III
II
J_{GT}
Region of qualified data
I
1.5 mm exclusion line
J-integral
$J_{02\,mm}$
0.2 mm offset line
Crack extension Δa

Toughness

J_{GT} corresponds to the onset of marked crack advance

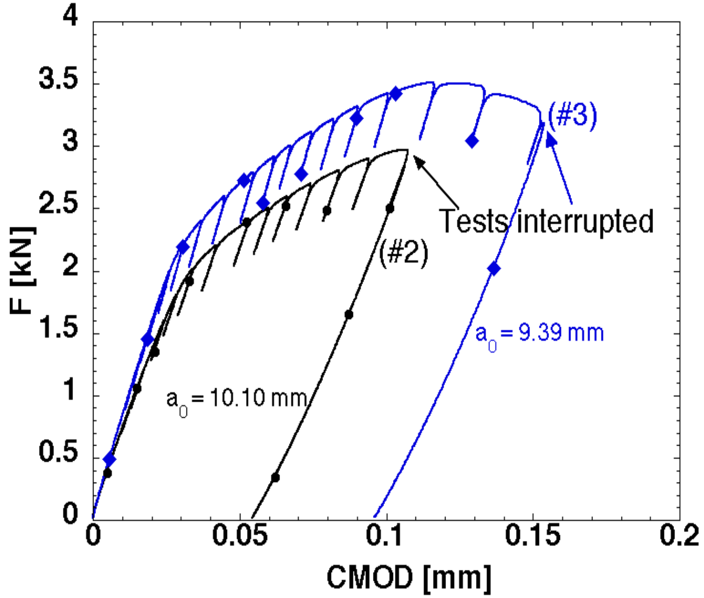

(pure Al/25 μm Al_2O_3 polyg. composites)

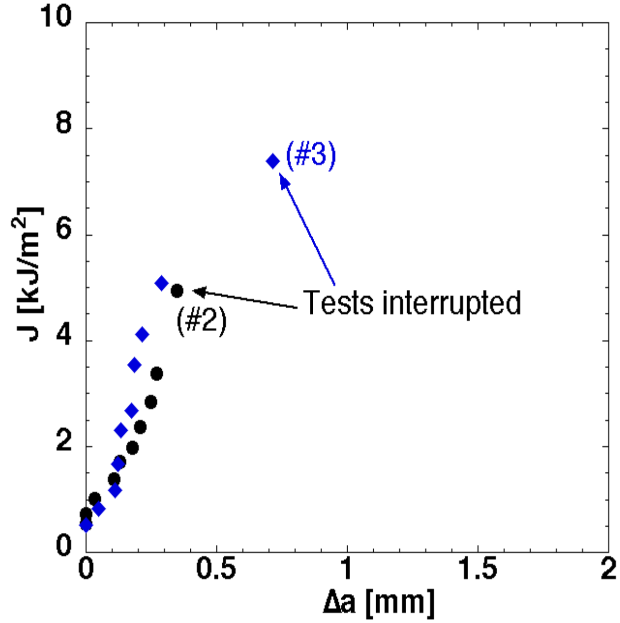

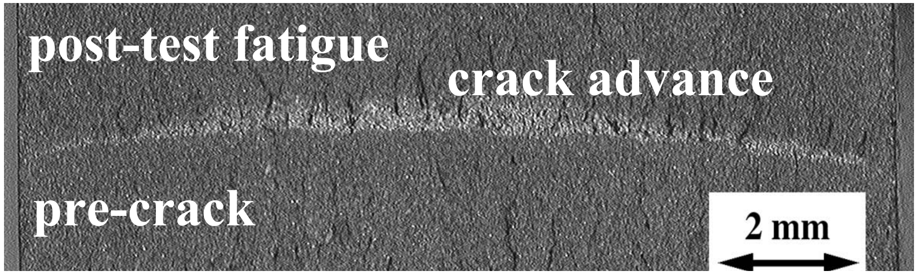

Crack front marked by fatigue, specimen #2

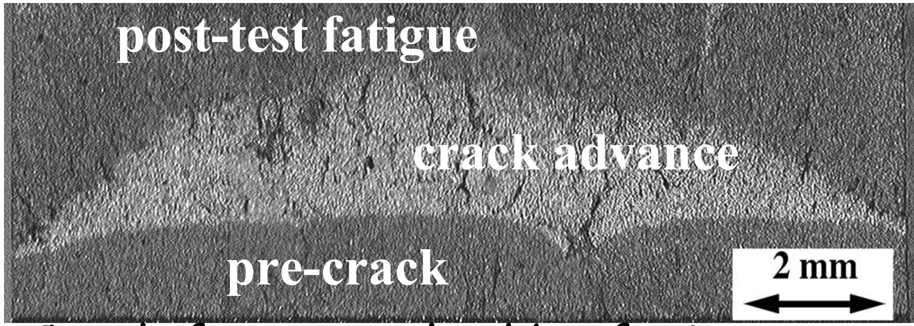

Crack front marked by fatigue, specimen #3

Toughness

Polygonal Al_2O_3 particles/pure Al: influence of particle size

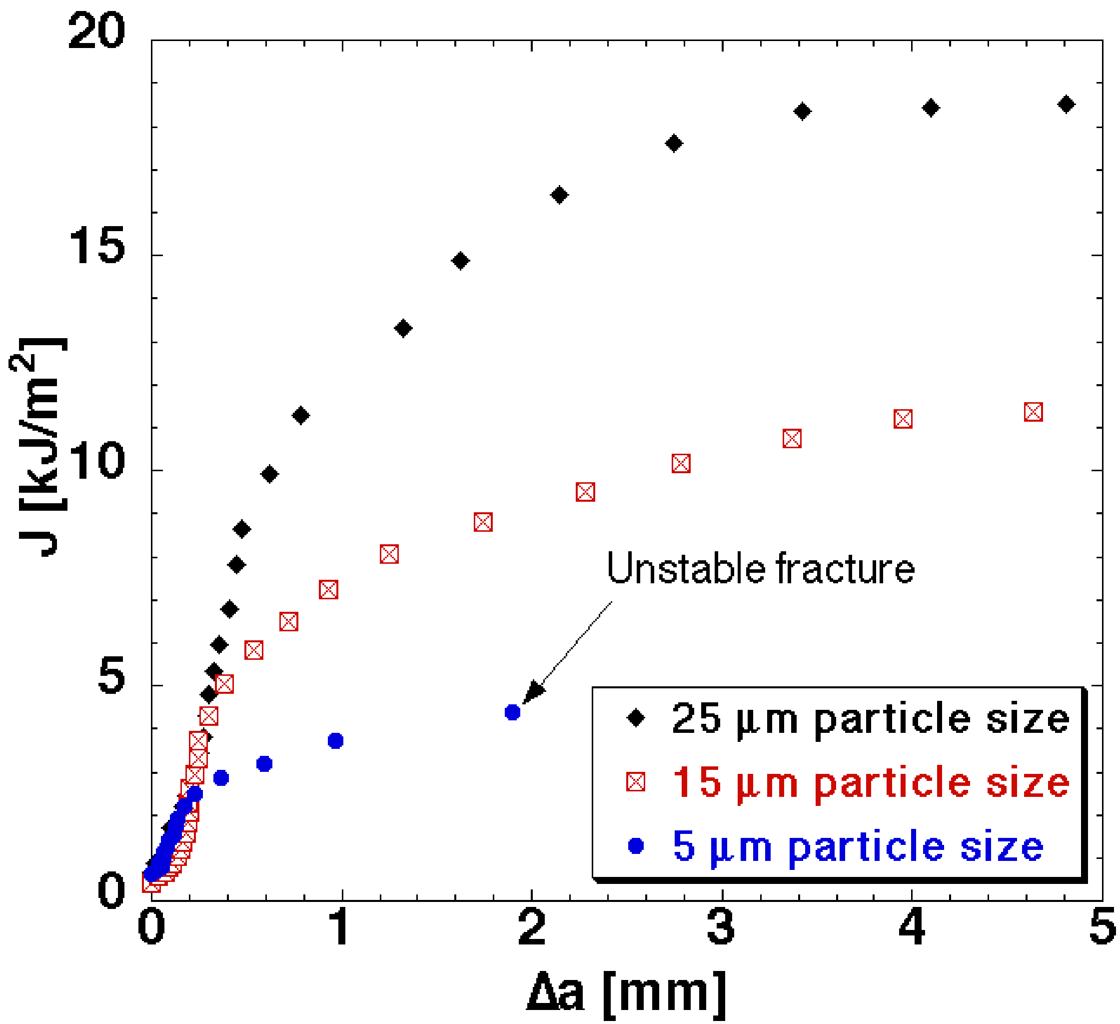

Toughness

B$_4$C particles/pure Al: influence of particle size

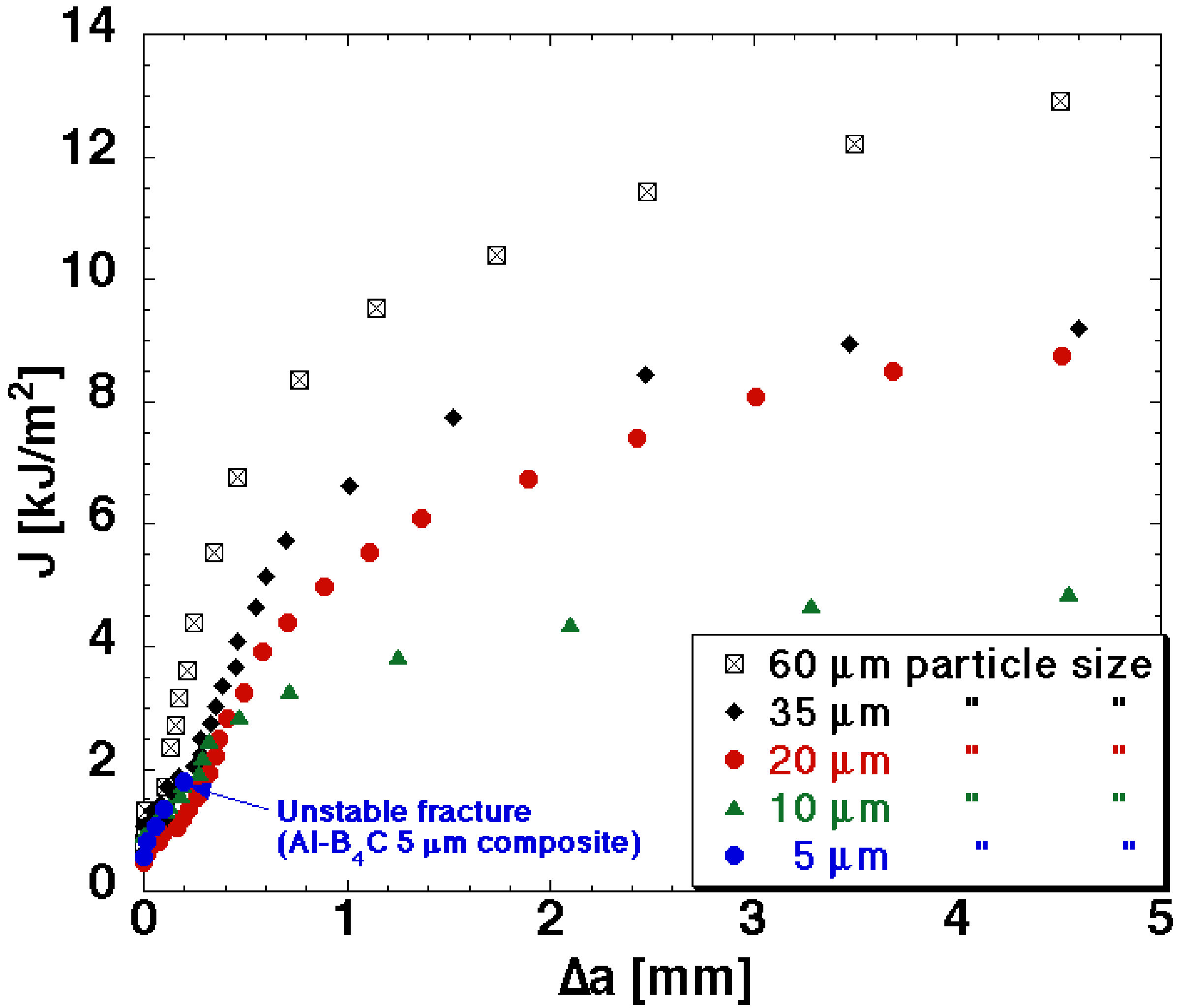

Toughness

Equal size: influence of reinforcement nature and quality

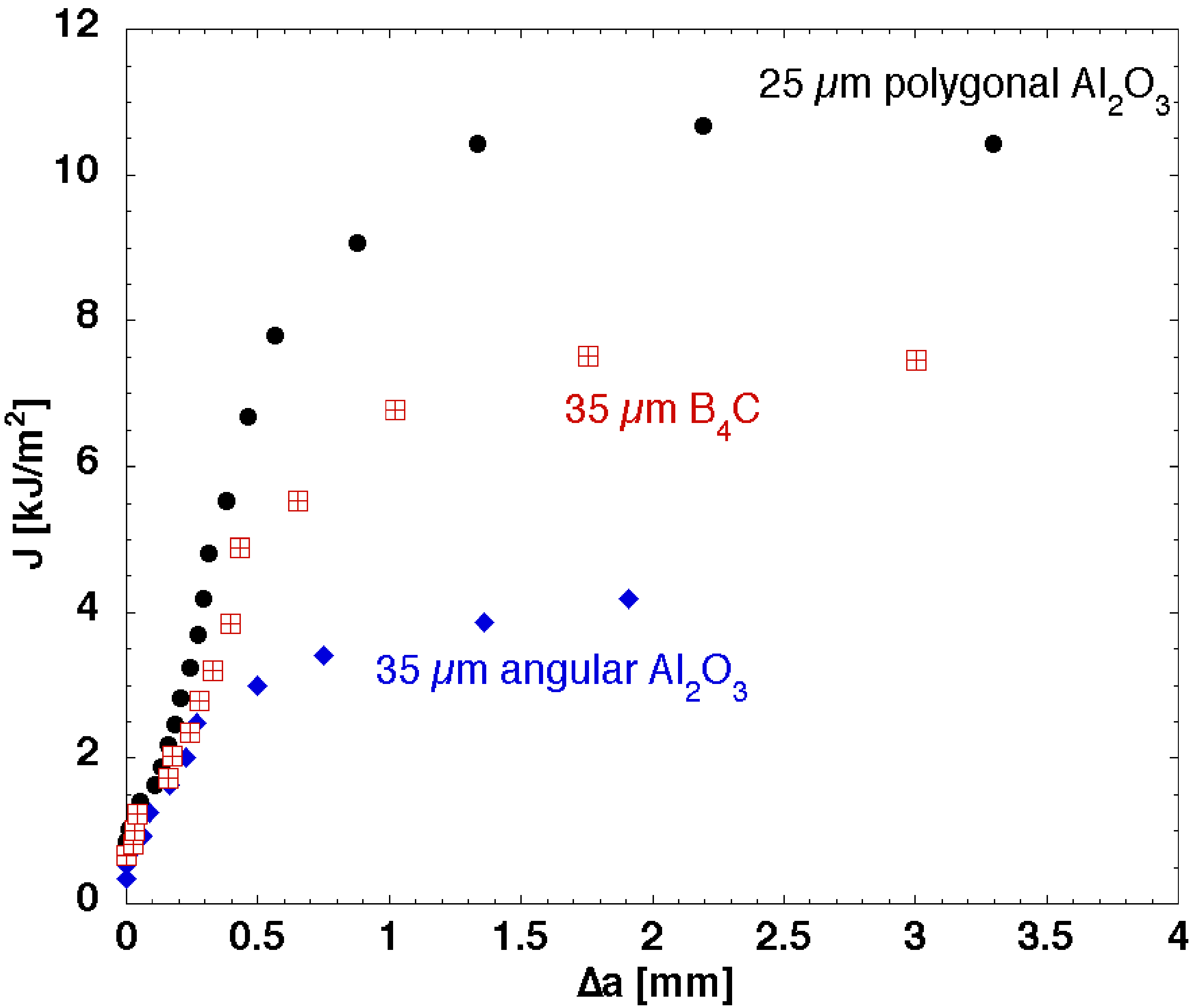

Toughness

Alloyed matrix composites were characterized in small-scale yielding using chevron-notched specimens (ASTM E-1304)

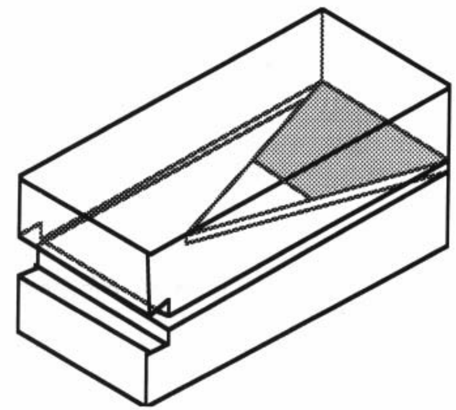

Consistency: *J*-integral test data for Al-Cu matrix composites are between 2 and 27% lower than chevron-notched test data.

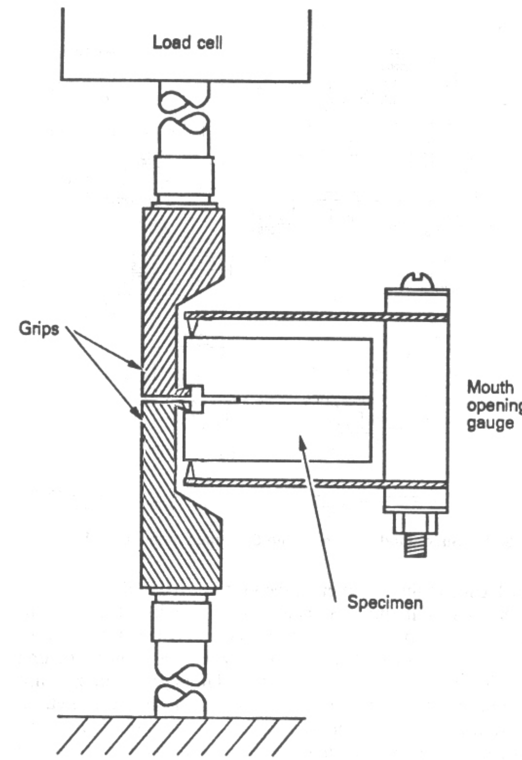

Toughness

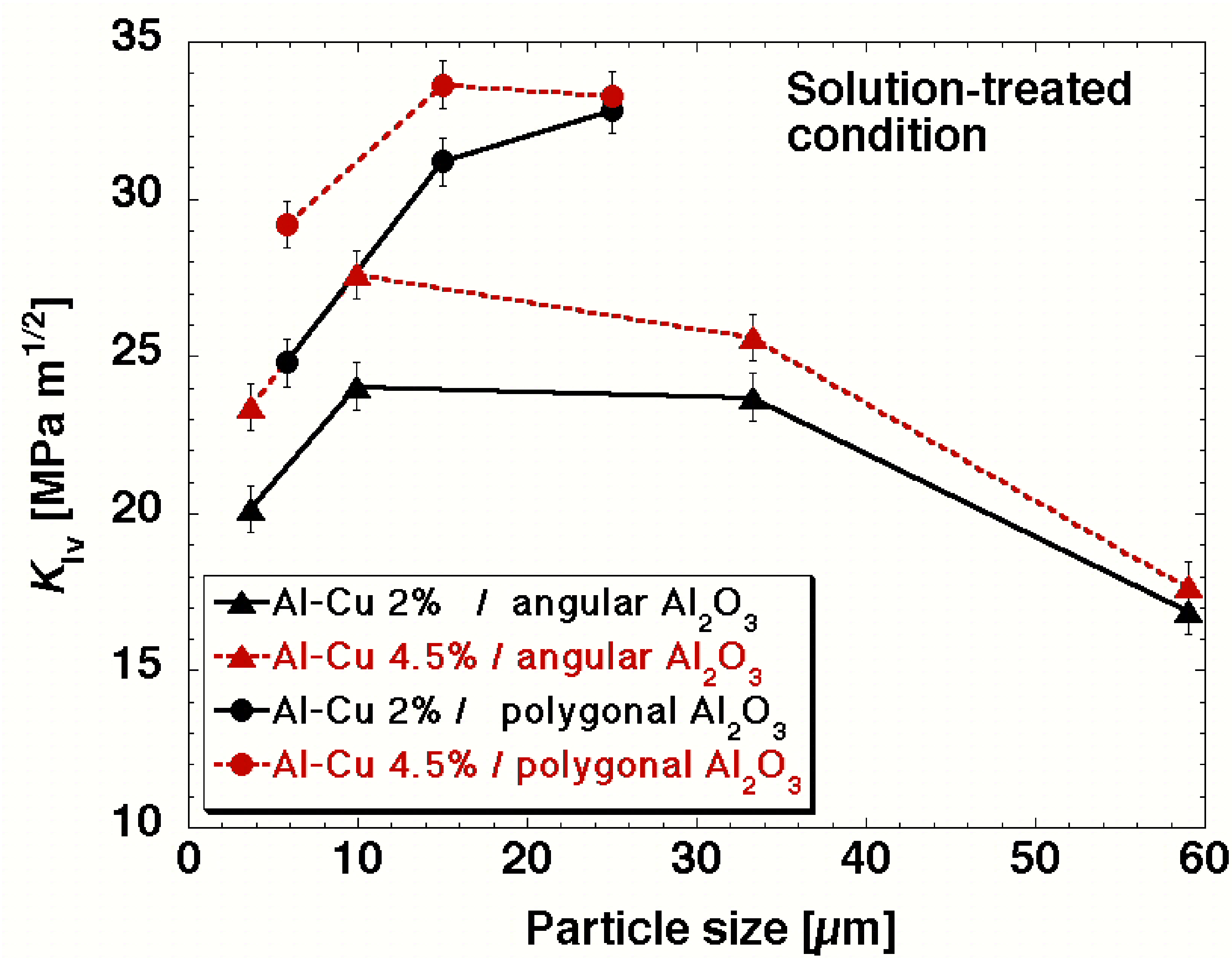

35
30
25
20
15
10
0
10
20
30
40
50
60
K_{Iv} [MPa m$^{1/2}$]
Particle size [μm]
Solution-treated condition
Al-Cu 2% / angular Al_2O_3
Al-Cu 4.5% / angular Al_2O_3
Al-Cu 2% / polygonal Al_2O_3
Al-Cu 4.5% / polygonal Al_2O_3

Strength/Toughness Combination

Strength/Toughness Combination

Overall summary of data:

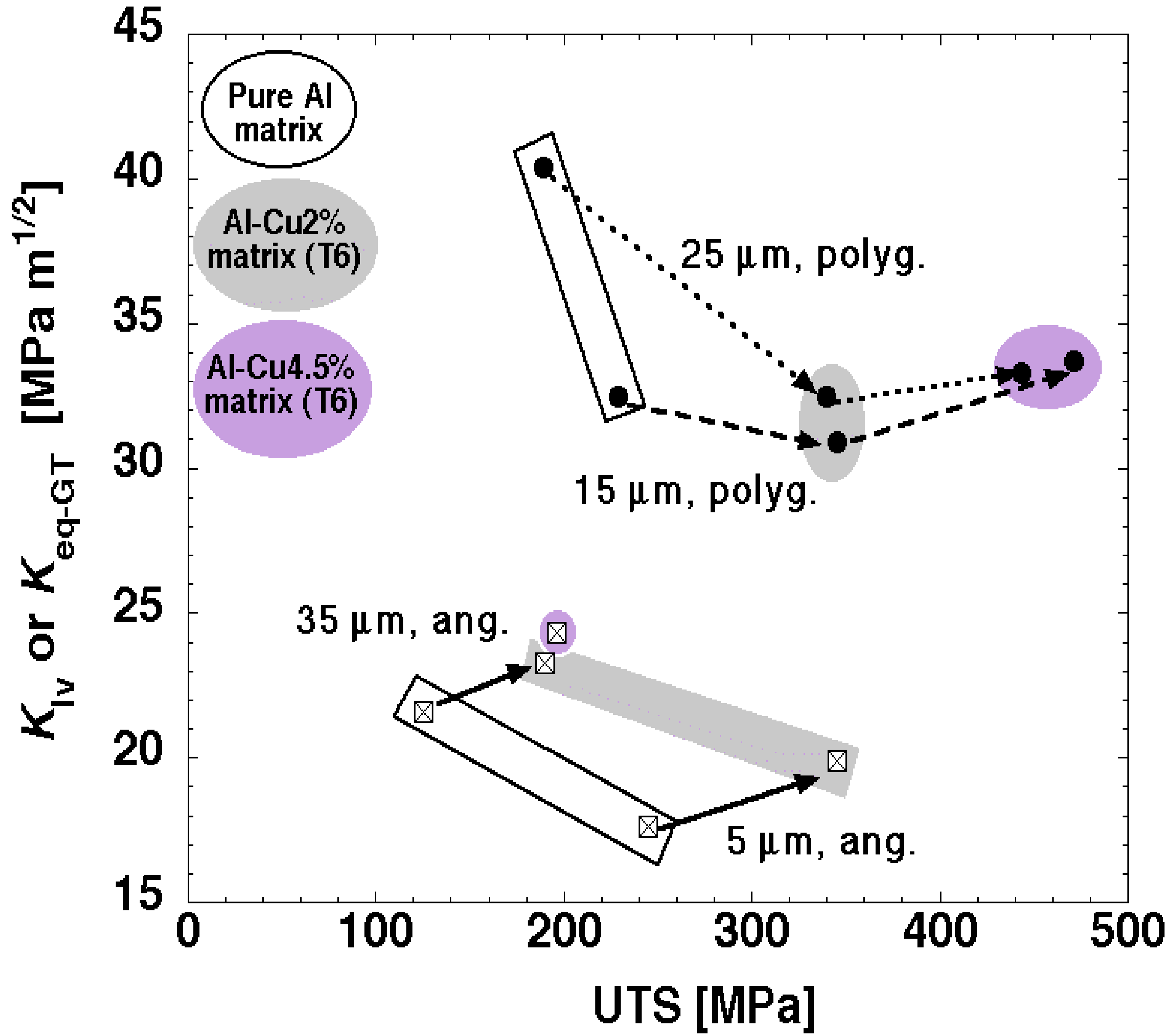

Strength/Toughness Combination

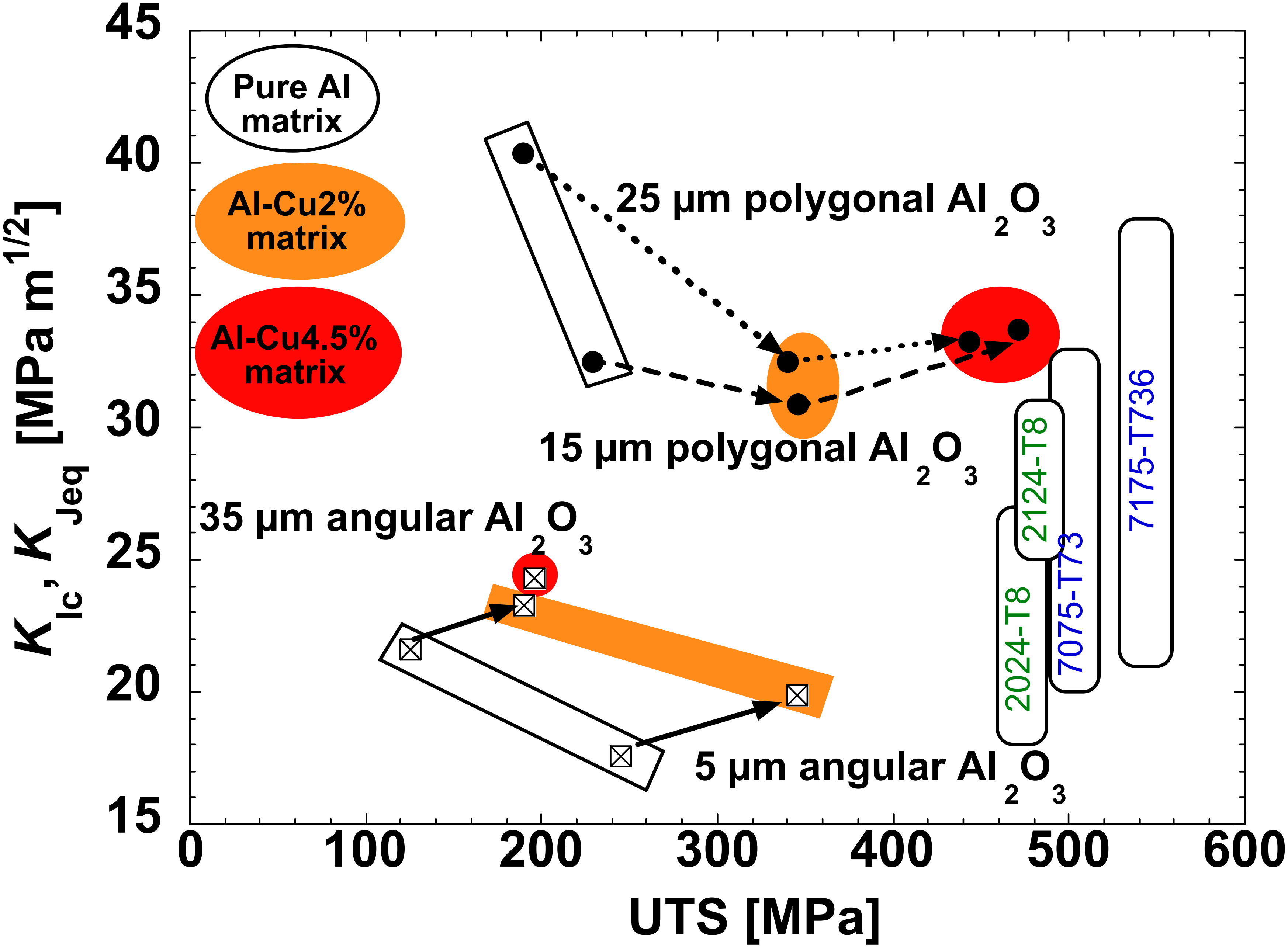

Toughening mechanisms

Toughening mechanisms

What makes these composites tough ?

• A first very simple mechanism:
$K \propto \sqrt{(G.E)}$
and E is 2.5 times higher than for *Al* alloys.

• Still, corresponding *G/(J)* values near 10 kJ/m^2 are high.

• There is significant *R*-curve behaviour: these *K* values are for near-steady crack advance.

Fracture micromechanisms

Fracture micromechanisms

Particle fracture

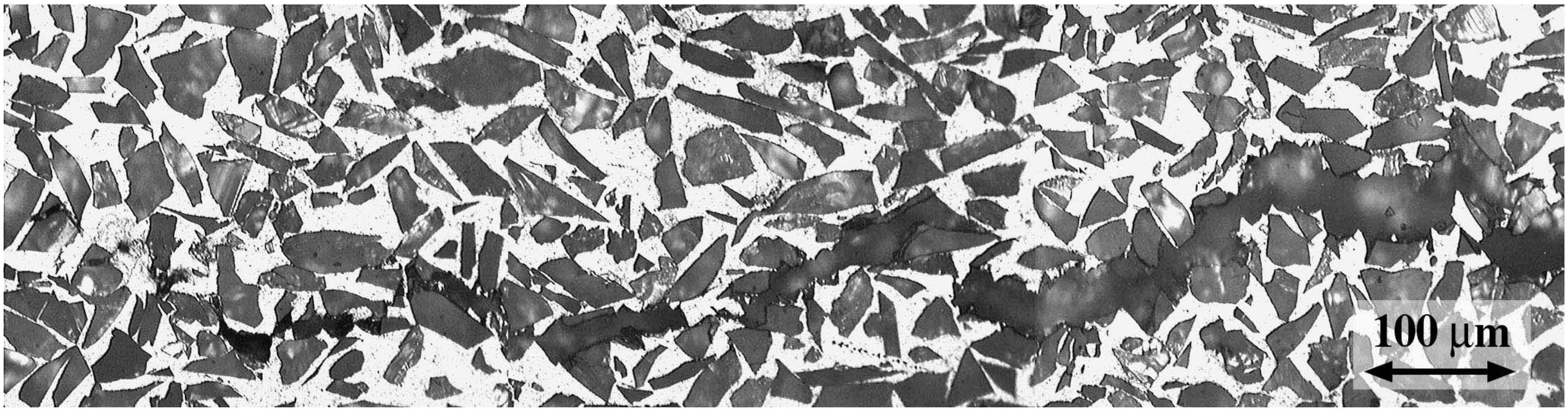

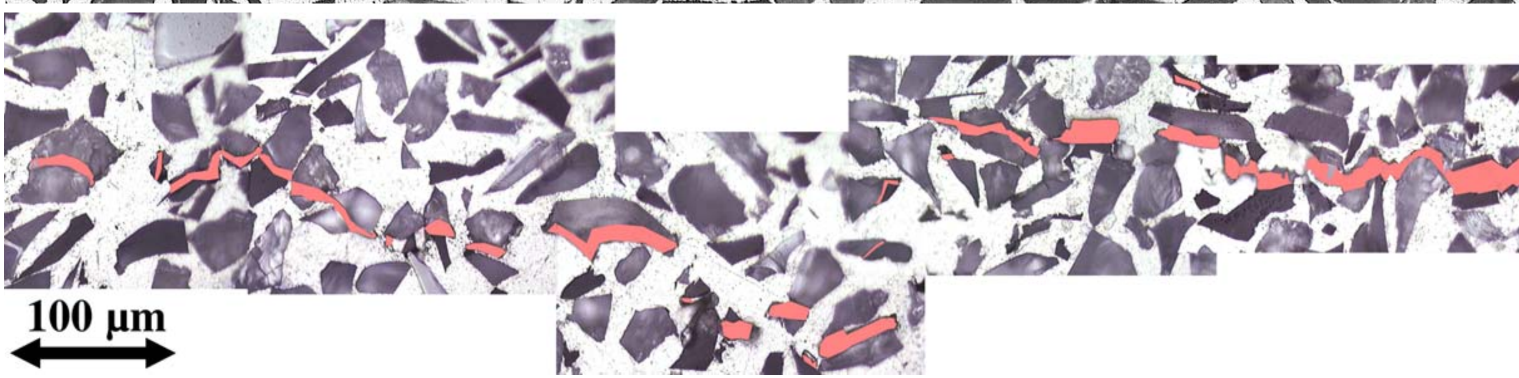

Pure Al/ 30 μm angular Al_2O_3

Fracture micromechanisms

Particle fracture

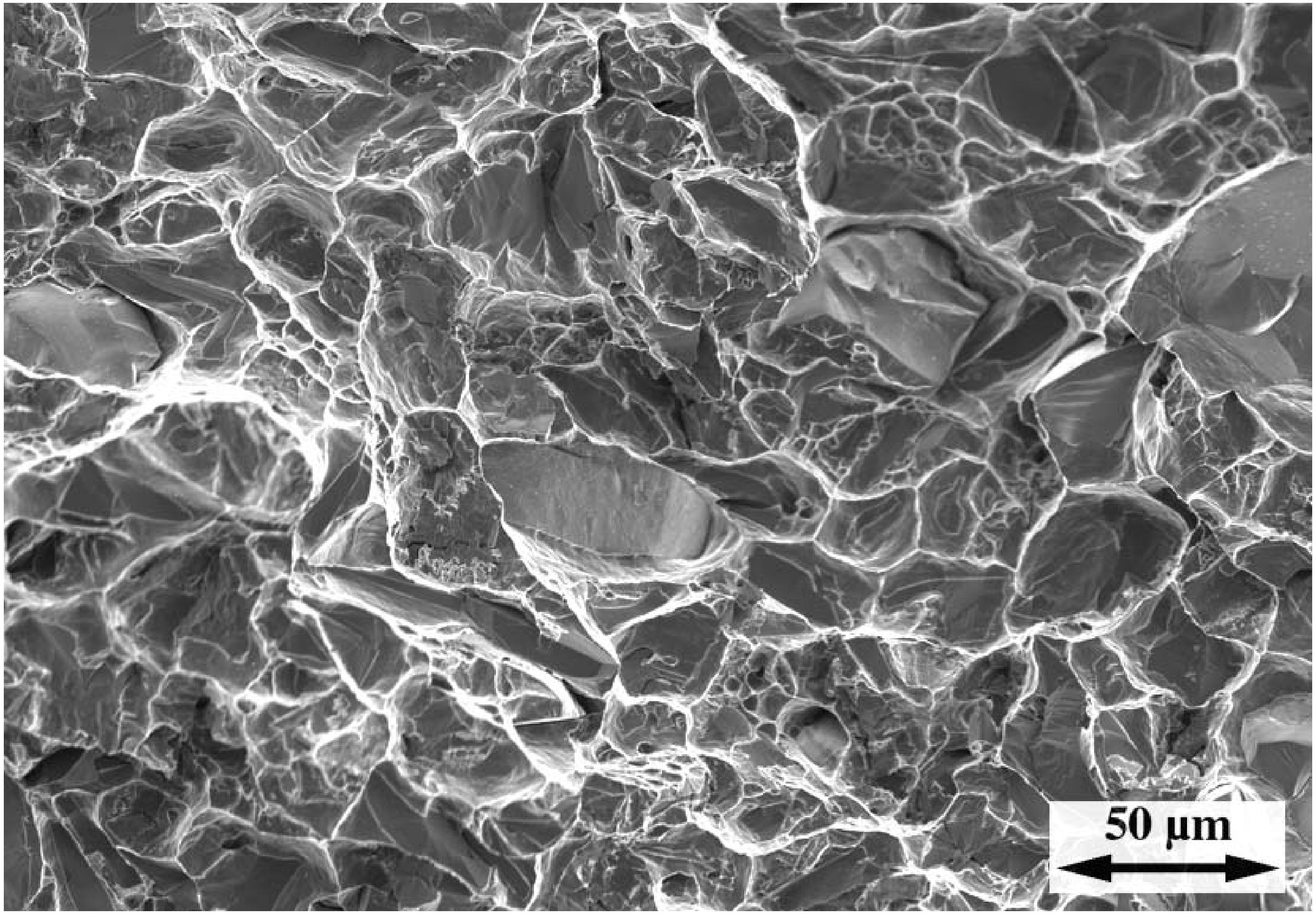

Pure Al/ 30 µm angular Al_2O_3

Fracture micromechanisms

Matrix void growth

Pure Al/10 μm polygonal Al_2O_3

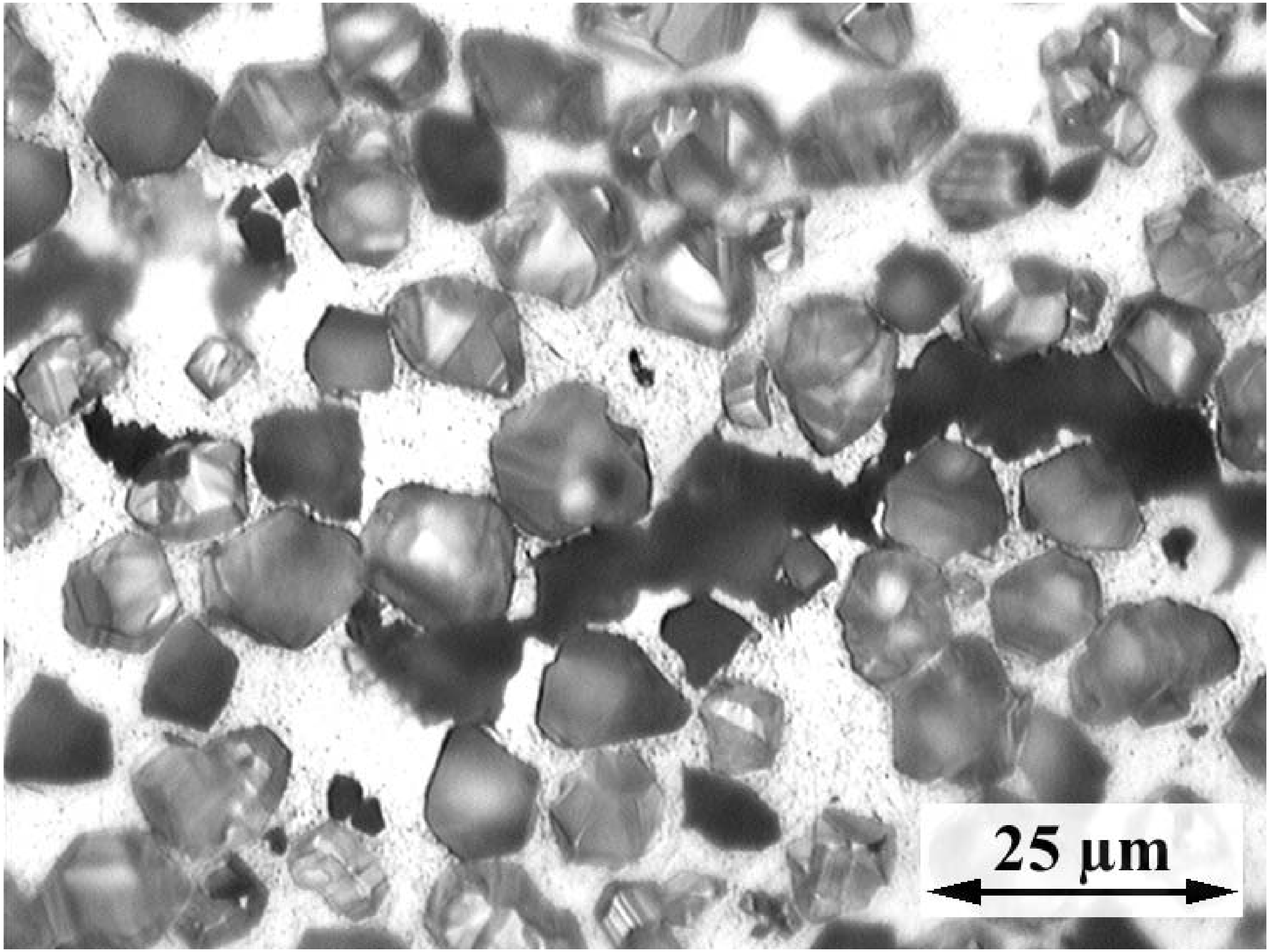

Fracture micromechanisms

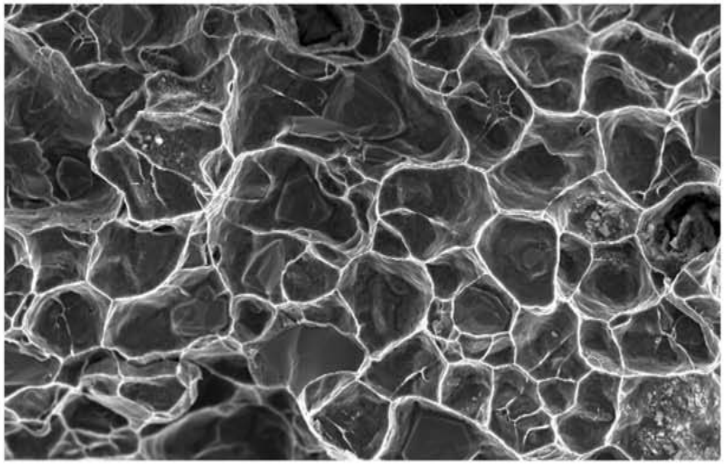

A 18

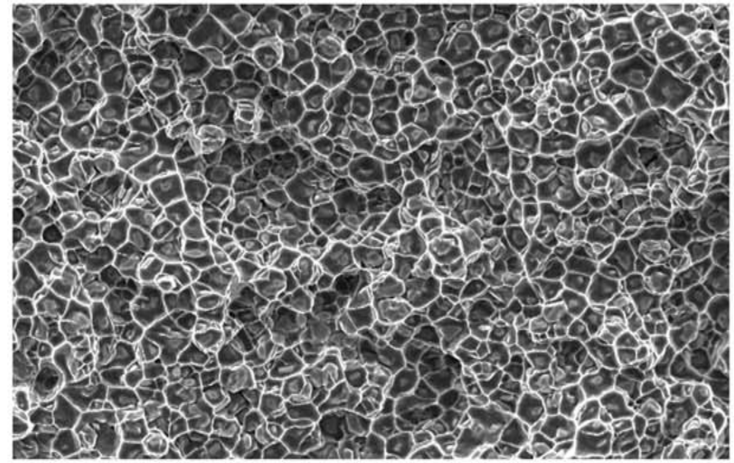

A 5

20 µm

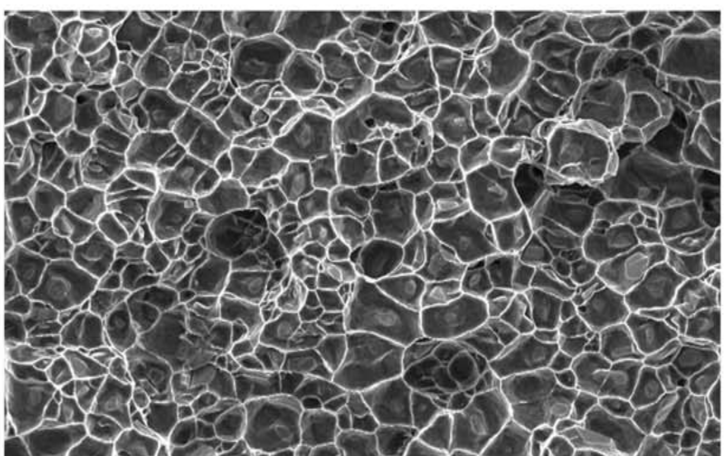

A 10

- Voids nucleate between particles

- Final void size scales with average particle size

Local fracture energy estimation

Local fracture energy estimation

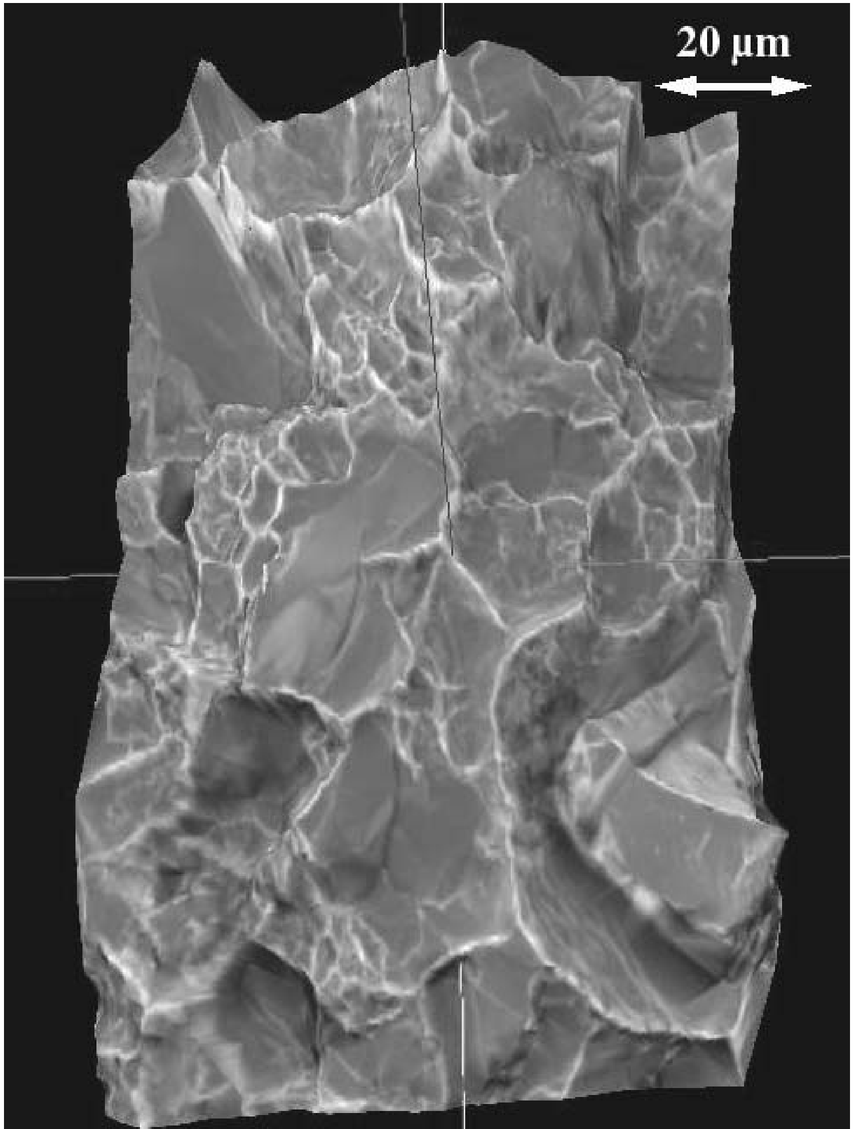

Pure Al composites: 3-D fracture surface topography measurement

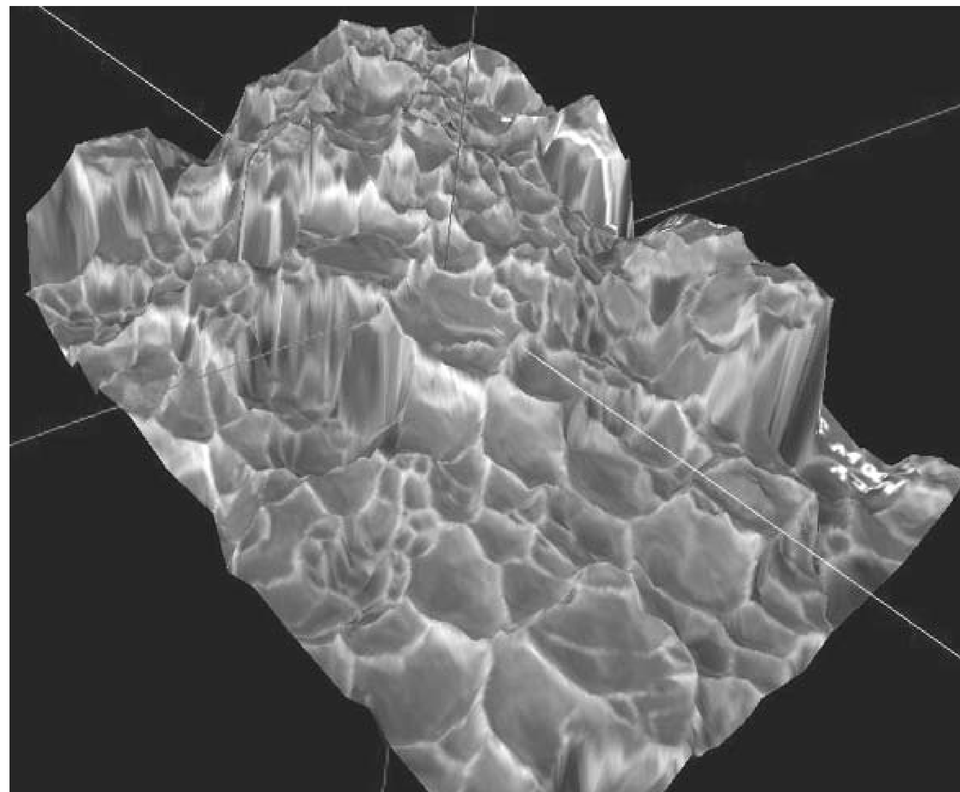

Local vs. total fracture energy

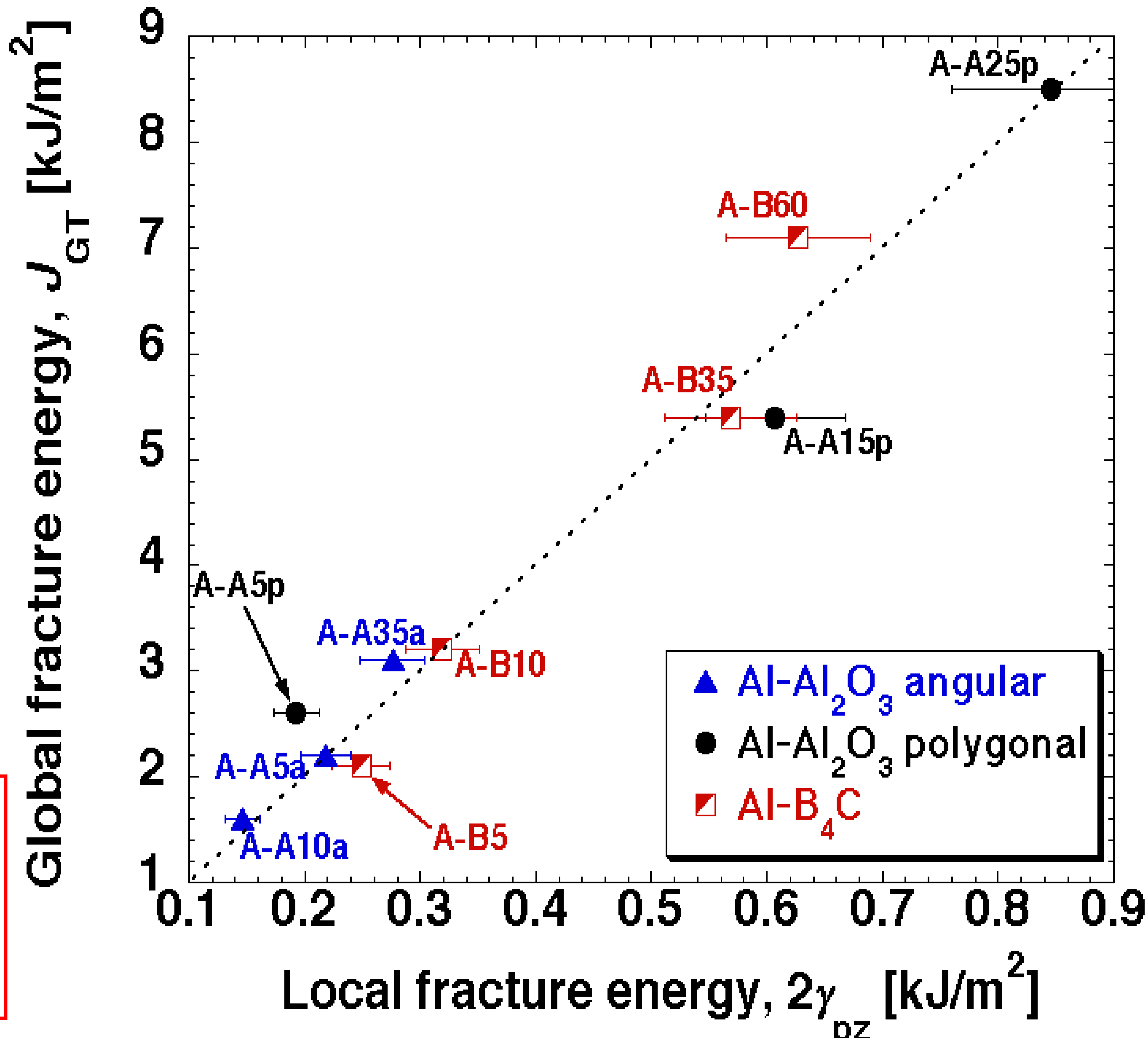

Pure Al matrix composites

Toughening mechanisms

Observation of crack tip plasticity using a photoelastic coating:

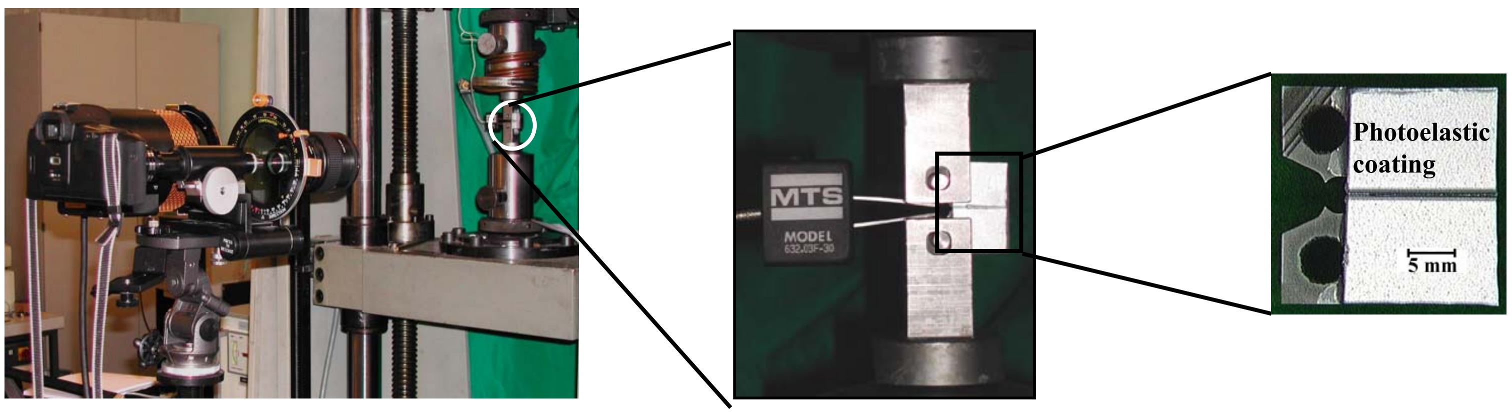

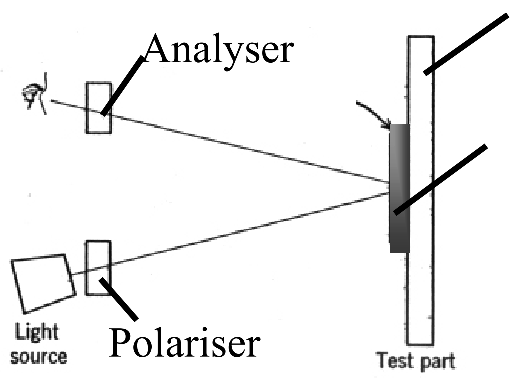

$\varepsilon_1 - \varepsilon_2 \approx 0.2\%$:

pale yellow - orange fringes

Toughening mechanisms

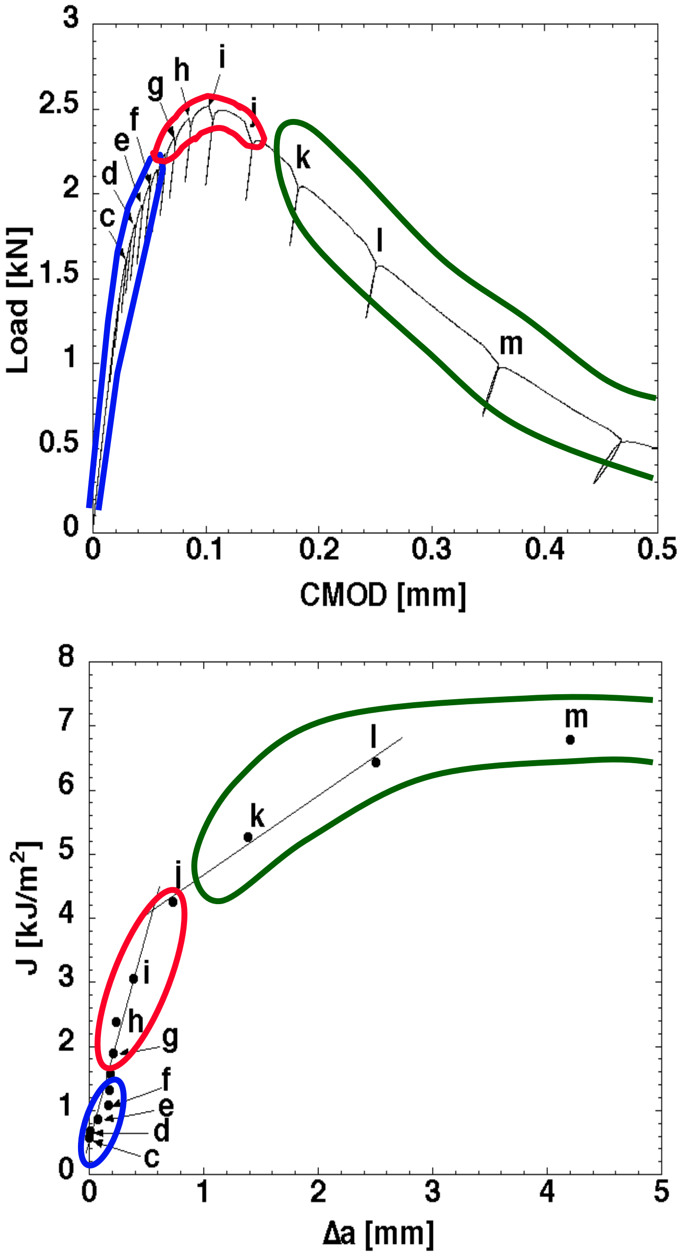

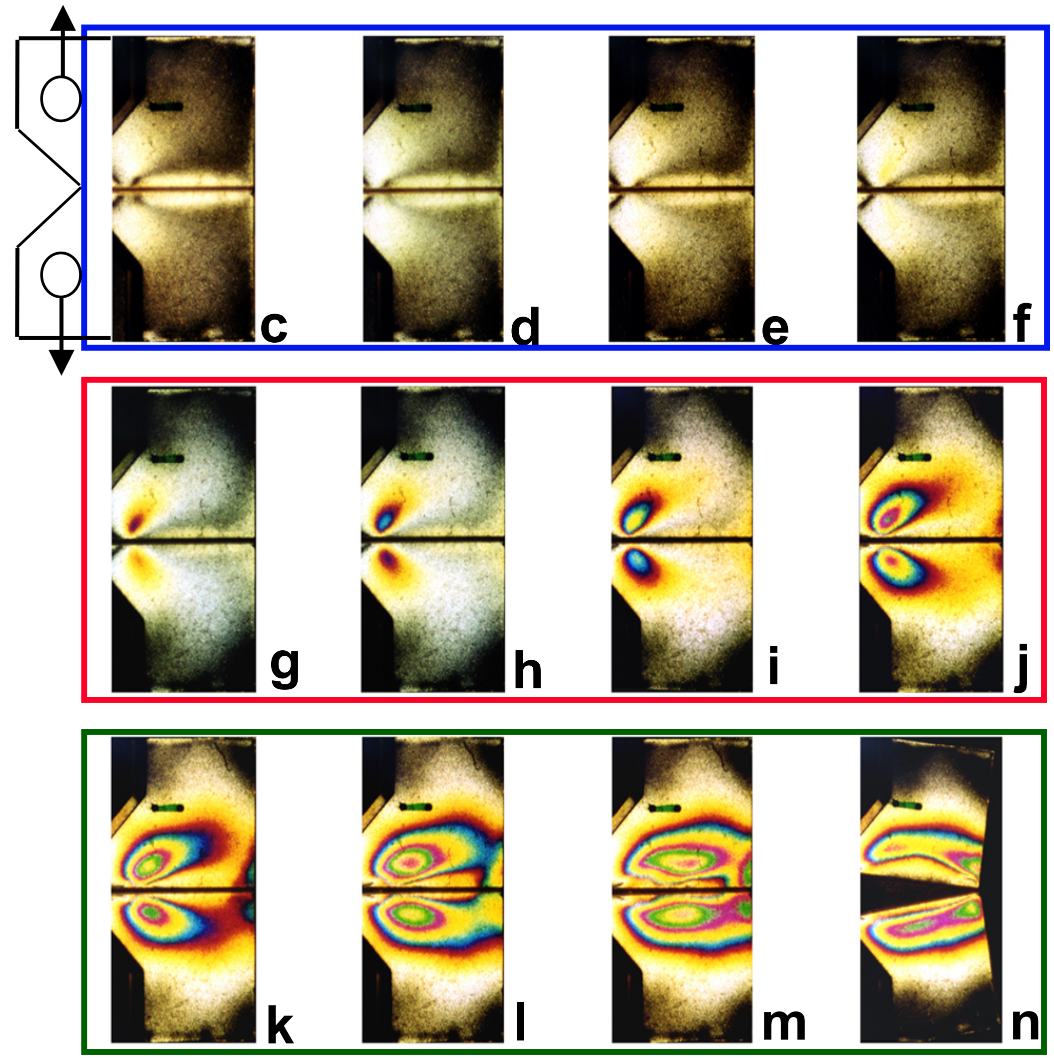

($Al/35\ \mu m$ ang. Al_2O_3)

Local vs. total fracture energy

In other words, the total fracture energy:
$J = 2\gamma_{pz} + W_p > 2\gamma_{pz}$

- $2\ \gamma_{pz}$ is the *local* « process zone » or « cohesive law » fracture energy;
- W_p is the energy dissipated in the surrounding macroscopic plastic zone

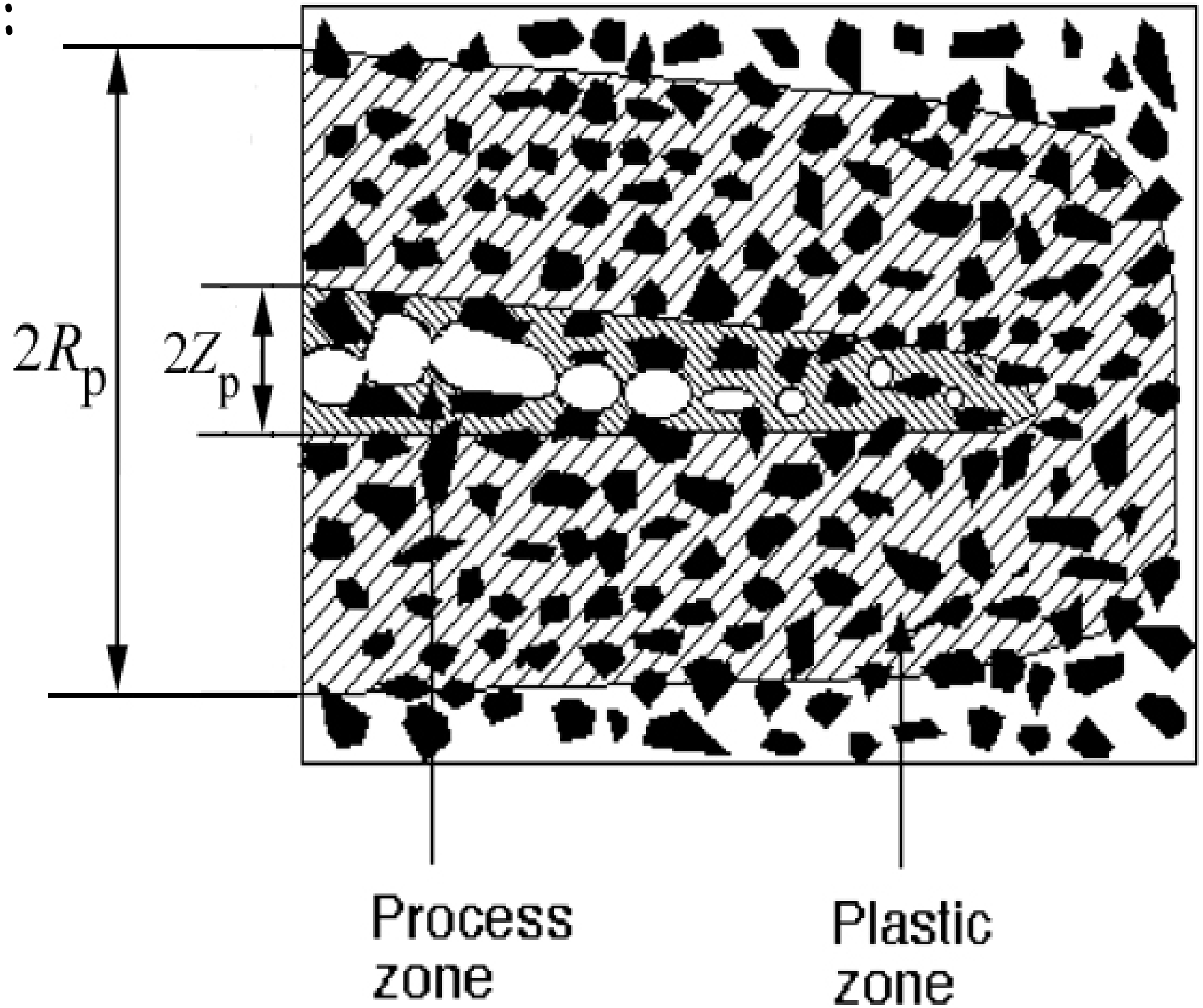

Toughening mechanisms

Tvergaard and Hutchinson (*JMPS* vol. 40 (1992) 1377)

Cohesive Zone Model :

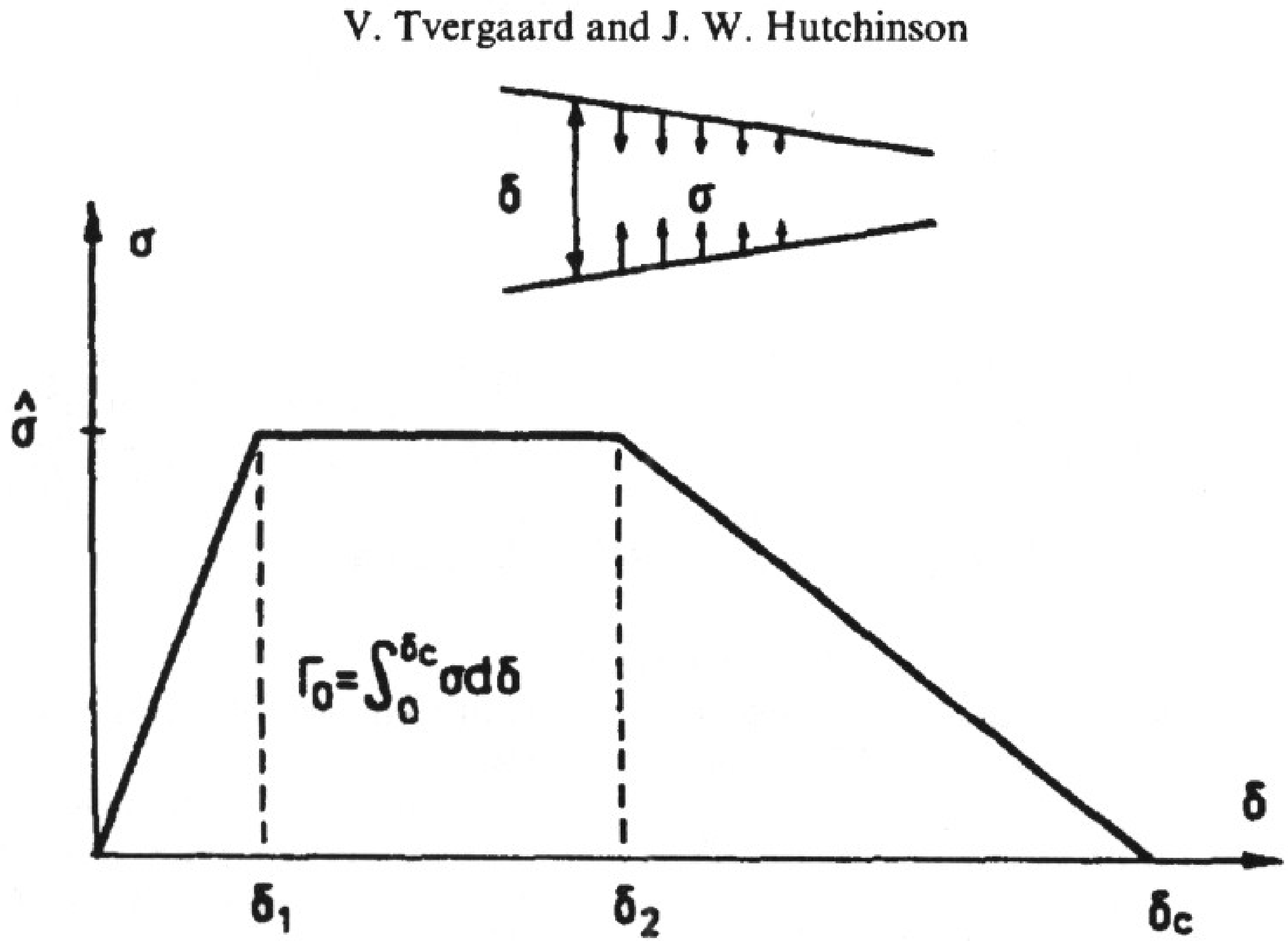

Fig. 1. Traction–separation relation for fracture process.

Toughening mechanisms

Tvergaard and Hutchinson (*JMPS* vol. 40 (1992) 1377):

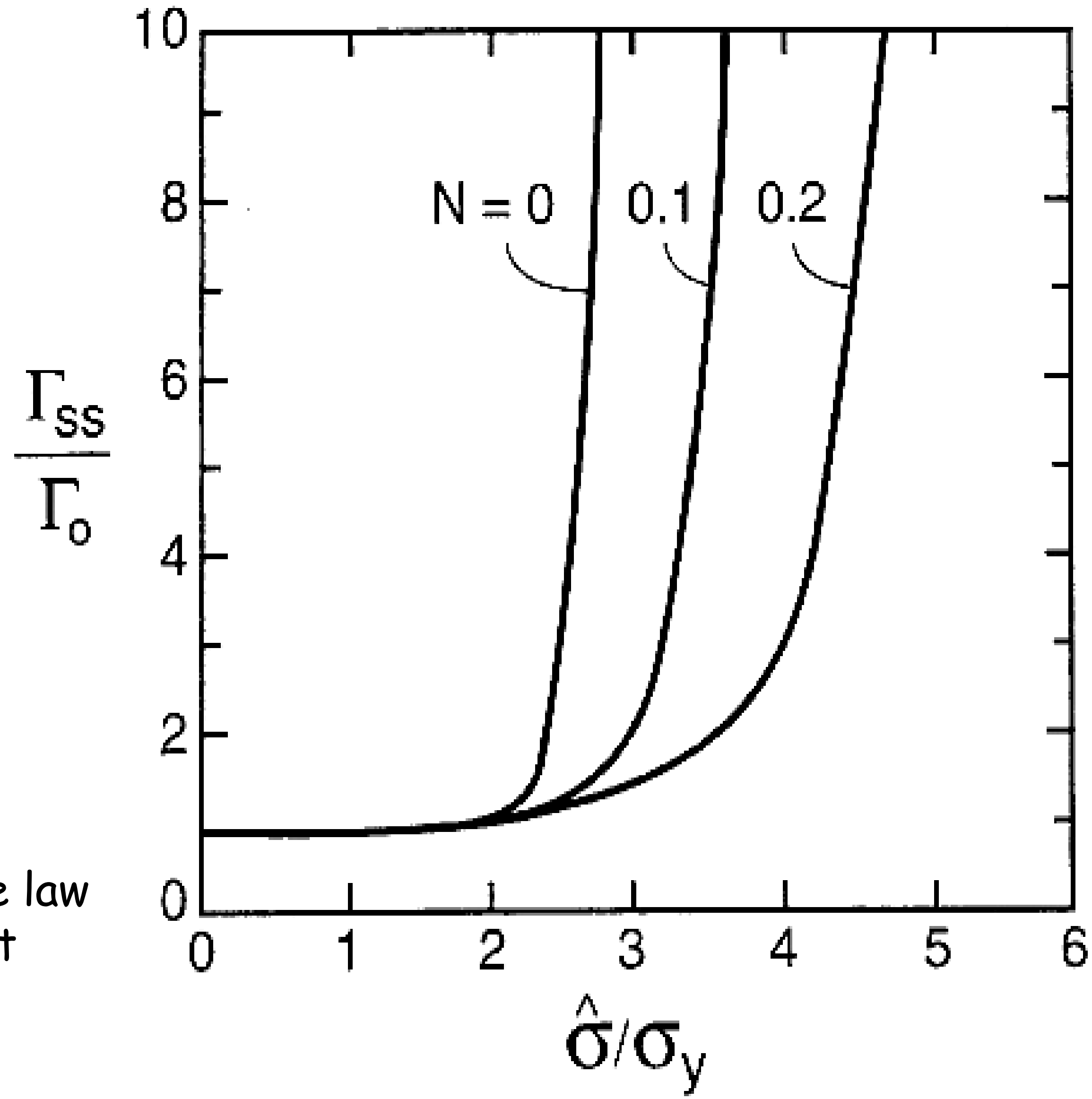

Γ_{ss}: steady-state toughness
Γ_0: local fracture energy ($2\gamma_{pz}$)
σ_y: composite yield strength
$\hat{\sigma}$: peak-stress of the cohesive law
N: strain-hardening coefficient

Toughening mechanisms

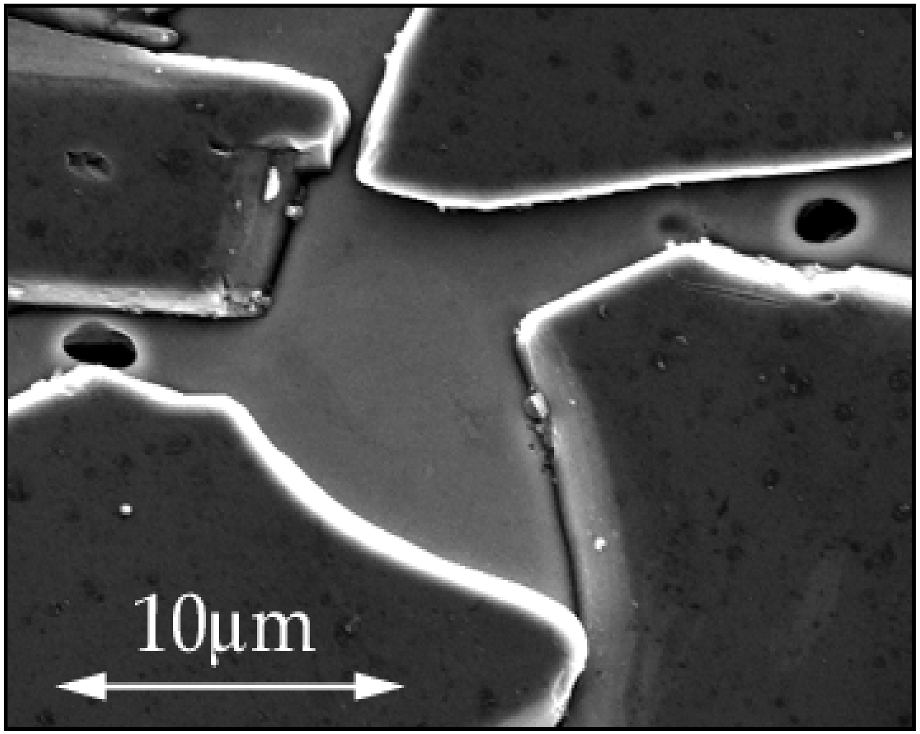

V. Tvergaard, Comput. Mechan. 20 (1997) 186

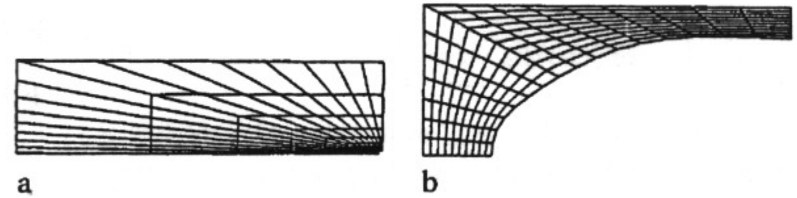

Fig. 7a,b. Meshes at two stages of deformation for $\sigma_y/E = 0.003, n = 10, H_0/B_0 = 0.25$ and $R_0/B_0 = 0.01$. **a** Initial mesh; **b** $\epsilon_1 = 0.522$ and $V/V_0 = 2.50 \cdot 10^5$

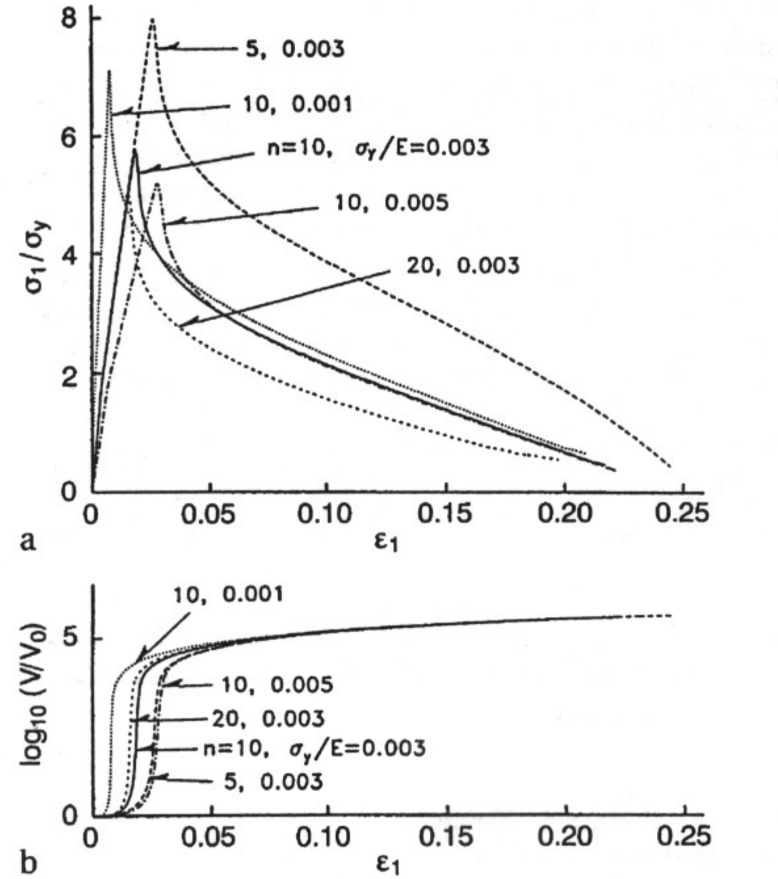

Fig. 8. Average true stress and void volume growth vs. average logarithmic strain, for $H_0/B_0 = 1$ and $R_0/B_0 = 0.01$. With remeshing

Metal sponge

The replication process

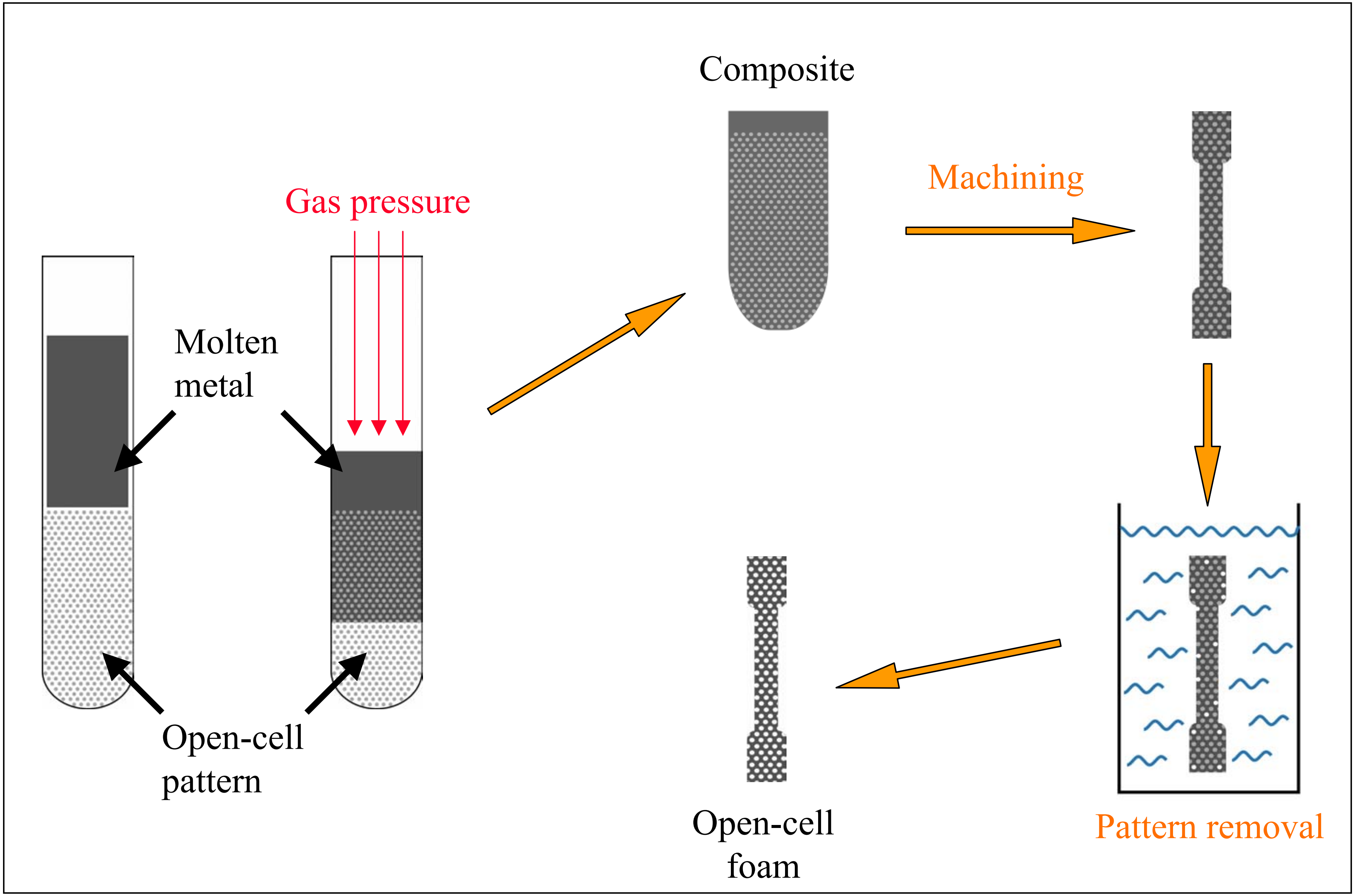

The replication process

Cold Isostatic Pressing (CIP) + sintering for 40 μm (32-45 μm) powder: 45 min. at 750°C.

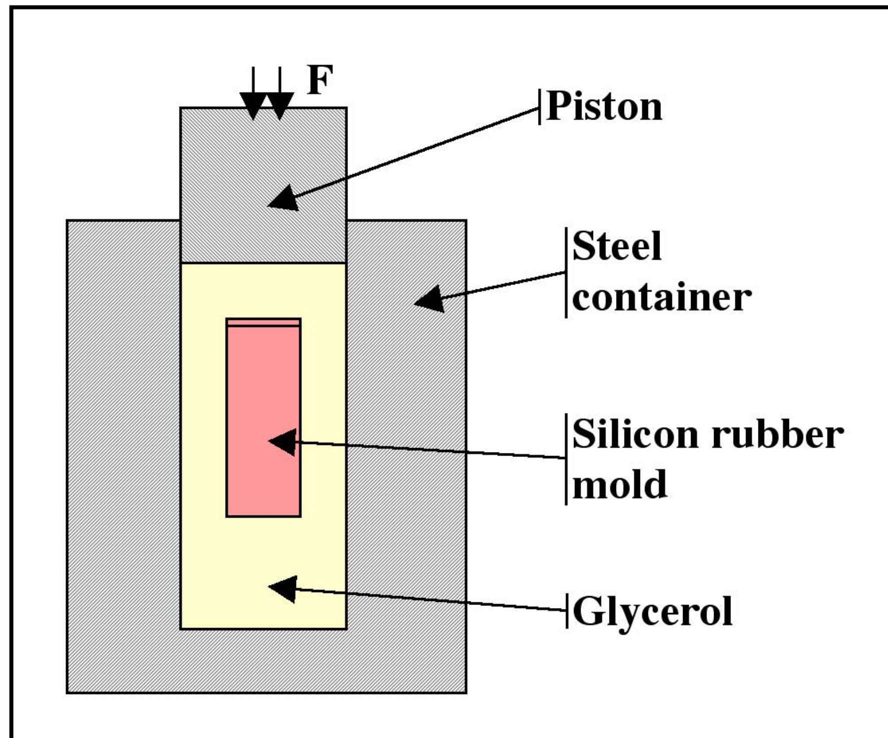

The replication process

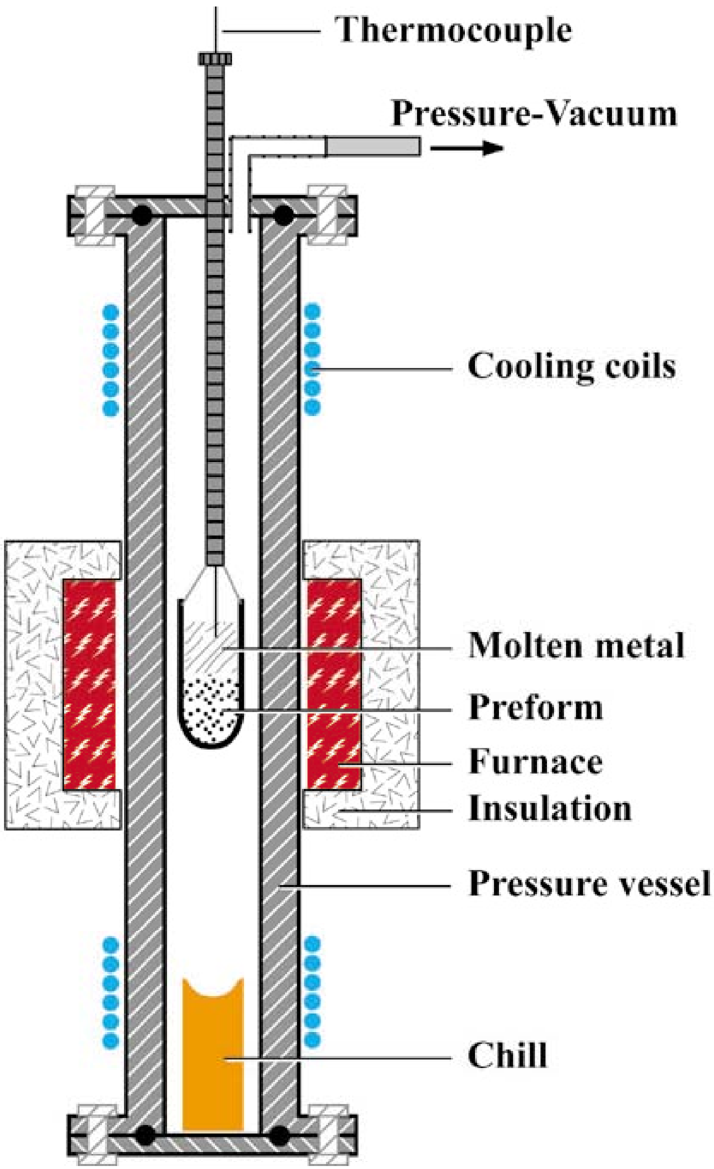

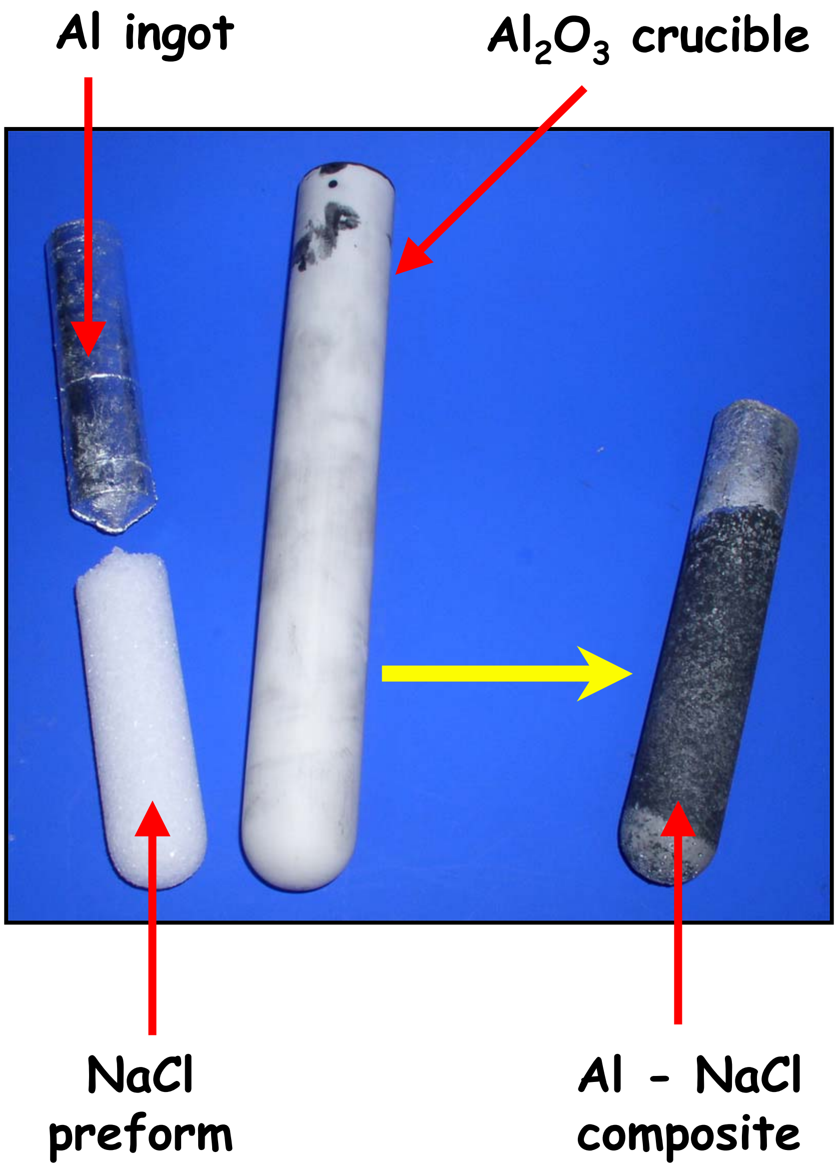

The replication process

Machining:
conducted prior to salt removal by dissolution on the (brittle) NaCl-Al composite;
Dissolution:
- **in distilled water.**
- **below 50 μm**, degassed water with forminggas (H_2 + N_2) bubbling(to minimize corrosion problems)

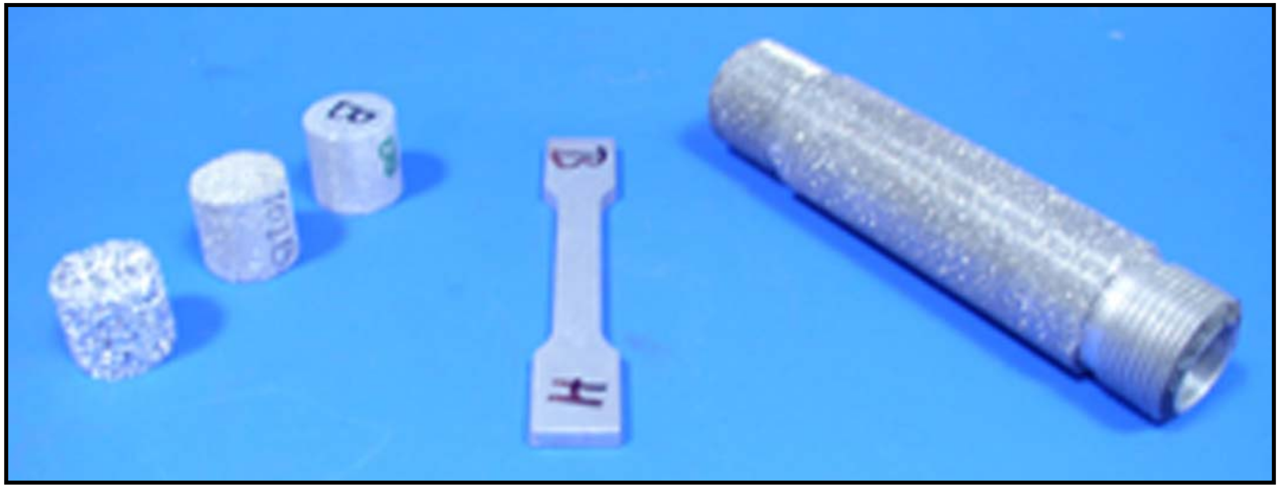

The replication process

Commercial NaCl powder, sieved to:

- 32-45 μm (40 μm);
- 63-90 μm (75 μm);
- >250 μm (ave. 400μm).

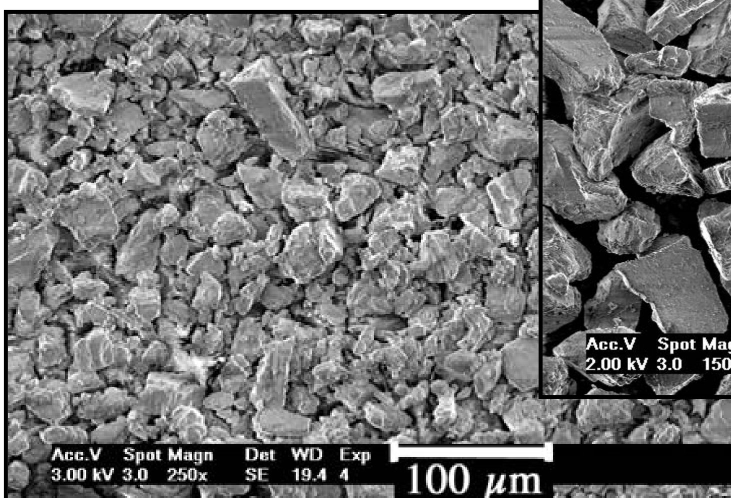

Sieving 32-45 μm

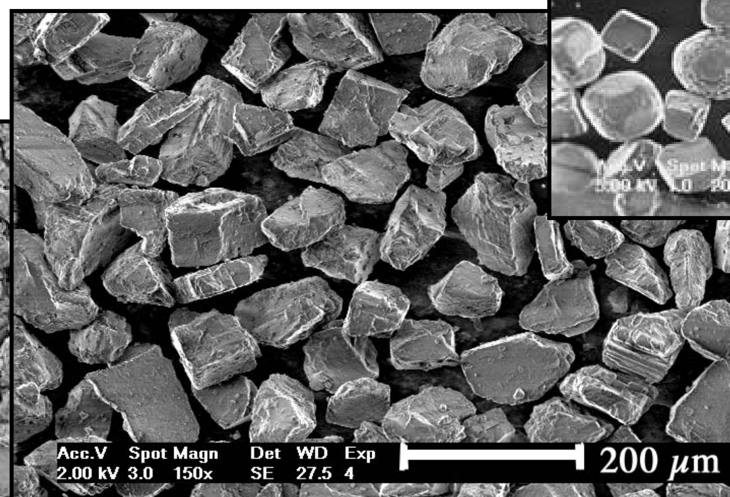

Sieving 63 - 90 μm

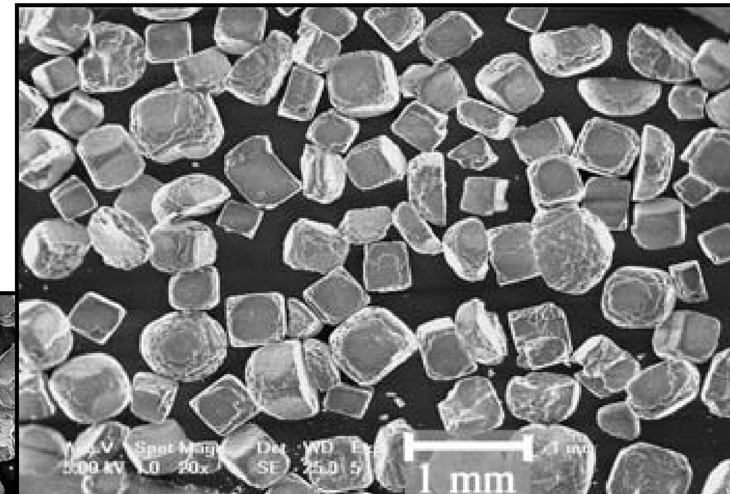

Sieving > 250 μm

Replicated Foams

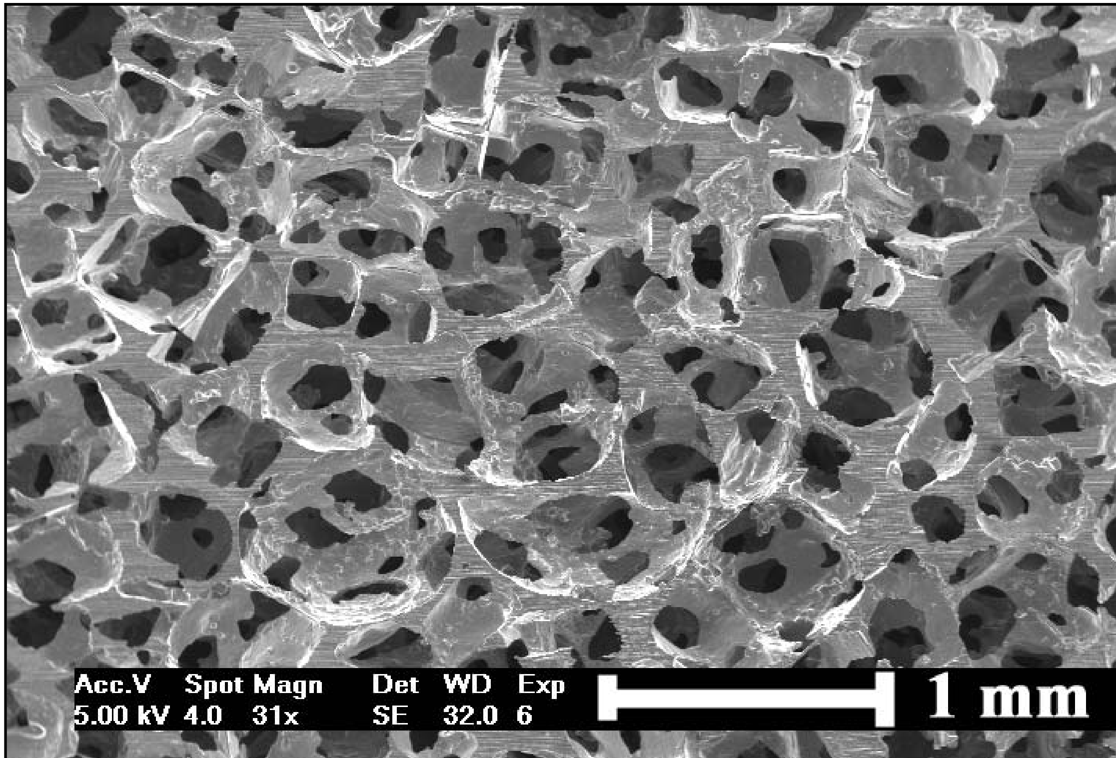

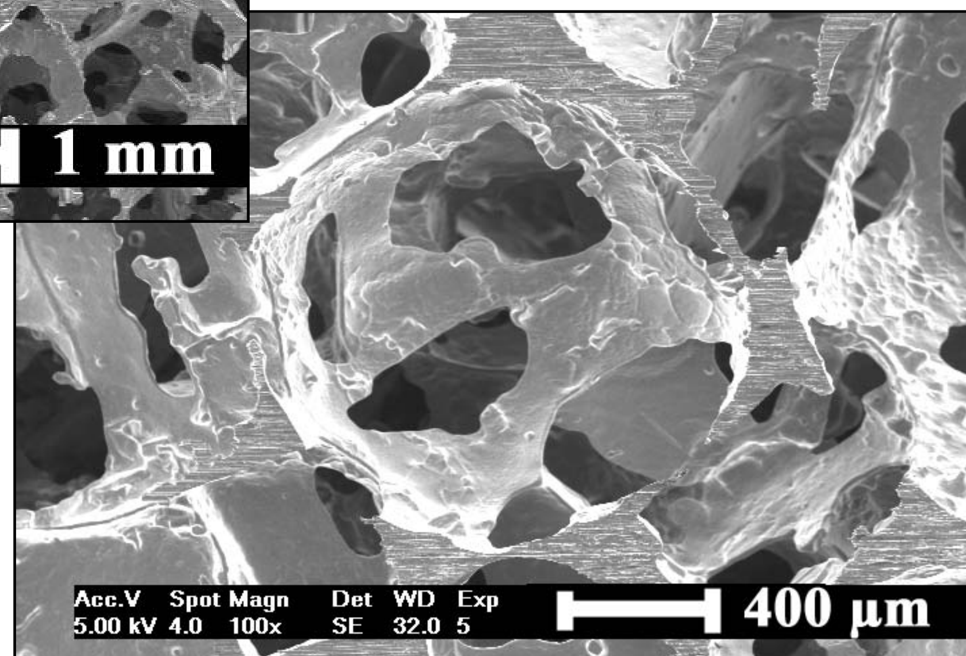

NaCl 400 μm ,
V_f Al = 16 %

Replicated Foams

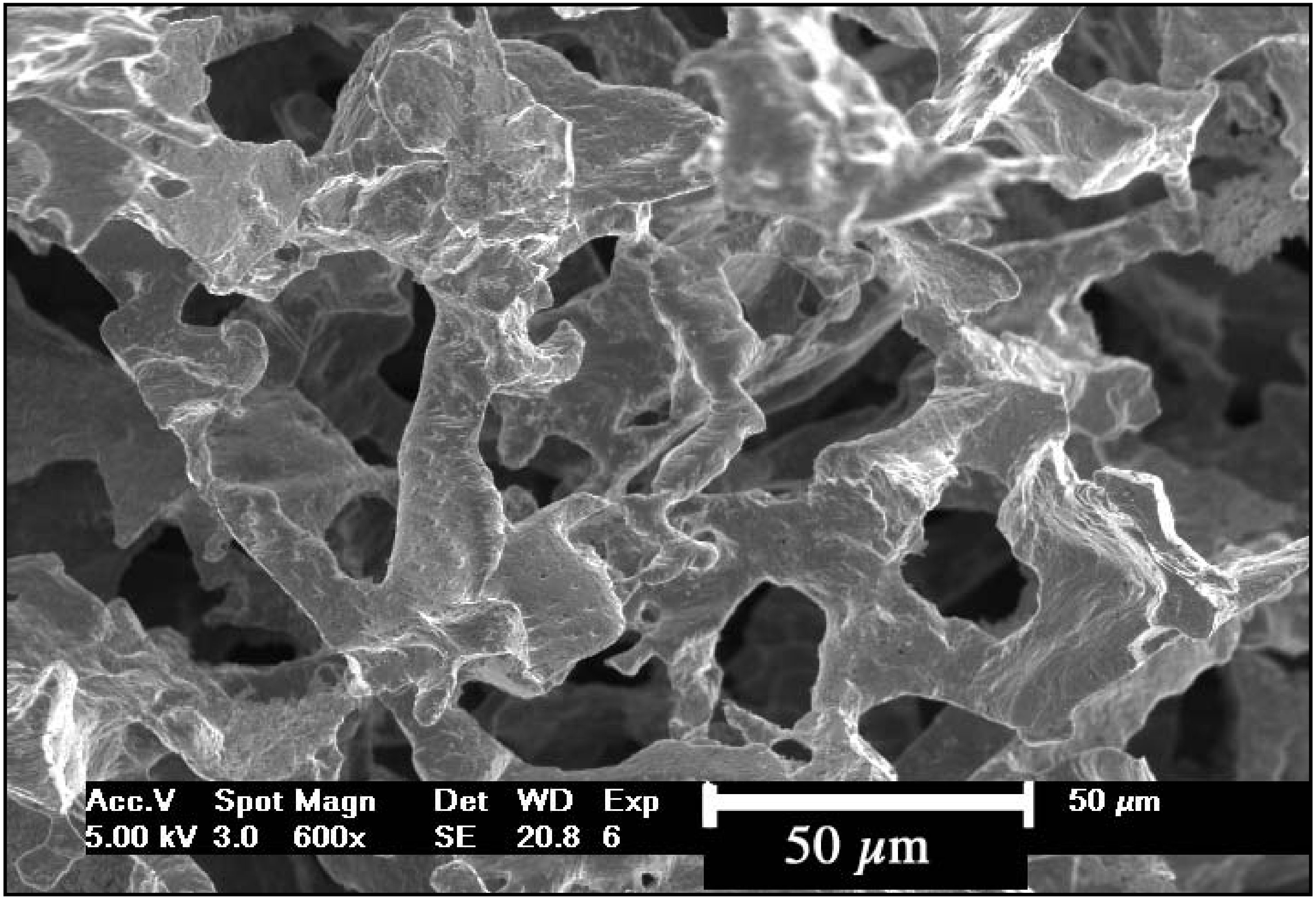

75 µm, Vf Al = 16 % (fracture surface)

Replicated Foams

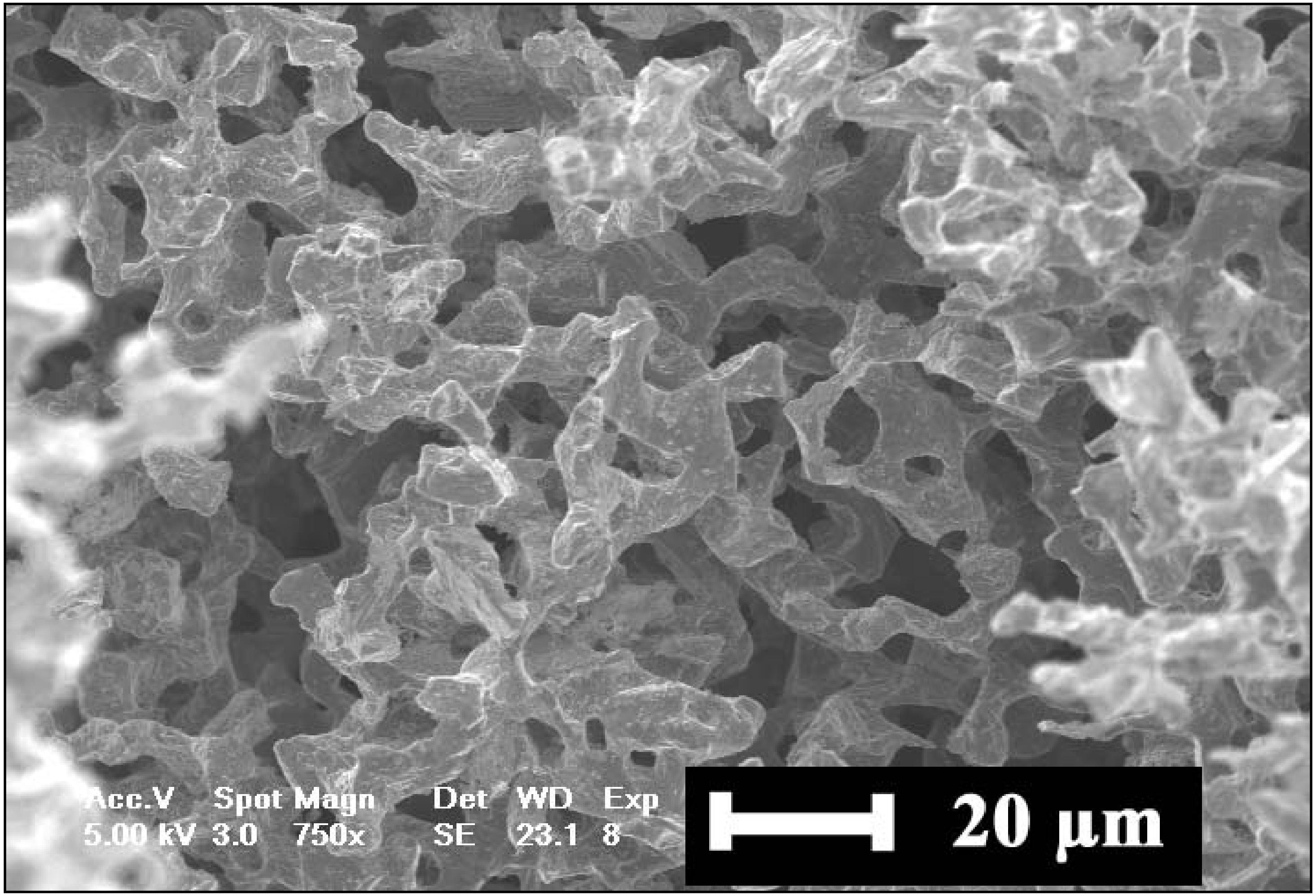

NaCl 20-32 μm , Vf Al = 18 % (fracture surface)

Mechanical Properties

Mechanical Properties

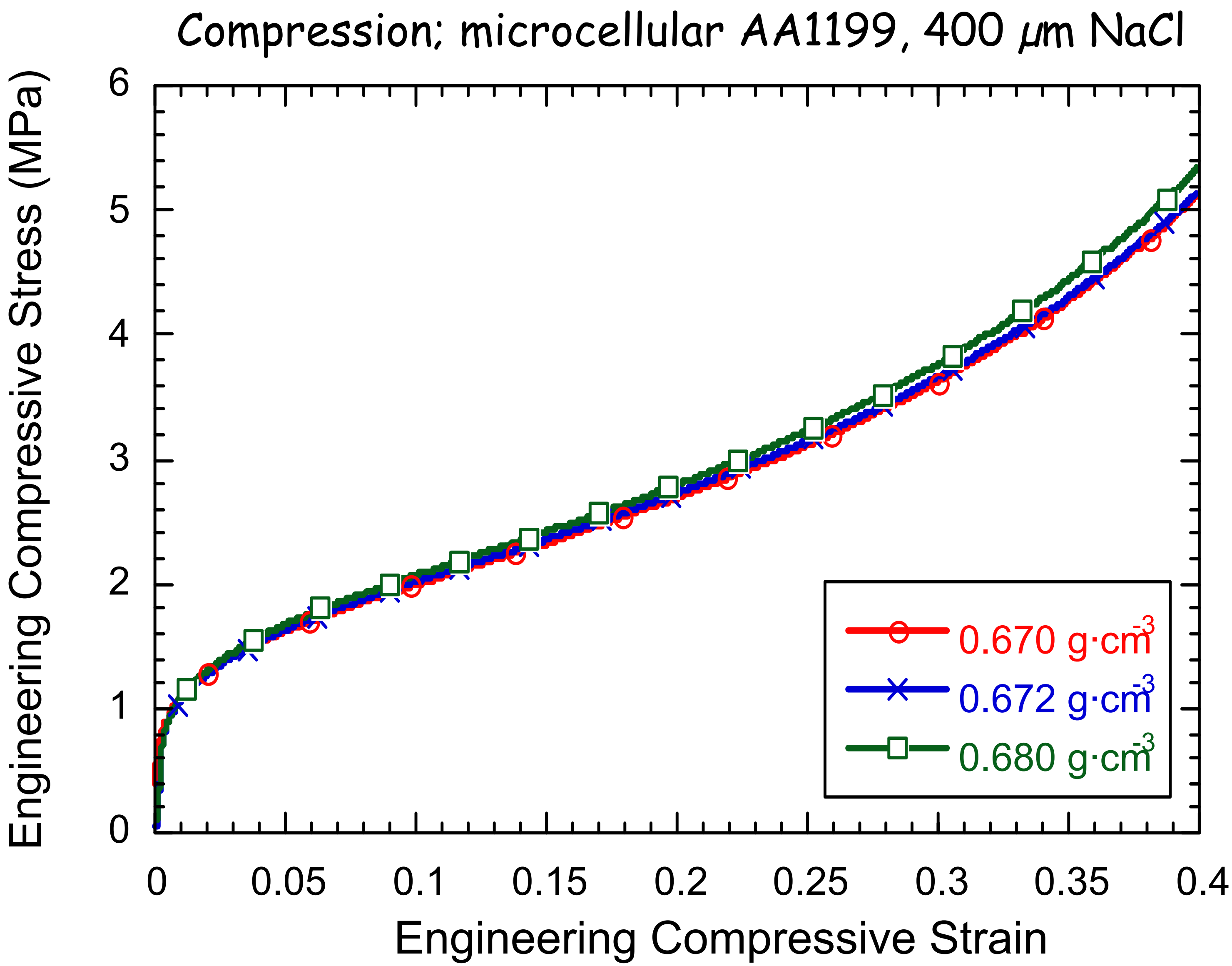

Influence of Density

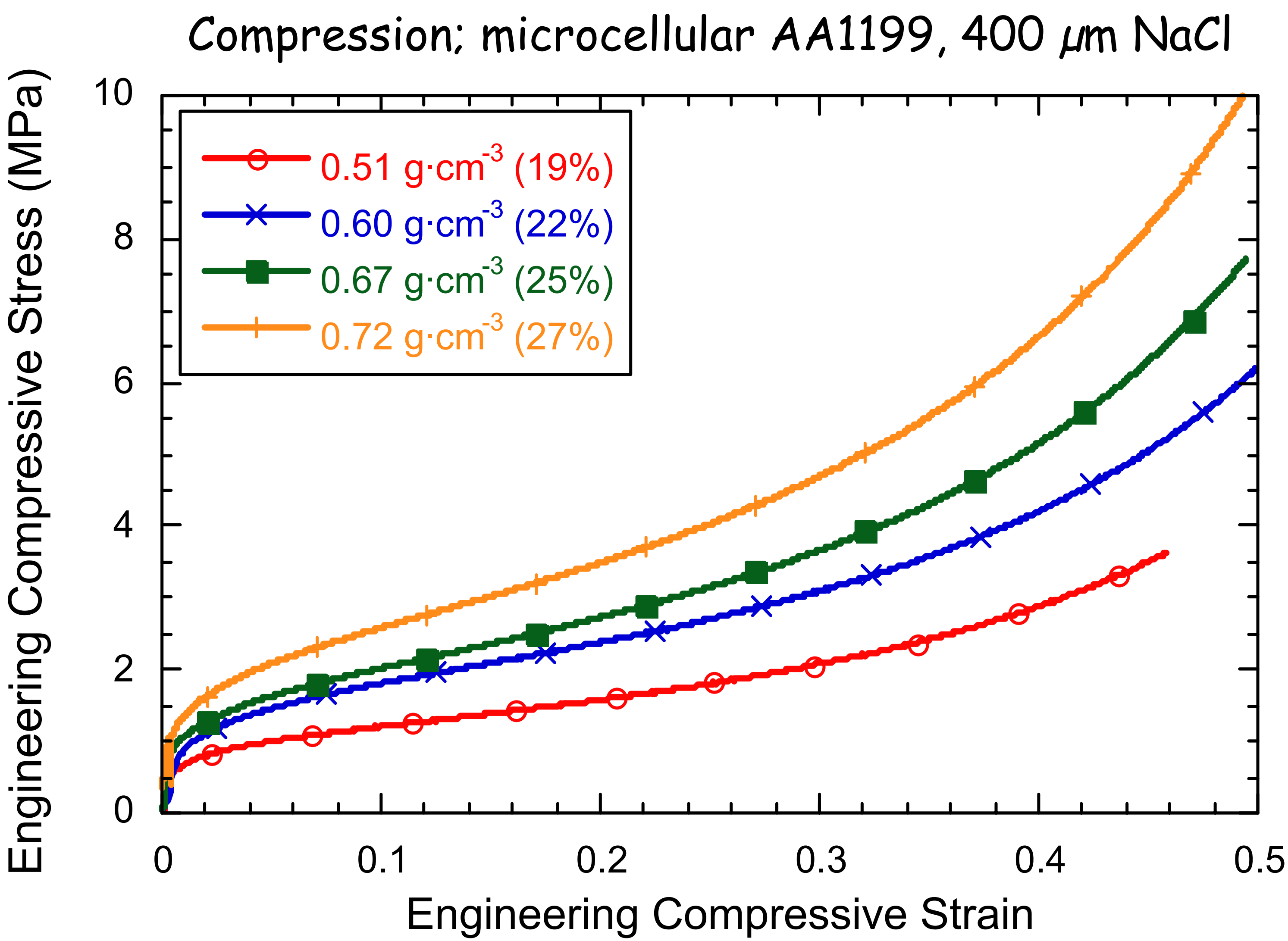

Influence of Density

Tension; microcellular AA1199, 400 μm NaCl

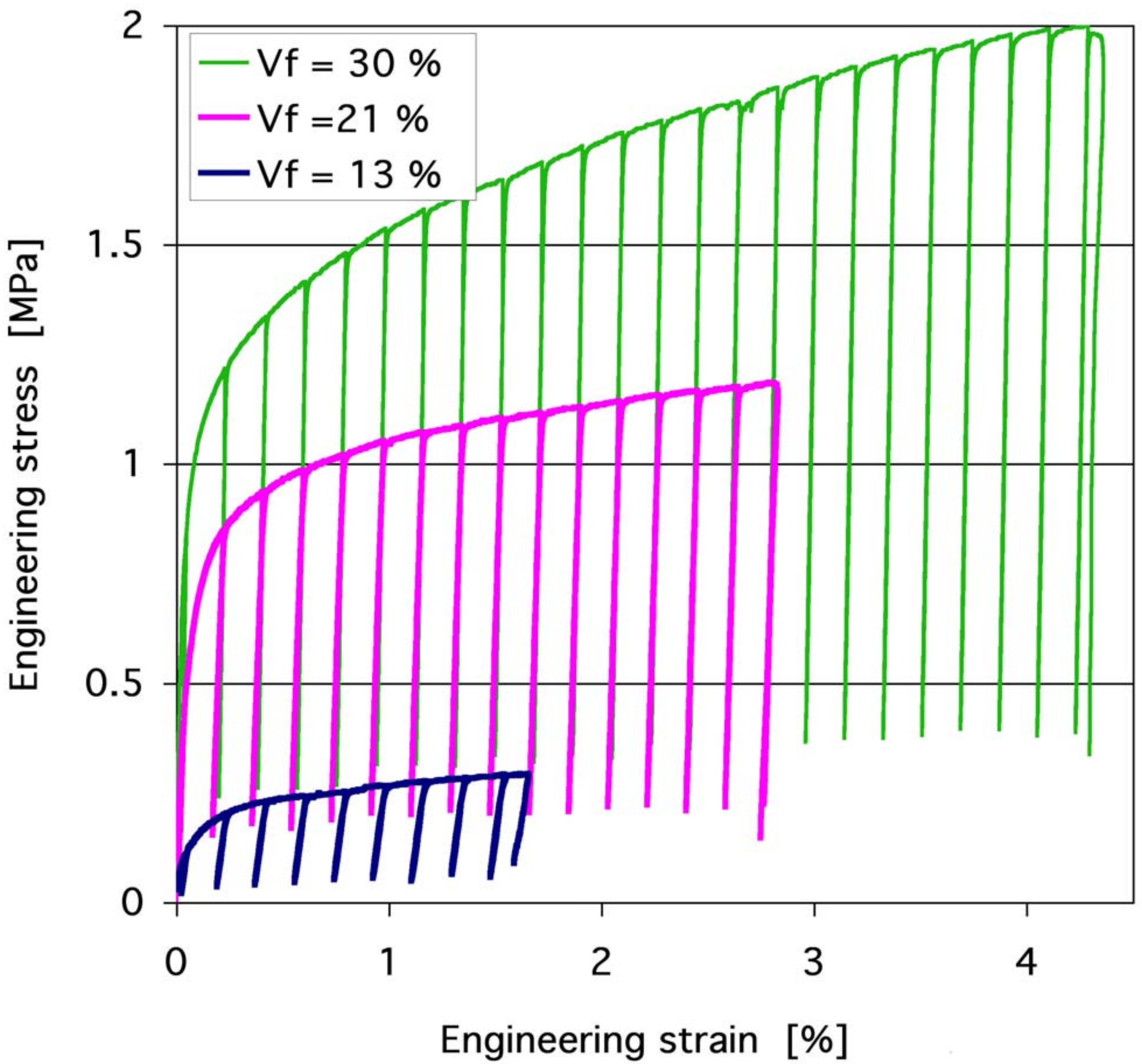

Influence of Density

Evolution of E_0 with Vf_{Al}, 400 μm NaCl

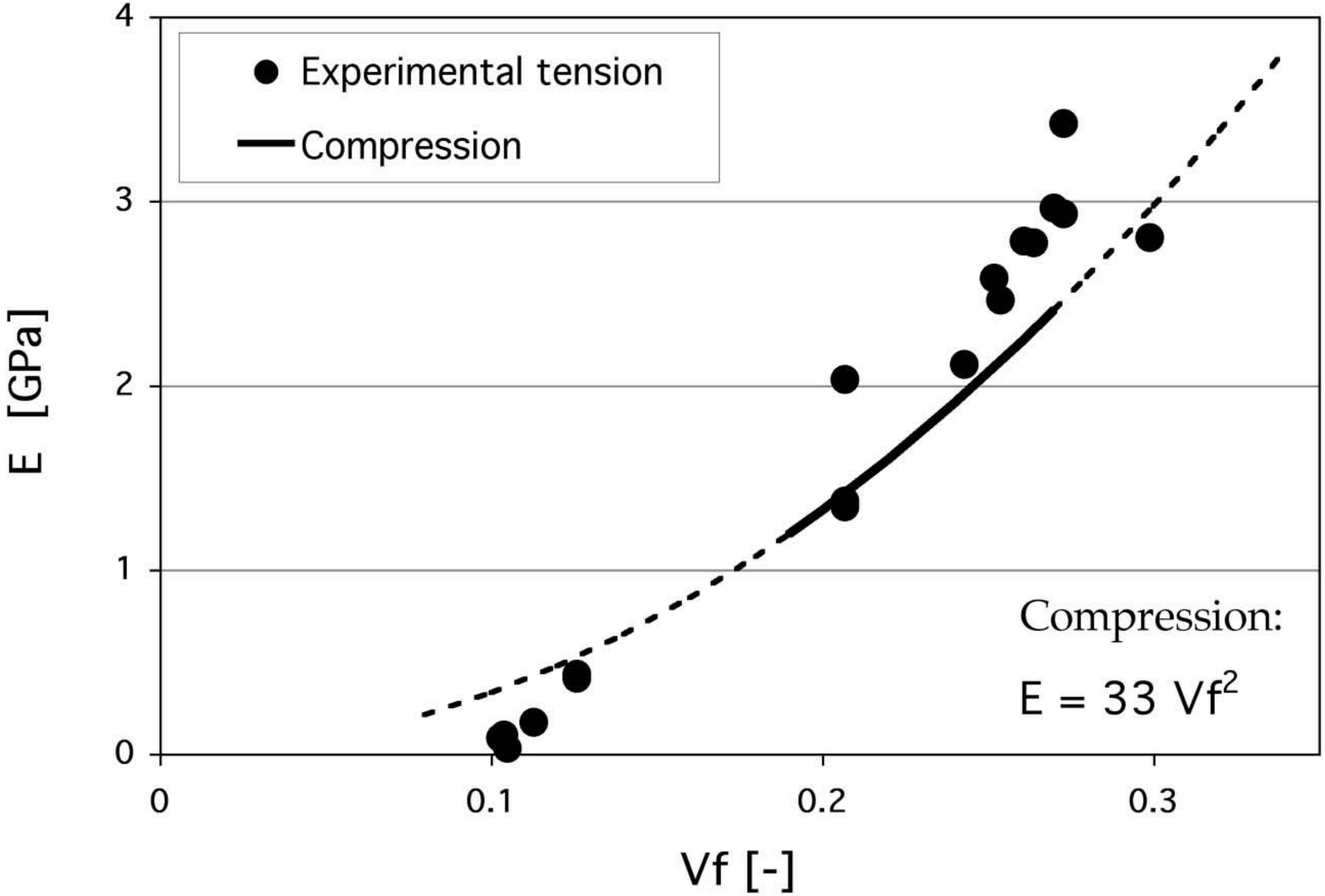

[*Acta Materialia*, 49 (19) 3959-3969 (2001); Proc. MetFoam 2003]

Influence of Density

Evolution of $\sigma_{2\%}$ with Vf_{Al}, 400 μm NaCl

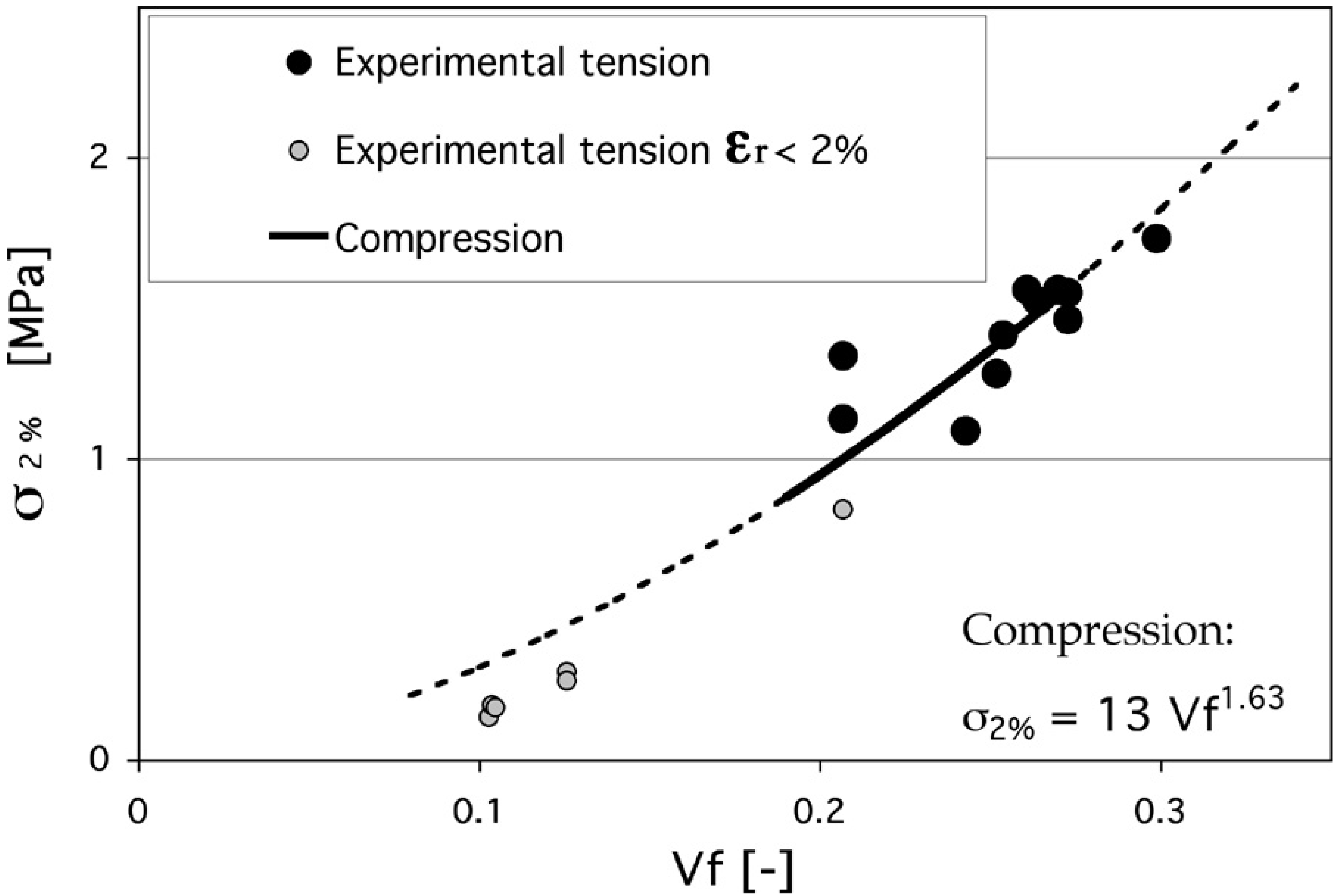

[*Acta Materialia*, 49 (19) 3959-3969 (2001); Proc. MetFoam 2003]

Size Effect

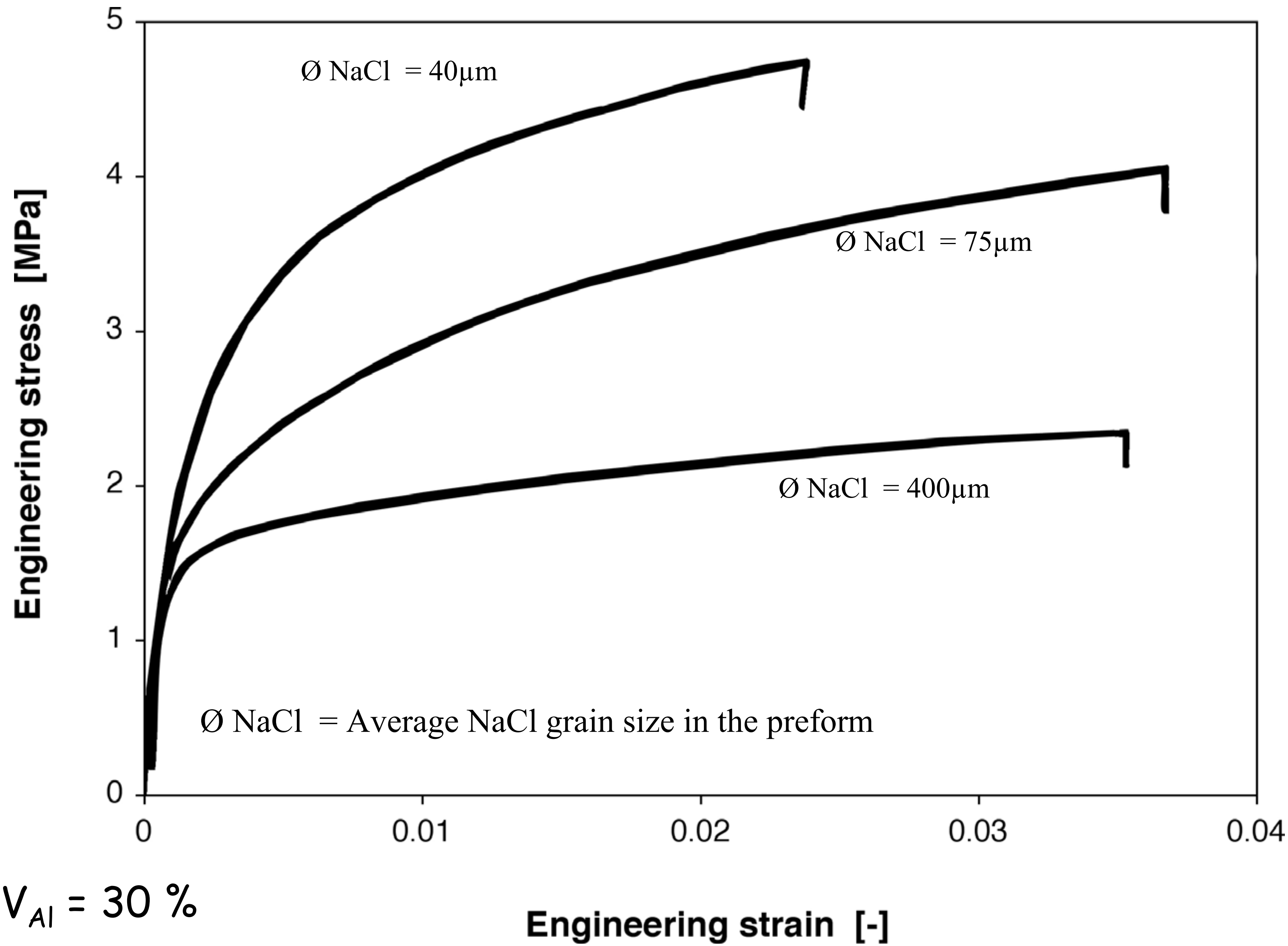

V_{Al} = 30 %

Size Effect

Sources of hardening at small cell sizes:

• Geometrically necessary dislocations when cooling after infiltration
$CTE_{Al} = 23.6 \cdot 10^{-6}$ [K^{-1}]
$CTE_{NaCl} = 44 \cdot 10^{-6}$ [K^{-1}]

• Oxidation during salt dissolution (hydroxide formation)

Damage

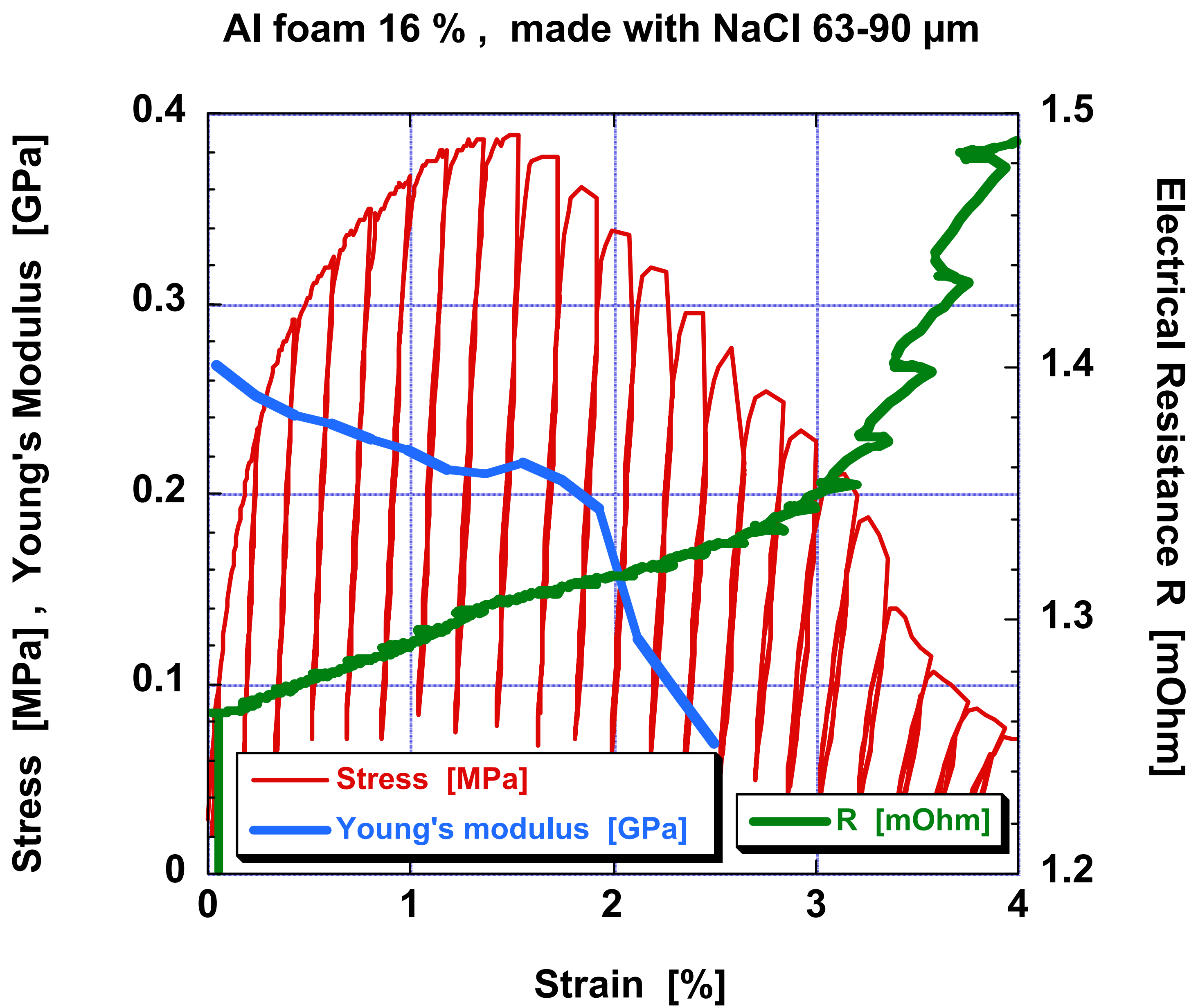

Al foam 16 % , made with NaCl 63-90 µm
Stress [MPa] , Young's Modulus [GPa]
Electrical Resistance R [mOhm]
Strain [%]
0
0.1
0.2
0.3
0.4
1.2
1.3
1.4
1.5
0
1
2
3
4
Stress [MPa]
Young's modulus [GPa]
R [mOhm]

Damage

Before necking, E decreases with e while R increases linearly with e.

This implies damage build-up during foam tensile deformation:
(the modulus would otherwise increase),

taking the form of foam strut tensile deformation and failure
(since the resistance increases linearly with strain before the peak).

Damage

Visualisation by X-Ray Microtomography:

At ESRF, in collaboration with:

• Ariane Marmottant, Luc Salvo, Rémy Dendiével
(INPG Grenoble, France)

• Eric Maire
(INSA Lyon, France)

Tensile test coupled with X-ray Microtomography

466_3

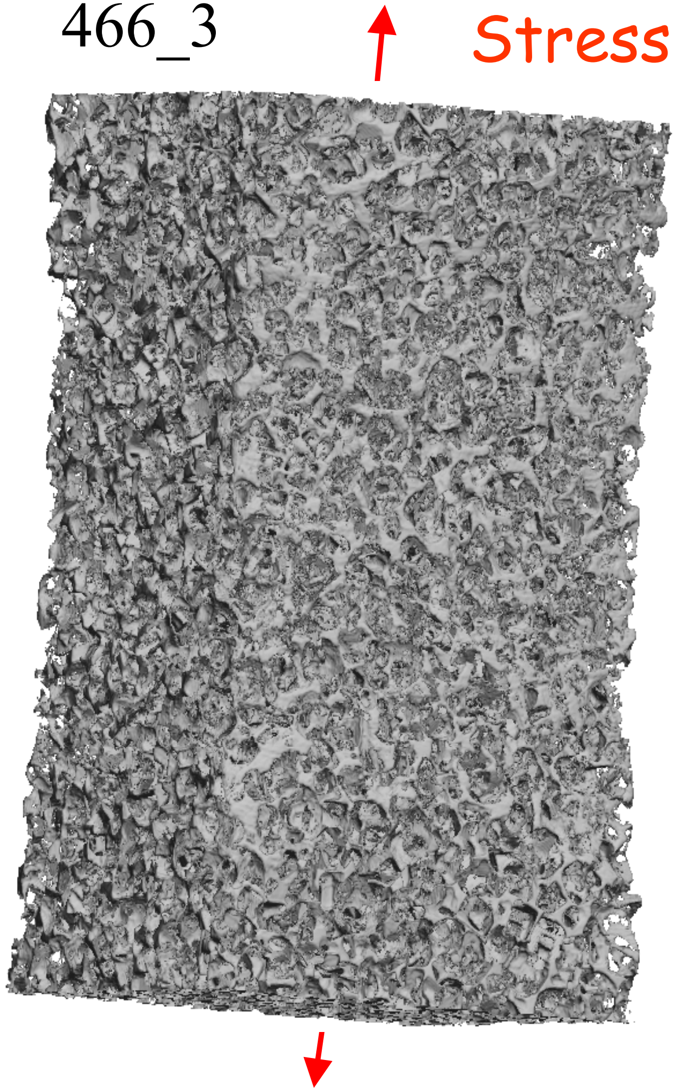

Salt: 400 μm
Vf preform = 75 %
Pinfiltration = 155 bars

Tensile test coupled with X-ray Microtomography

466_4

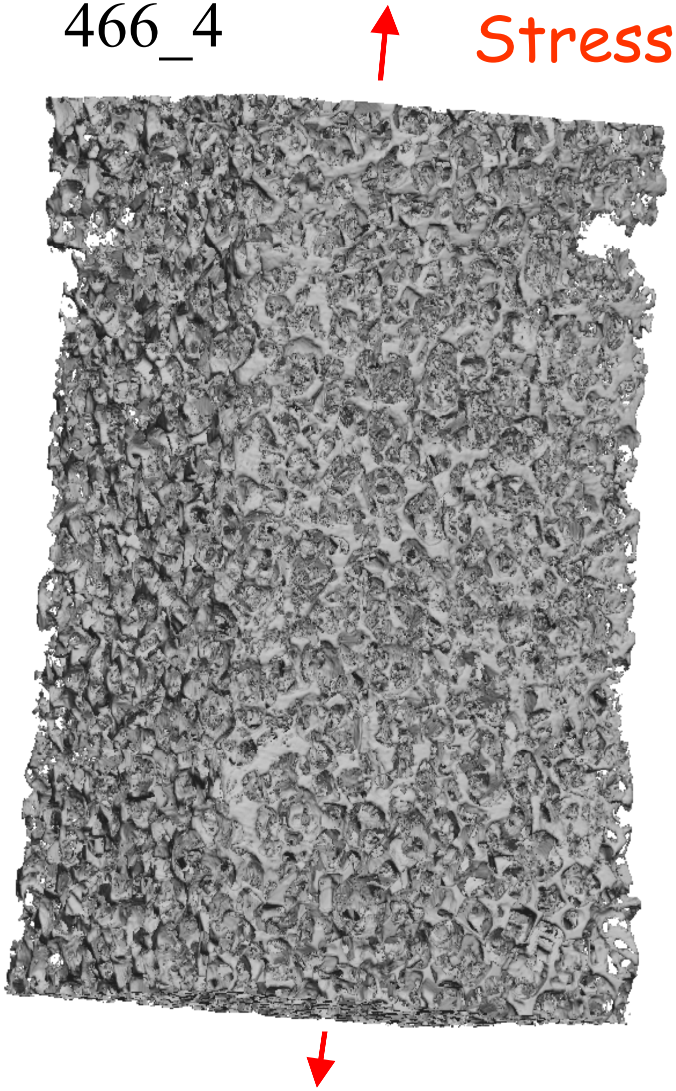

Salt: 400 μm
Vf preform = 75 %
Pinfiltration = 155 bars

Tensile test

467_0

Stress axis

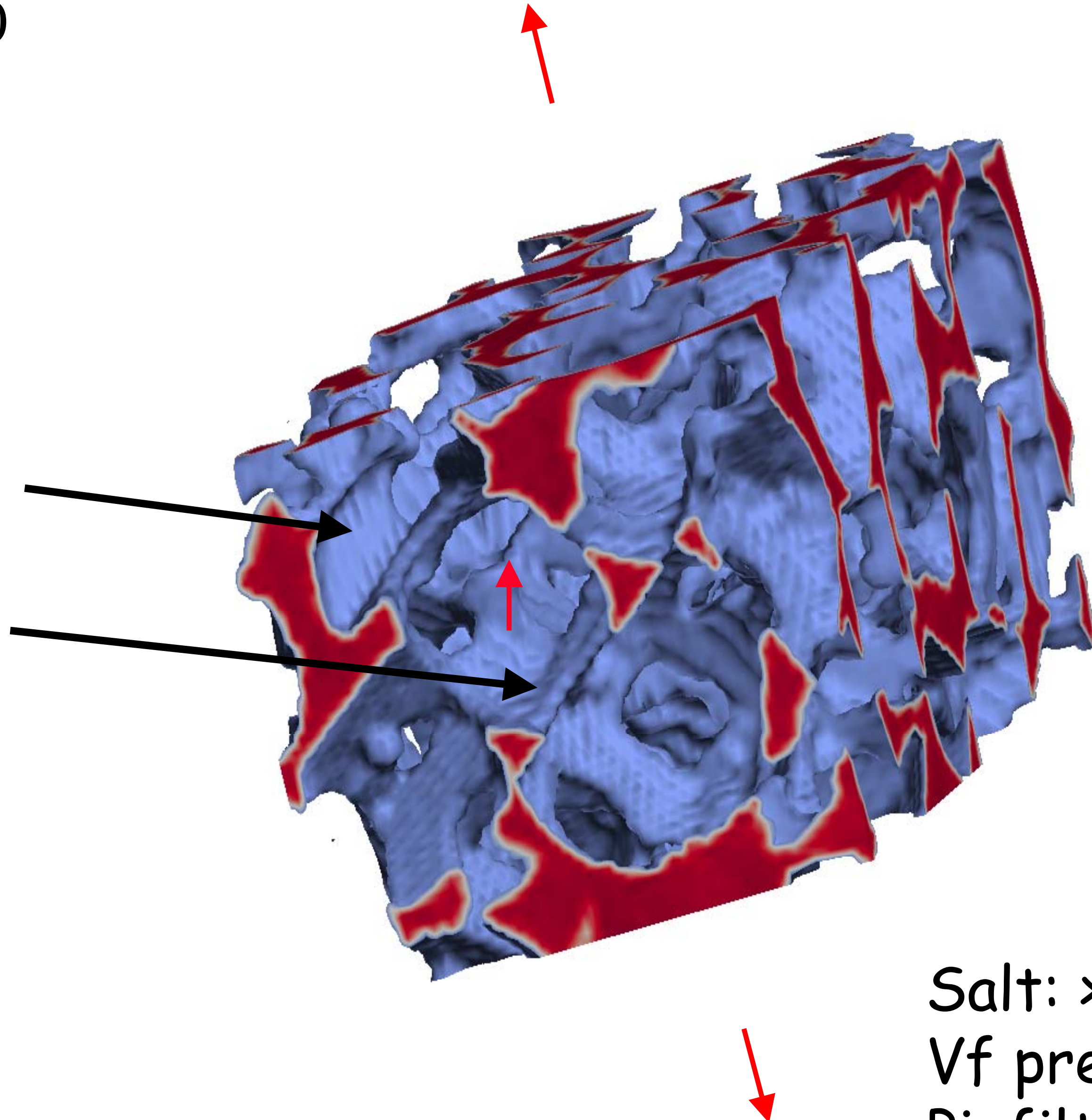

Salt: > 250 µm
Vf preform = 75 %
Pinfiltration = 1 bar

Tensile test

467_1

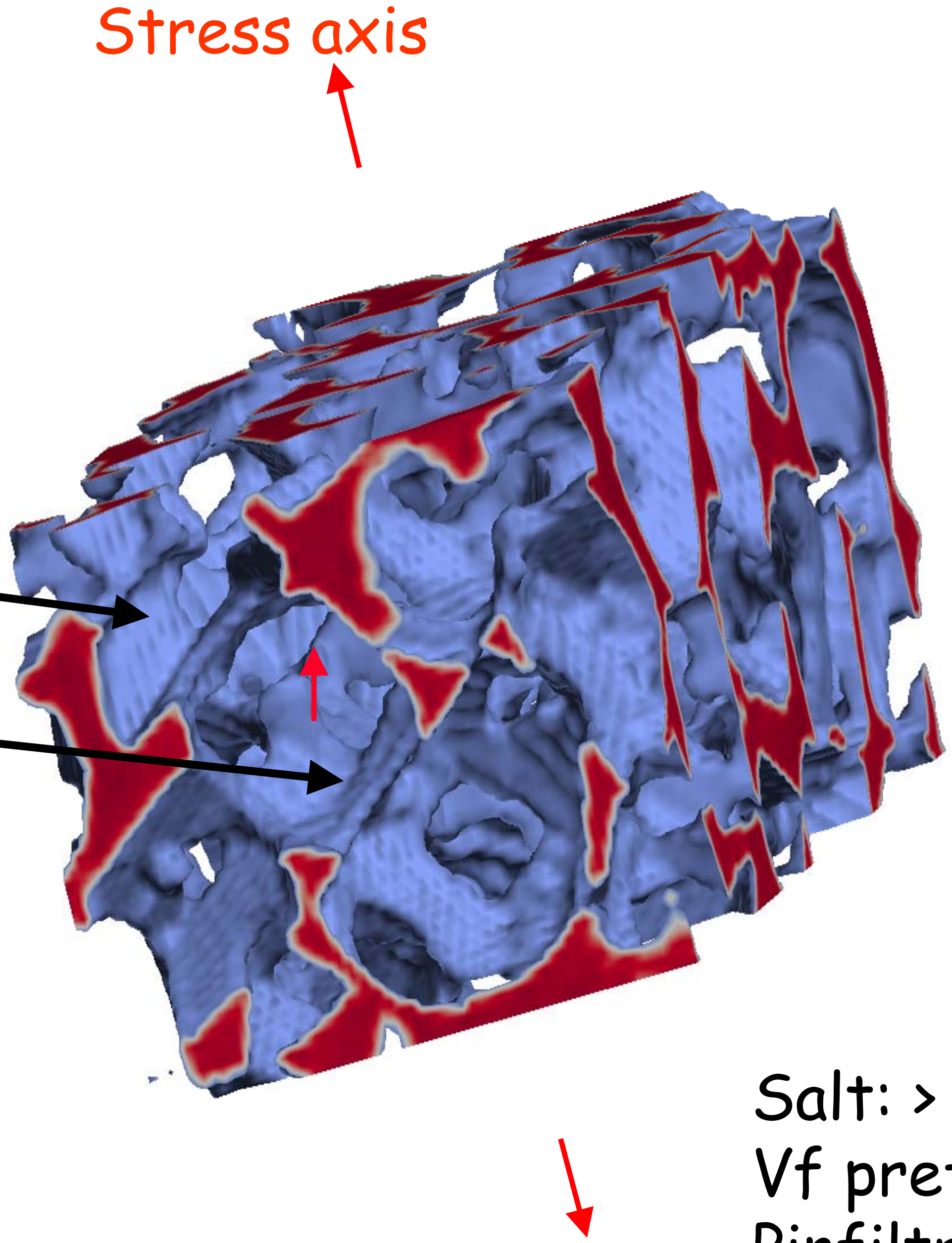

Salt: > 250 µm

Vf preform = 75 %

Pinfiltration = 1 bar

Tensile test

467_2

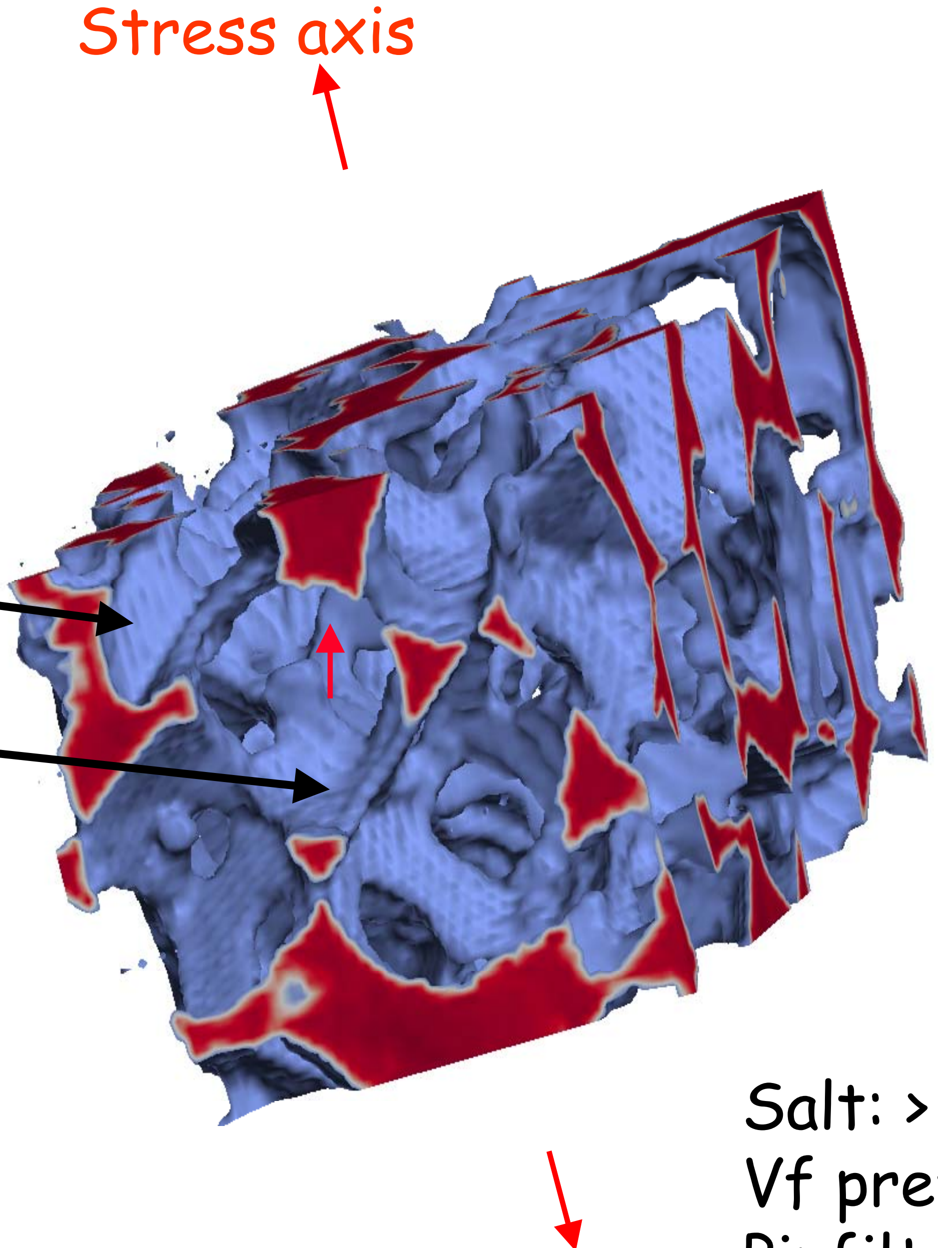

Salt: > 250 µm
Vf preform = 75 %
Pinfiltration = 1 bar

Tensile test

467_3

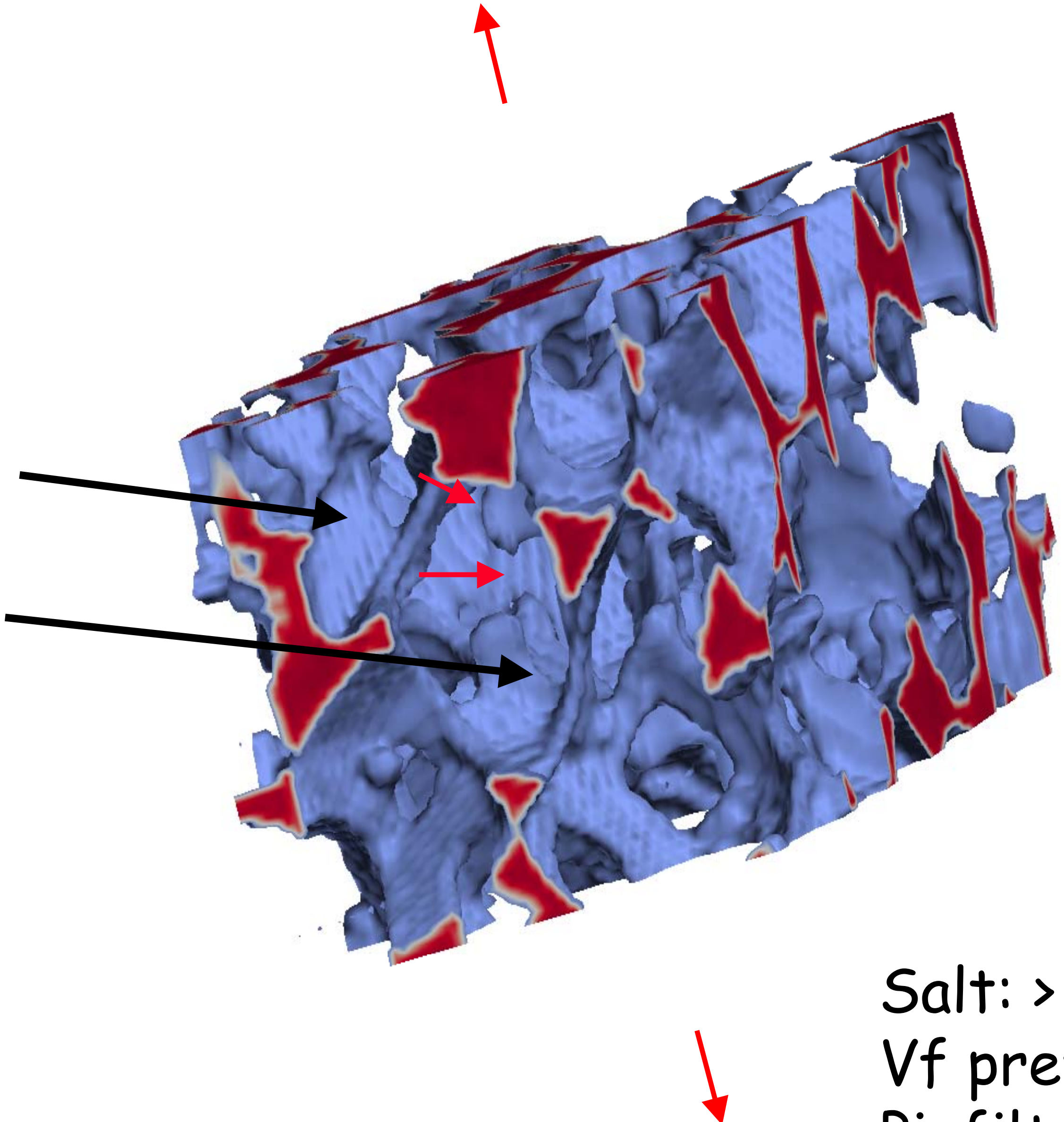

Salt: > 250 µm

Vf preform = 75 %

Pinfiltration = 1 bar

Tensile test

467_0

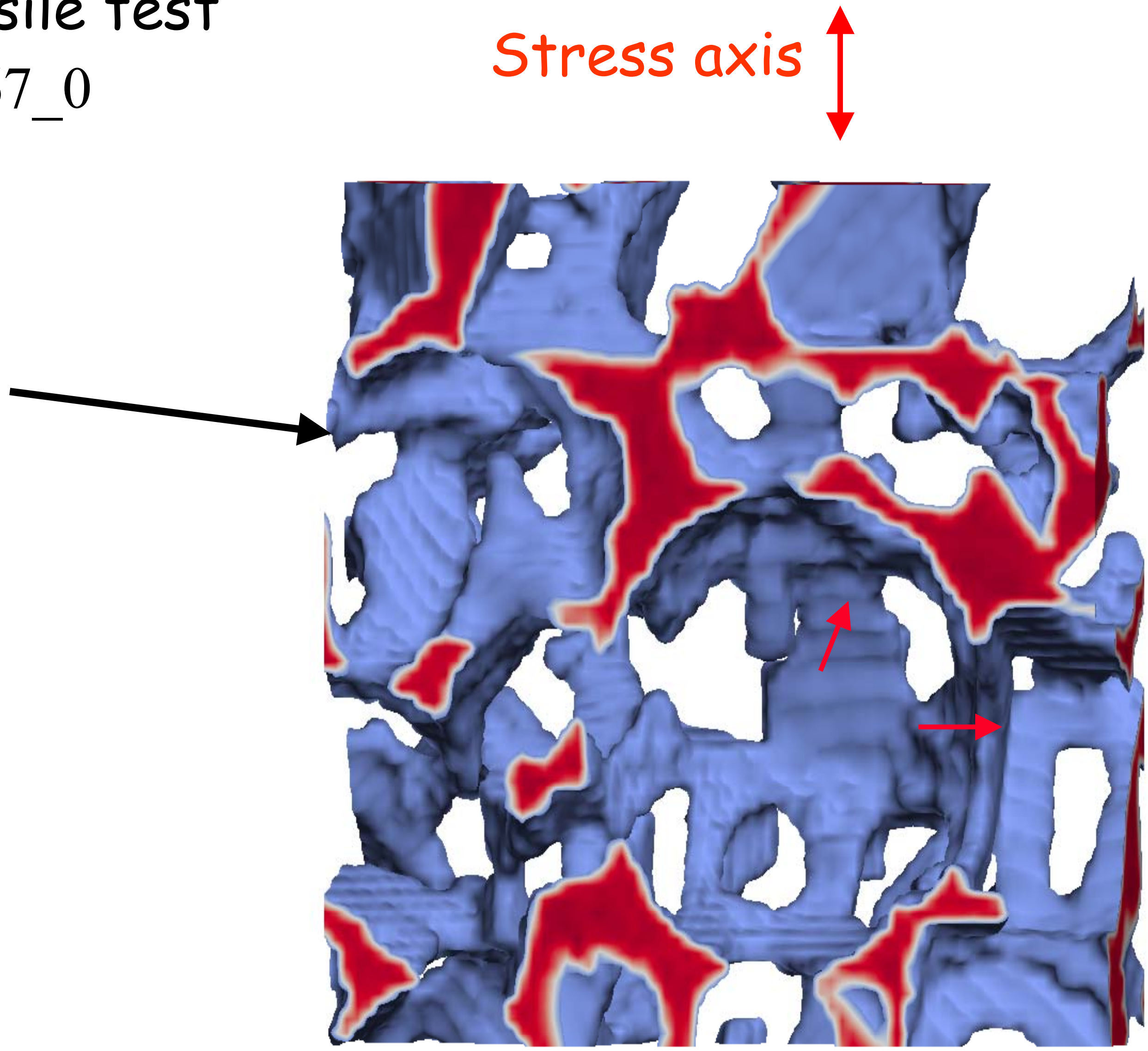

Salt: > 250 µm

Vf preform = 75 %, Pinfiltration = 1 bar

Tensile test

467_1

Stress axis

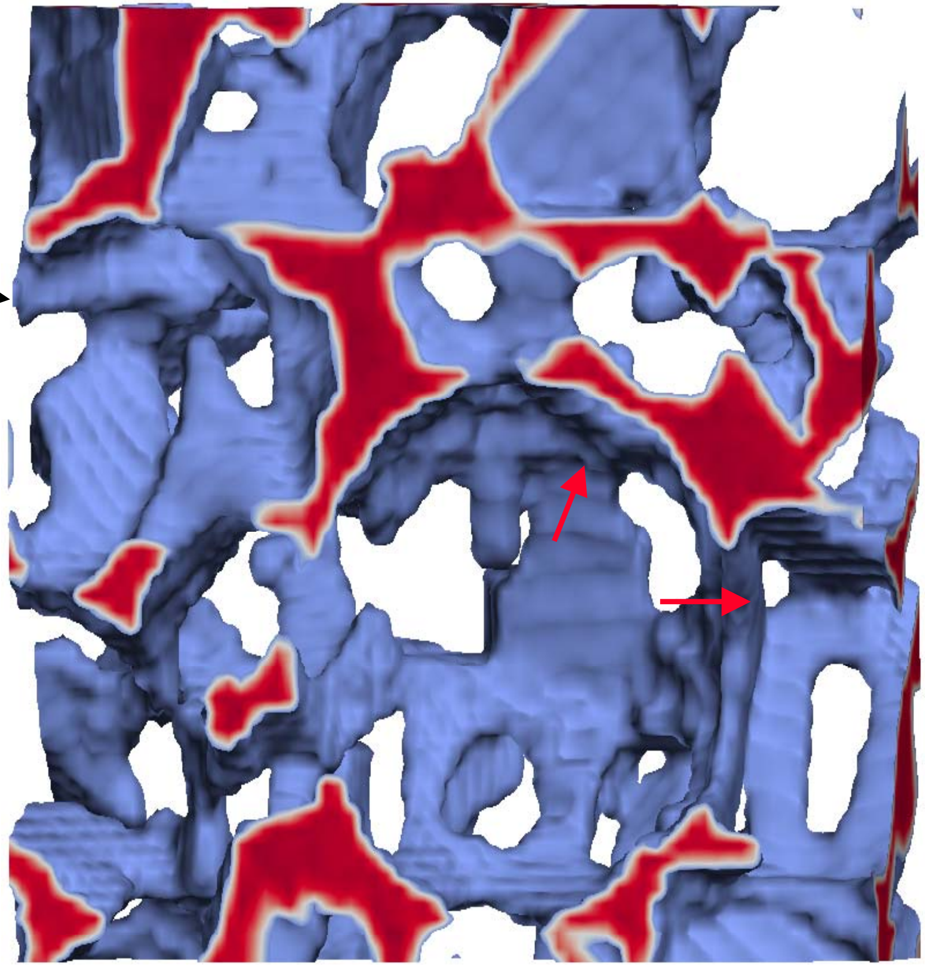

Salt: > 250 μm

Vf preform = 75 %, Pinfiltration = 1 bar

Tensile test

467_2

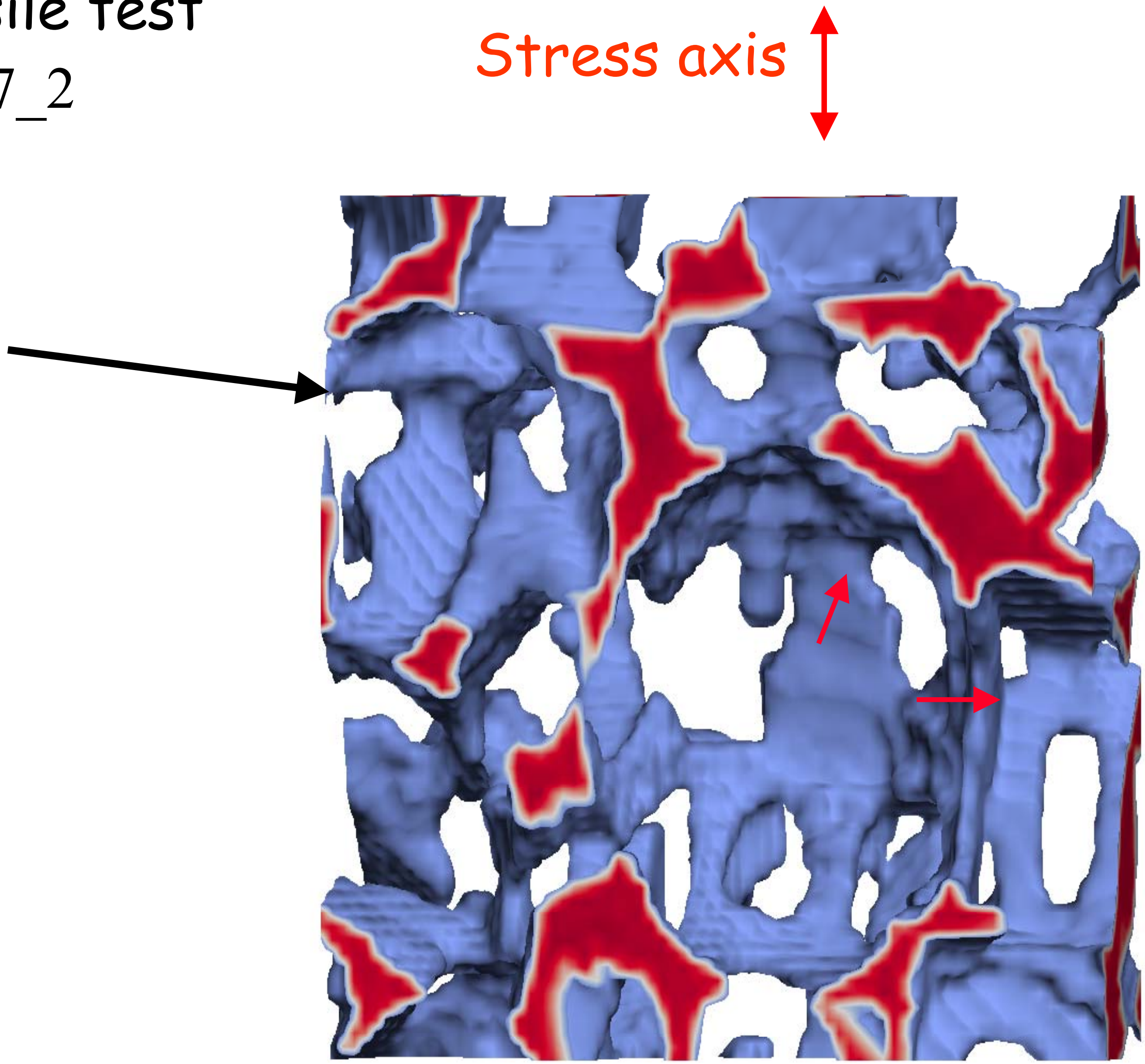

Salt: > 250 µm

Vf preform = 75 %, Pinfiltration = 1 bar

Tensile test

467_3

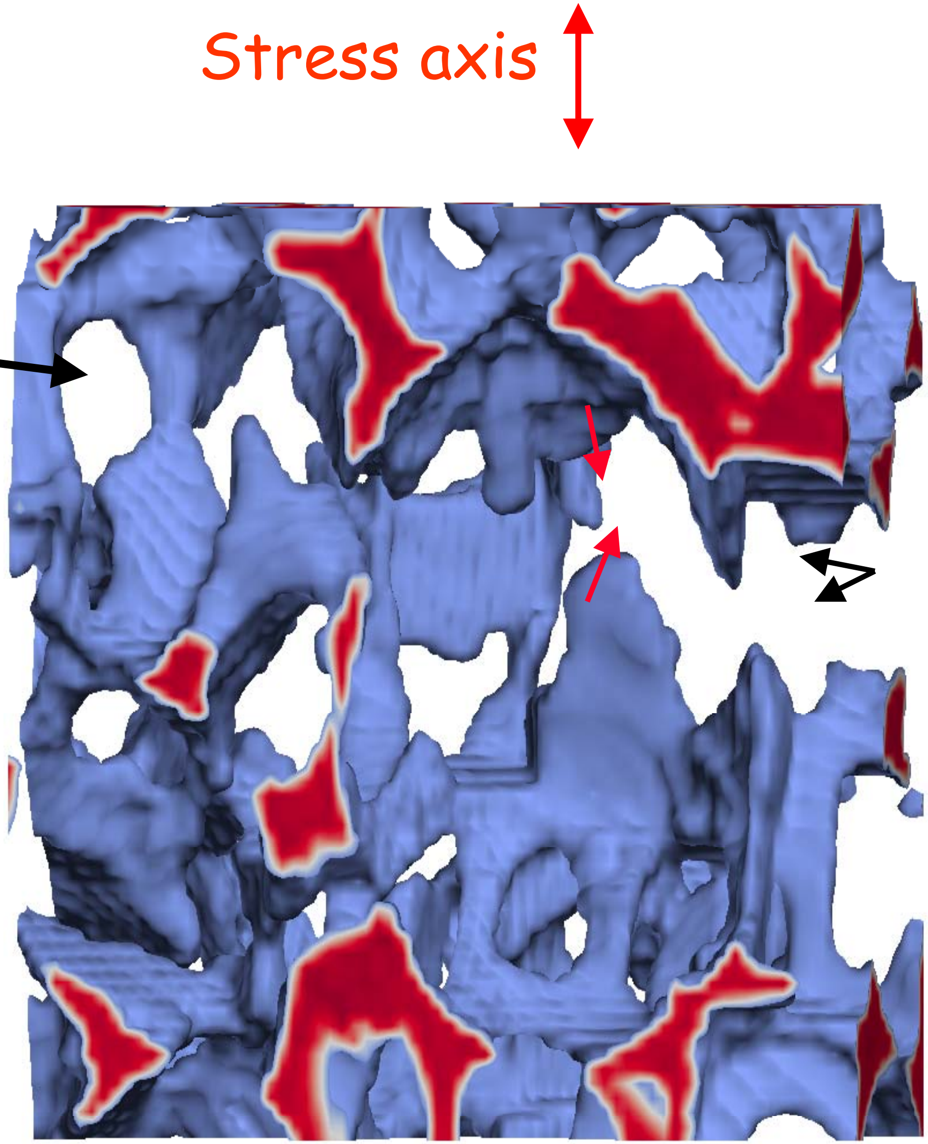

Salt: > 250 µm

Vf preform = 75 %, Pinfiltration = 1 bar

Damage as seen in the SEM

Far from fracture zone

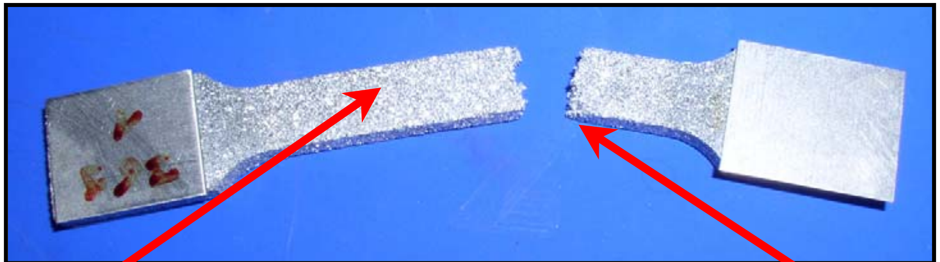

Fracture surface

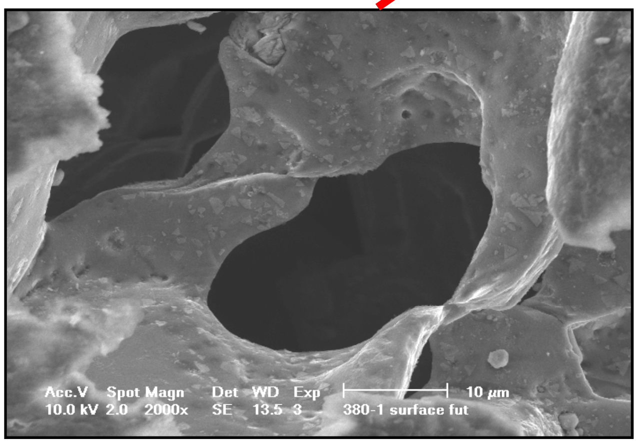

NaCl 75µm , Vf_{Al} =31 %

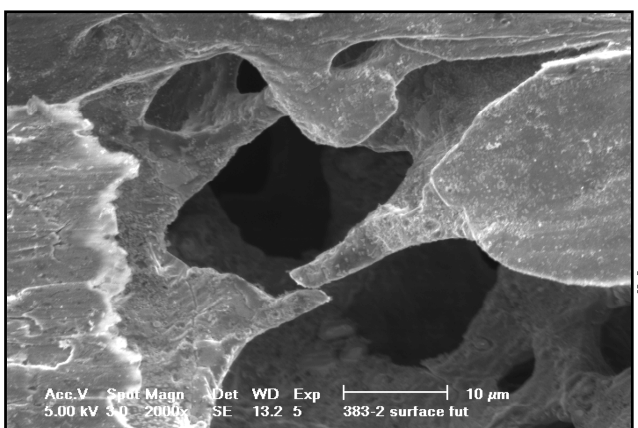

NaCl 75µm , Vf_{Al} =28 %

NaCl 400µm , Vf_{Al} =25 %

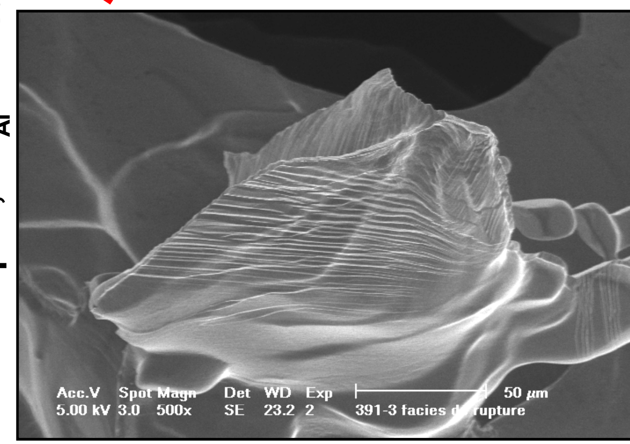

NaCl 75µm , Vf_{Al} =28 %

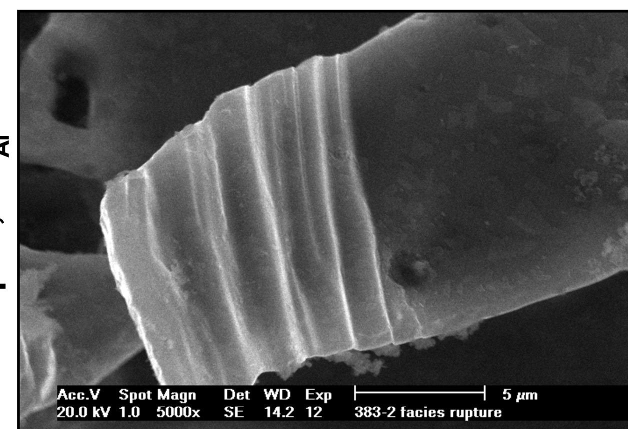

Microstructural tailoring

Microstructural tailoring

Influence of NaCl Sintering:

T sintering = 755 °C; V_f = 66%; particle size: 63-90 μm

t = 0 [h]

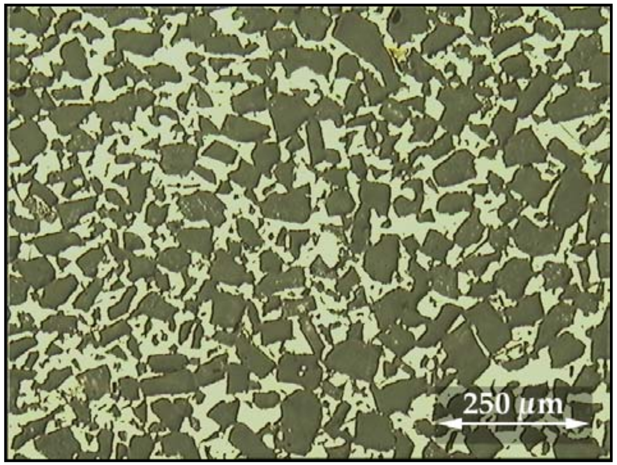

t = 2 [h]

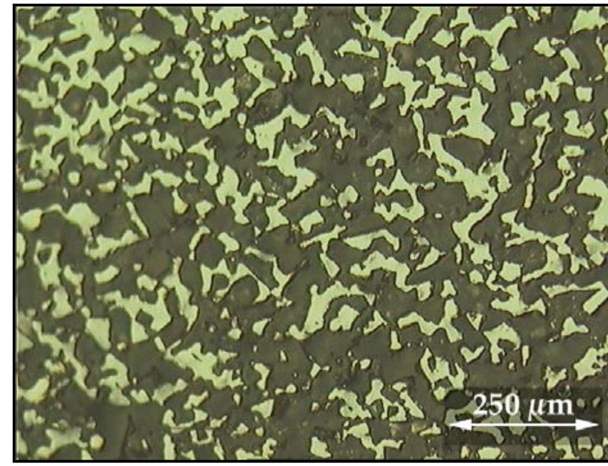

t = 9 [h]

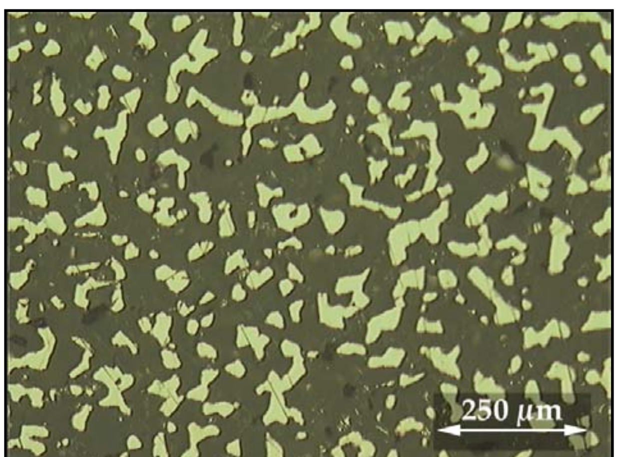

t = 25 [h]

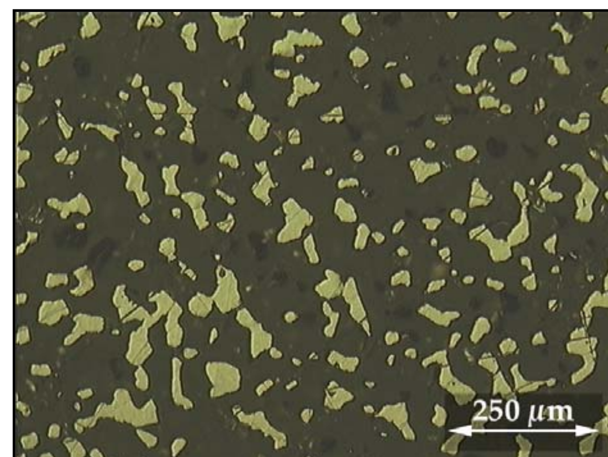

Microstructural tailoring

Influence of NaCl sintering

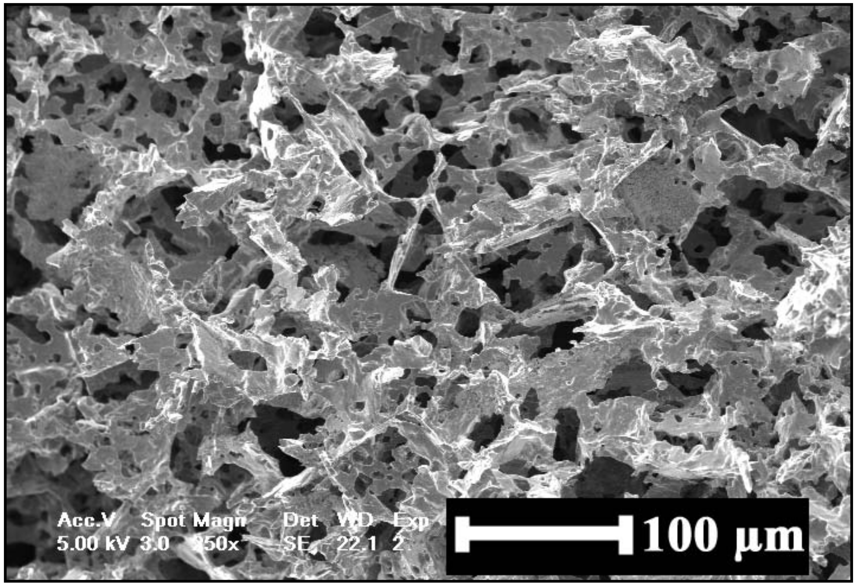

NaCl 63-90 μm,
no sintering
Vf Al = 18 %

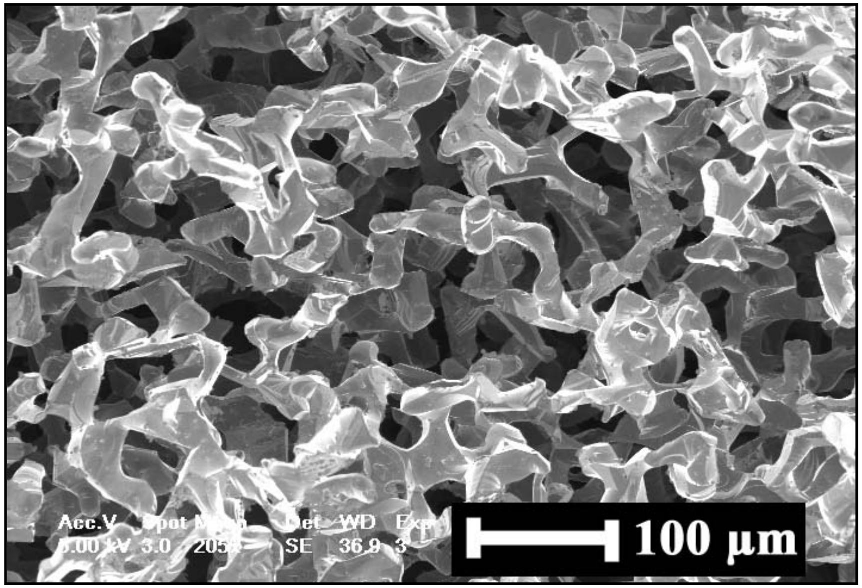

NaCl 63-90 μm,
sintered 24h@750°C
Vf Al = 18 %

Microstructural tailoring

Commercial powders

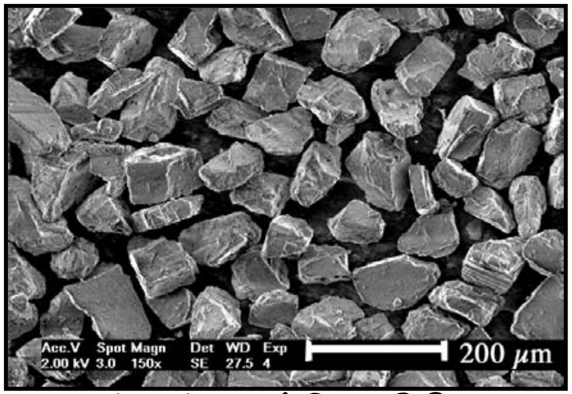

Sieving 63 - 90 μm

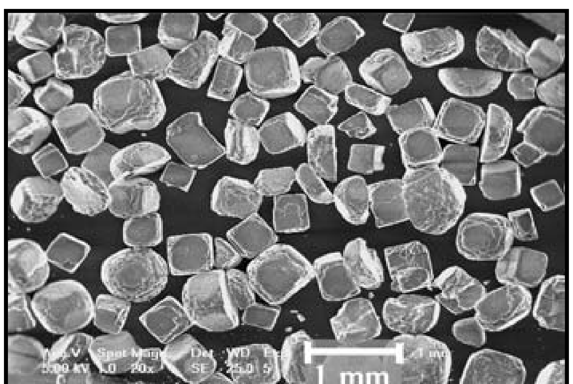

Sieving > 250 μm

Precipitated powders

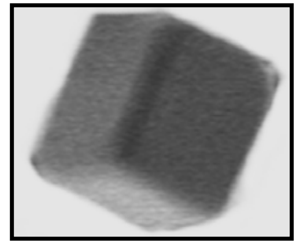

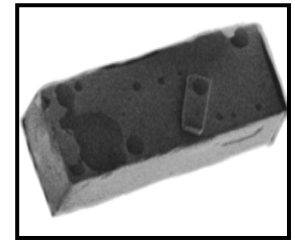

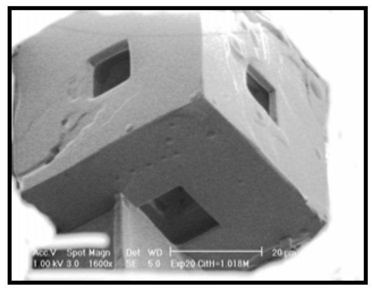

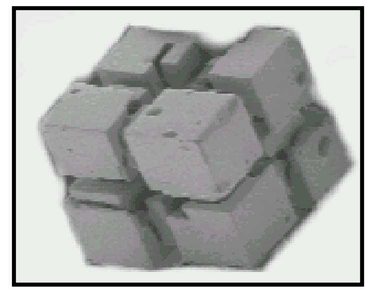

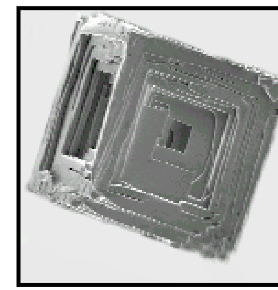

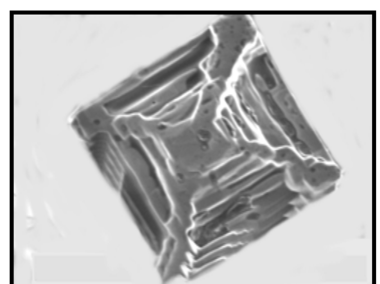

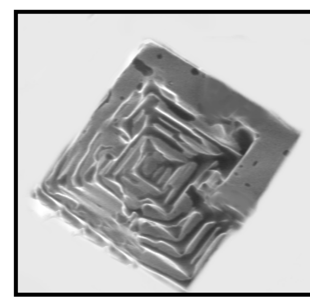

(a few μm in diameter)

Microstructural tailoring

Influence of Infiltration Pressure (preform 75% dense)

P = 1 bar

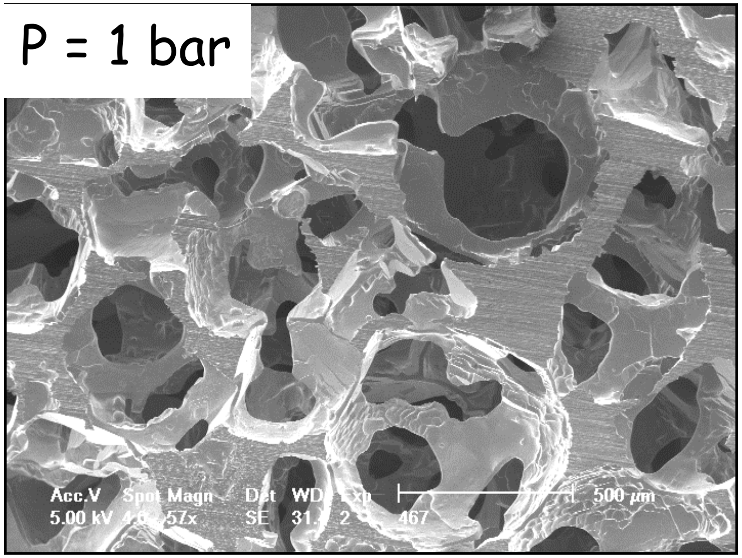

P = 5 bar

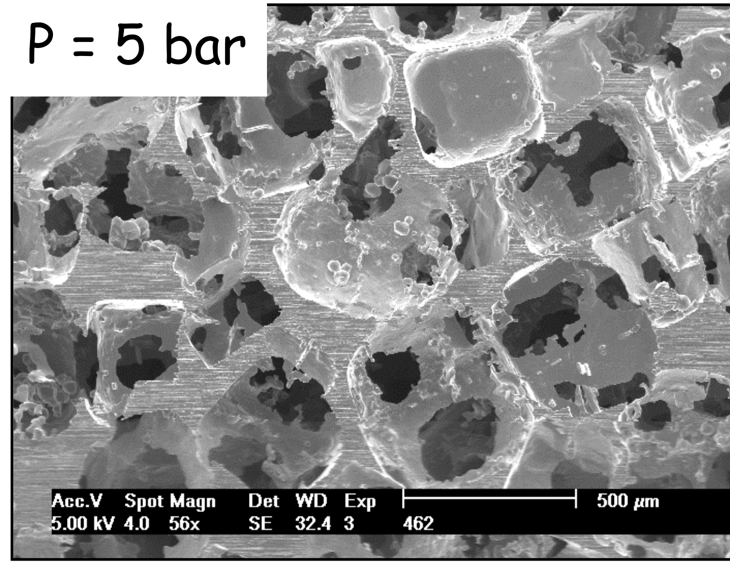

P = 10 bar

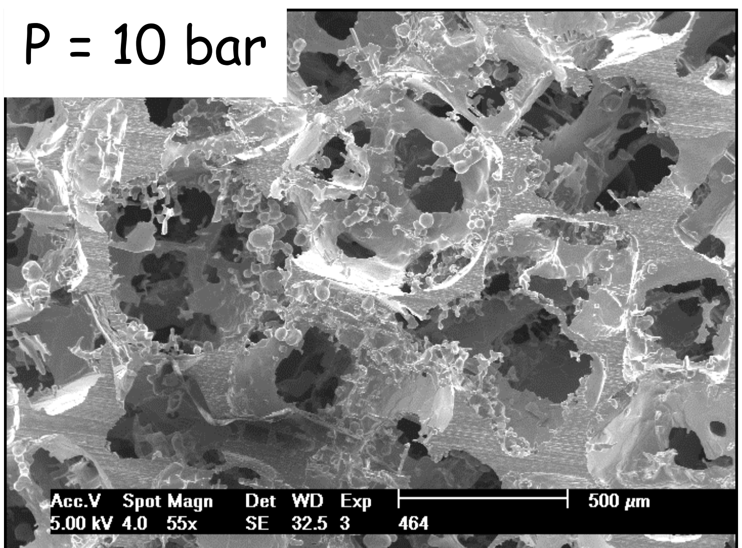

P = 155 bar

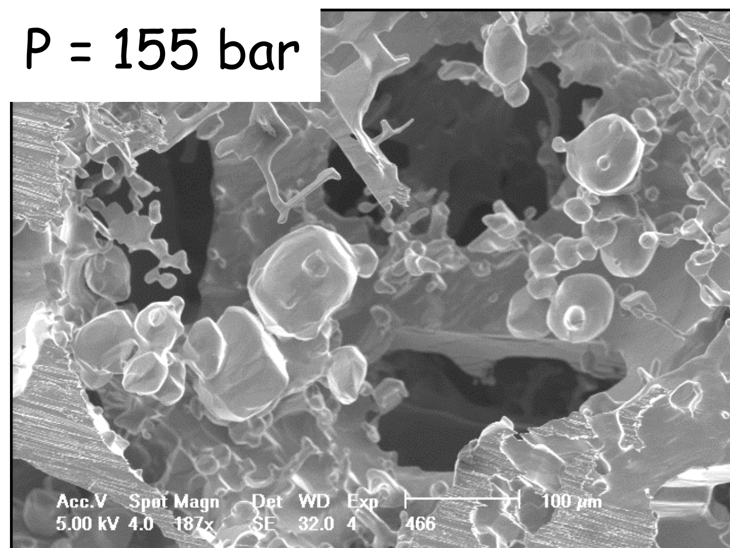

Conclusion

Infiltration: definition, engineering advantages, usefulness in research;

High V_f ceramic particle reinforced metal: can be made relatively tough, strong and ductile.

Open-cell aluminium foams (sponges): exploration of processing/microstructure/property relations for this class of materials.

Acknowledgement

This research program is supported by the Swiss National Science Foundation,
Projects No. 200020-100287 and 200020-100179